

***IN VIVO AND IN VITRO* INVESTIGATION OF THE TISSUE-  
SPECIFIC ACTIVITY OF THE HUMAN *CYP3A4* AND *CYP3A5*  
PROMOTERS**

Dissertation

zur Erlangung des Grades

Doktor der Naturwissenschaften

(Dr. rer. nat.)

Am Fachbereich Biologie

der Johannes Gutenberg-Universität Mainz

**Dieudonné Nem**

aus

**Bayangam, Kamerun**

Mainz, 2011

**Dekan:** [REDACTED]

**1. Berichtstatter:** [REDACTED]

**2. Berichtstatter:** [REDACTED]

Tag der mündlichen Prüfung: 18.10.2011

To [REDACTED],

[REDACTED] and [REDACTED]

**For love and for having always been with me all the times**

## **Acknowledgements**

This study was carried out at the Department of pharmacology, University Medical Center, Johannes Gutenberg University Mainz from April 2008 to October 2011. It is a pleasure for me to thank those who made this thesis possible.

First, I owe my deepest gratitude to my supervisor, [REDACTED] for having admitted me to his group and for introducing me to the broad world of cytochrome P450s. His sage advice, insightful criticisms, patient and discreet encouragement inspired me throughout the completion of my thesis.

It is an honour for me to thank the [REDACTED] and [REDACTED], since without their financial support the work presented herein would not have been possible.

I am also grateful to [REDACTED] for the pronuclear injections to generate the transgenic CYP3A5 mouse strains, [REDACTED] for his technical assistance with mice bioluminescent imaging, [REDACTED] for her excellent help with the P-Match and Western Blot analyses, [REDACTED], [REDACTED], [REDACTED], and [REDACTED] for kindly providing construct and expression vectors.

I am indebted to my colleagues for their enthusiasm and friendly atmosphere implemented in our group and the whole Department. Thank you so much [REDACTED] for your dynamism and technical guidance. I thank [REDACTED] for his friendship, encouragement and for sharing with me his knowledge of comparative genomic and bioinformatic analyses. Thank you [REDACTED], [REDACTED], [REDACTED], and [REDACTED]. Your constructive criticisms and unconditional collaboration helped me to correct my mistakes and enabled me to improve myself and move deeper into my topic. Unforgettable are all conversations that make our office such a pleasant place to work in.

I am heartily thankful to all my friends for the exiting times spend together and the valuable life experience during this period. I would also like to show my gratitude to my family. My special gratitude to my cousin, [REDACTED] for always supporting me to follow my dreams. [REDACTED], [REDACTED], [REDACTED], [REDACTED] and [REDACTED] for sustaining and encouraging me. I thank my wife, [REDACTED] for allowing me to experience a balanced life.

Finally, I reserve my blessings to all of those who supported me in any respect during the completion of this work but who are not specifically cited herein.

## Table of contents

Table of contents .....	i
List of figures .....	iii
List of tables .....	iv
List of abbreviations .....	v
1. Introduction .....	1
1.1 The Cytochrome P450 superfamily .....	1
1.1.1 General considerations .....	1
1.1.2 Classification .....	1
1.1.3 Function .....	2
1.2 Human CYP3A family .....	2
1.2.1 The evolutionary history of the <i>CYP3</i> gene family .....	2
1.2.2 The evolution of primate CYP3A genes .....	3
1.2.3 Structure of human CYP3A genes .....	4
1.2.4 CYP3A substrate spectrum .....	5
1.2.5 CYP3As genetic polymorphisms and variability of expression .....	7
1.2.6 CYP3A genes expression .....	9
1.2.7 CYP3As regulation .....	10
1.2.7.1 Transcription regulation of CYP3As .....	10
1.2.7.1.1 Nuclear receptor superfamily .....	10
1.2.7.1.2 Regulation of CYP3As by Nuclear receptors: PXR and CAR .....	11
1.2.7.1.3 Regulation of CYP3As by other nuclear factors .....	13
1.2.8 <i>In Vivo</i> known investigation of CY3As regulation and expression .....	15
1.2.8.1 Molecular based-mechanism for the generation of transgenic mice .....	15
1.2.8.2 Known CY3As transgenic mice .....	16
2. Aims of the study .....	19
3. Materials and methods .....	20
3.1 Materials .....	20
3.1.1 Instruments .....	20
3.1.2 Chemicals* .....	21
3.1. 3 Reagents/Kits/enzymes/Antibodies/solvents .....	21
3.1. 4 Solvents .....	22
3.1.5 Tools data analysis .....	22
3.1.5.1 Local software .....	22
3.1.5.2 Online data banks and software .....	23
3.1.6 Consumable materials* .....	23
3.1.7 Oligonucleotides .....	24
3.2 Methods .....	26
3.2.1 CYP3A promoter sequence analysis .....	26
3.2.2 Construction of <i>CYP3A5</i> reporter gene constructs .....	26
3.2.3 Generation of CYP3A5-luc transgenic mice .....	27
3.2.3.1 Isolation of genomic tail-tip DNA .....	27
3.2.3.2 PCR genotyping of CYP3A5-luc transgenic mice .....	27
3.2.3.3 Determination of the tissue distribution of CYP3A5-luc transgene .....	28
3.2.3.4 Animal treatment with PCN and TCPOBOP agonists .....	28
3.2.3.5 Transgenic mice bioluminescent imaging assay .....	28
3.2.4 <i>In vitro</i> analyses of the human CYP3A4 and CYP3A5 promoters .....	29
3.2.4.1 Inverted PCR-based mutagenesis .....	29
3.2.4.2 Site-directed mutagenesis of the YY1 and NF1 binding sites .....	29
3.2.4.3 Expression vector constructs .....	30

---

3.2.4.4 Bacterial cell transformation and plasmid isolation.....	30
3.2.4.5 Cell Culture .....	30
3.2.4.6 Transient transfection and luciferase assays .....	31
3.2.4.7 <i>In vitro</i> transcription and translation .....	31
3.2.4.8 RNA isolation and cDNAs synthesis .....	31
3.2.4.9 RT-PCR and amplification of the YY1 and NF1 cDNAs .....	32
3.2.4.10 Nuclear extract preparation .....	32
3.2.4.11 Annealing of labeled oligonucleotides.....	33
3.2.4.12 Electrophoretic mobility gel shift assay (EMSA) and supershift assay .....	33
3.2.5 Statistical analyses.....	33
4. Results .....	34
4.1 <i>In vivo</i> analysis of <i>CYP3A5</i> promoter activity.....	34
4.1.1 Generation and identification of the <i>CYP3A5</i> -luc mice .....	34
4.1.2 <i>In vivo</i> determination of the basal activity of the <i>CYP3A5</i> transgene .....	34
4.1.3 <i>In vitro</i> determination of the tissue distribution of <i>CYP3A5</i> transgene activity.....	36
4.1.4 Photonic localisation and segmental determination of the <i>CYP3A5</i> -luc activity along the small intestine.....	37
4.1.5 The dose-effect on the PXR-driven <i>CYP3A5</i> -luc transgene activity in the small intestine and kidney.....	38
4.1.6 The time-effect on the PXR- or CAR-driven <i>CYP3A5</i> -luc transgene induction in the small intestine.....	39
4.1.7 Induction activity of the <i>CYP3A5</i> -luc transgene along the small intestine .....	40
4.2 <i>In vitro</i> evaluation of the determinants of the differential tissue-specific activity of <i>CYP3A4/CYP3A5</i> promoters .....	41
4.2.1 Identification of the minimal <i>CYP3A5</i> promoter.....	41
4.2.2 Comparative analysis of <i>CYP3A5</i> -6.2 and chimeric XREM- <i>CYP3A5</i> constructs in LS174T cells .....	41
4.2.3 Evaluation of <i>CYP3A5</i> and <i>CYP3A4</i> proximal promoter activities in renal and intestinal cells.....	42
4.2.4 Function of the 57 bp promoter fragment in <i>CYP3A4/5</i> expression and comparison of the proximal <i>CYP3A5</i> and <i>CYP3A4</i> promoters.....	43
4.2.5 Evolutionary history of the 57 bp region in primates.....	46
4.2.6 The 57 bp region contains conserved regulatory elements .....	48
4.2.7 The effect of the mutation of the NF1 and the E-box on <i>CYP3A4</i> and <i>CYP3A5</i> - 57ins activities.....	49
4.2.8 Functional characterization of the human <i>CYP3A4</i> YY1 binding site.....	50
4.2.8.1 Determination of the tissue expression of YY1 .....	50
4.2.8.2 EMSA analysis of the <i>CYP3A4</i> YY1 binding .....	51
4.2.8.3 Mutational analysis of the YY1 binding site in MDCK.2 cells in the <i>CYP3A5</i> - 57ins construct.....	52
4.2.8.4 The effect of overexpression of YY1 on <i>CYP3A4</i> promoter in LS174T and MDCK.2 cells.....	53
4.2.8.5 Identification of YY1 domain(s ) required for the <i>CYP3A4</i> promoter inhibition .....	55
4.2.8.6 Mutational analysis of the YY1 binding site in LS174T cells in the <i>CYP3A4</i> construct .....	57
4.2.9 The Effect of PXR on the differential activity of <i>CYP3A4</i> and <i>CYP3A5</i> promoters .....	58
4.2.10 Functional characterization of the human <i>CYP3A4</i> -NF1 binding site .....	60
4.2.10.1 Endogenous and overexpression analysis of NF1 in LS174T and MDCK.2 cells.....	61

4.2.10.2 Mutational analysis of the NF1 binding site .....	61
5. Discussion .....	64
5.1 <i>In vivo</i> regulation of CYP3A5 promoter in the small intestine.....	64
5.2 Differential regulation of the human CYP3A4 and CYP3A5 proximal promoters in renal and intestinal cells .....	66
5.3 Evolution of the YY1 binding site within the <i>CYP3As</i> promoters.....	66
5.4 The CYP3A5 proximal promoter had acquired an altered ancestral function .....	67
5.5 Identification of factors overriding YY1 inhibitory effect in CYP3A4-expressing organs .....	68
5.6 The physiological significance of the YY1 binding site from the <i>CYP3A5</i> proximal promoter .....	70
5.7 Molecular mechanism of the differential renal and intestinal expression of CYP3A5 and CYP3A4 .....	71
6. Conclusion.....	74
7. Perspectives .....	75
8. Abstract .....	77
9. Zusammenfassung .....	79
10. References .....	81
11 Appendix .....	91
Curriculum vitae.....	95

## List of figures

Fig. 1. A reconstruction of the evolution of primate CYP3A loci. ....	3
Fig. 2. Plots of sequence identity between human <i>CYP3A4</i> (left) and <i>CYP3A5</i> (right), and all other available primate <i>CYP3A</i> promoter sequences. ....	5
Fig. 3. Drug metabolism by Phase I enzymes. ....	6
Fig. 4. CYP3A locus. ....	8
Fig. 5. Structure of nuclear receptors. Identified domains are shown.....	11
Fig. 6. The molecular mechanism of transcriptional regulation by PXR and CAR and the structure of nuclear receptor response elements.....	12
Fig. 7. Difference between homology-directed genome modification and illegitimate DNA integration.....	16
Fig. 8. PCR screening of CYP3A5-luc mice.....	34
Fig. 9. Bioluminescent images of basal CYP3A5-luc transgene activity <i>in vivo</i> .....	35
Fig. 10. The expression of the CYP3A5-luc transgene in different organs. ....	36
Fig. 11. Determination of the CYP3A5-luc transgene activity along the small intestine. ....	37
Fig. 12. The dose- and sex- effect on the PCN induction of the CYP3A5-luc transgene activity in the duodenum (A) and kidney (B). ....	38
Fig. 13. The time- and sex-effect on the induction of the CYP3A5-luc transgene activity in the duodenum. ....	39
Fig. 14. The effect of the PCN on the CYP3A5-luc transgene induction in different parts of the small intestine. ....	40
Fig. 15. Induction conferred by <i>CYP3A5</i> promoter with serial of deletions.....	42
Fig. 16. The activities of proximal <i>CYP3A4</i> and <i>CYP3A5</i> promoters in kidney-derived MDCK.2 and in small intestine-derived LS174T cells.....	43
Fig. 17. Sequence identity and distribution of regulatory elements in the proximal promoters of human <i>CYP3A4</i> and <i>CYP3A5</i> . ....	44
Fig. 18. The effect of the <i>CYP3A4</i> -derived 57 bp region on the activities of the proximal <i>CYP3A4</i> and <i>CYP3A5</i> promoters in MDCK.2 cells. ....	45

Fig. 19. Genomic and functional conservation of the 57 bp <i>CYP3A</i> promoter region in primates. ....	47
Fig. 20. Conservation of the regulatory elements in the 57 bp region. ....	49
Fig. 21. Mutational analysis of the NF1 and the E-box in <i>CYP3A4</i> and <i>CYP3A5-57ins</i> constructs in MDCK.2 cells. ....	50
Fig. 22. The determination of the YY1 expression in LS174T, MDCK.2 and HepG2 cells. ...	51
Fig. 23. Binding of YY1 to the 57 bp element of the <i>CYP3A4</i> promoter. ....	52
Fig. 24. Mutational analysis of the <i>CYP3A4</i> -derived YY1 binding site in the <i>CYP3A5-57ins</i> construct. ....	53
Fig. 25. The effect of YY1 overexpression in LS174T and MDCK.2 cells.....	54
Fig. 26. Structure of the YY1 transcription factor. Functional domains are shown. ....	55
Fig. 27. The effect of the wild-type and mutated YY1 proteins on the <i>CYP3A4</i> -driven luciferase construct.....	56
Fig. 28. Mutational analysis of the YY1 binding site within the human <i>CYP3A4</i> promoter...	57
Fig. 29. The effect of PXR overexpression on the <i>XREM-CYP3A4</i> - and <i>XREM-CYP3A5-57ins</i> -driven luciferase activity. ....	59
Fig. 30. Functional analysis of the NF1 binding site within the wild-type <i>CYP3A4</i> construct. ....	62
Fig. 31. Models for the differential transcriptional regulation of <i>CYP3A4</i> and <i>CYP3A5</i> . ....	72

## List of tables

Table 1: Nuclear receptors involved in the transcriptional regulation of <i>CYP3As</i> gene.....	13
Table 2: Primers used for cloning of the 370 bp, 990 bp, 1.35 kb, 2.0 kb and 6.2 kb <i>CYP3A5</i> proximal promoter constructs.....	24
Table 3: Primers used for insertions and deletions of the 370 bp <i>CYP3A5</i> (1-4) proximal promoter construct and of the 374 bp <i>CYP3A4</i> (5-8) promoter construct. ....	24
Table 4: Primers sequences used for site-directed mutagenesis of nuclear factor binding sites. ....	25
Table 5: Primers used for RT-PCR quantification of YY1 (1-2), NF1 (3-4) and internal standard 18SRNA (5-6). And for the EMSA analysis, IRDye-800 labeled YY1 <i>CYP3A4</i> -derived probe (7-8) and YY1 positive control (9-10). ....	25



## List of abbreviations

abbreviation	Explanation
AF-1/2	Transactivation region 1 or 2
APS	Ammonium persulfate
AR	Androgen receptor
BAC	Bacterial artificial chromosome
BSA	Bovine serum albumine
BTE	Basic transcription element
C/EBP	CCAAT/enhancer binding protein
CAR	Constitutive androstane receptor
CLEM	Constitutive liver enhancer module
CMV	Cytomegalovirus
COUP-TF	Chicken ovalbumin upstream promoter-transcription factor
CYP	Cytochrome P450
CYP3A5-luc	Transgenic CYP3A5-luciferase
C57BL/6N	C57 black 6 mouse
DBD	DNA-binding domain
DEHAS	Dehydroepiandrosterone 3-sulfate
DMEM	Dulbecco's Modified Eagle Medium
DMSO	Dimethylsulfoxid
DNA	Deoxyribonucleic acid
DR	Direct repeat
DTT	Dithiothreitol
EDTA	Ethylenediamine tetraacetic acid
EGTA	Ethylene glycol tetraacetic acid
EMSA	Electrophoretic mobility shift assay
ER	Everted repeat
ER	Estrogen receptor
ERR	Estrogen related receptor
Fw	Forward
GA	Glycine and alanine rich region
GAPDH	Glyceraldehyde-3-phosphate dehydrogenase
GH	Growth hormone
GR	Glucocorticoid receptor
GRE	Glucocorticoid receptor element
HAT	Histone acetylase
HDAC	Histone deacylase
HEPES	(4-(2-hydroxyethyl)-1-piperazineethanesulfonic acid)
HepG2	Human hepatocarcinoma cells

Continued ...

HNF3 $\beta$	Hepatocyte nuclear factor 3 $\beta$
HNF4- $\alpha$	Hepatocyte nuclear factor 4 $\alpha$
IGEPAL	Octylphenoxypolyethoxyethanol
i.p.	Intraperitoneal
IL-6	Interleukine-6
IR	Inverted repeat
LB	Luria-Bertani
LBD	Ligand-binding domain
LIP	C/EBP $\beta$ -liver inhibitory protein
LS174T	Human colon carcinoma cells
MDCK.2	Madin-Darby Canine Kidney Cells type 2
mRNA	Messenger ribonucleic acid
NADPH	Nicotinamide adenine dinucleotide phosphate
NF1	Nuclear factor 1
NF-K $\beta$	Nuclear factor K $\beta$
NF-Y	Nuclear factor Y
NR	Nuclear receptor
PAGE	Polyacrylamide gel electrophoresis
PB	Phenobarbital
PBS	Phosphate-buffered saline
PCN	Pregnenolone 16 $\alpha$ -carbonitrile
Poly (dI-dC)	Poly (deoxyinosinic-deoxycytidylic acid)
PPAR	peroxisome proliferator-activated receptor
PR	Progesterone receptor
PXR	Pregnane X receptor
RAR	Retinoic acid receptor
RNA	Ribonucleic acid
RT-PCR	Reverse transcription polymerase chain reaction
RU486	Mifepristone
Rv	Reverse
RXR	Retinoid X receptor
SDS	Sodium dodecyl sulfate
SEM	Standard error of the mean
SHP	Small/short heterodimer partner
SMRT	Silencing mediator for retinoid and thyroid hormone receptors
SNP	Single nucleotide polymorphism
SP	Spacer
SP1	Specific protein 1
SP3	Specific protein 3

---

Continued ...

TBE	Tris-Boric acid EDTA
TBP	Transcription binding protein
TCPOBOP	1,4-bis-[2, -(3,5-dichloropyridyloxy)]benzene
TE	Tris-EDTA
TEMED	N, N, N', N' - Tetramethylethylenediamine
TG	Transgenic mice
TR	Thyroid hormone receptor
Tris	Tris (hydroxymethyl)aminomethane
VDR	Vitamine D receptor
WT	Wild-type
XREM	xenobiotic-responsive enhancer module
YY1	Yin Yang 1

---

# 1. Introduction

## 1.1 The Cytochrome P450 superfamily

### 1.1.1 General considerations

Exogenous lipophilic compounds penetrate easily into the lipid membranes of living cells, which may result in toxicity. Therefore, cellular survival requires detoxifying systems. Prokaryotes export principally toxic compound via their membrane transport system directly into the surrounding environment (Nikaido 2001), while multi-cellular organisms are mostly equipped with detoxification system, which, among others, includes a large variety of Cytochrome P450 (CYP) detoxifying enzymes. CYP enzymes are a superfamily of hemoproteins capable of converting the nonpolar lipophilic compounds into more polar, mostly inactive or non-toxic metabolites that can be readily eliminated by the kidney or other organs. Thus, CYPs are fundamental for the viability of most animal life forms.

The experimental discovery of CYP dates back to the year 1955, when an enzyme system capable of oxidizing xenobiotic compounds was identified in the endoplasmic reticulum of the liver (Axelrod 1955). Three years later, a carbon monoxide (CO)-binding pigment was detected in liver microsomes in two independent studies (Garfinkel 1958; Klingenberg 1958). This protein was characterized by an absorption maximum at 450 nm and demonstrated to be a hemoprotein of b-type class (Omura and Sato 1964; Omura and Sato 1964). It was named CYP450 after the distinguishing strong feature in its absorption spectrum. Eukaryotic CYP enzymes are membrane-bound. They are mainly localized at the cytosolic side of the endoplasmic reticulum and inner membranes of mitochondria (Werck-Reichhart and Feyereisen 2000). Mitochondrial CYPs are involved in steroid-biosynthesis reactions and do not metabolize foreign compounds.

### 1.1.2 Classification

The CYP enzymes are classified into families and subfamilies based on their amino acid sequence similarity. The enzymes are designated with the root CYP followed by an arabic numeral indicating family, a capital letter indicating the subfamily and other numerals for the individual enzymes. Members of the same family share more than 40% identity of the amino acid level sequence identity (e.g., CYP3) and 55% or more greater for members of the same subfamily (e.g., CYP3A; (Nelson, Koymans et al. 1996). All information regarding the CYP sequences and corresponding classifications are available at the homepage of the Cytochrome P450 committee (<http://drnelson.utmem.edu/CytochromeP450.html>). Human genome contains 57 different CYP genes and 58 pseudogenes (Nelson, Zeldin et al. 2004).

### 1.1.3 Function

CYP enzymes metabolize a large array of compounds, including endobiotics (such as e.g., bile acids, steroid hormones, fatty acids, prostaglandins, leukotrienes and biogenic amines) and xenobiotics (such as e.g., drugs, carcinogens, and environmental pollutants) (Shimada, Yamazaki et al. 1994; Li, Kaminski et al. 1995). The metabolism of the latter class of substances are mainly carried out by CYP1 and 2, and particularly CYP3 enzymes. Families CYP1, CYP2 and CYP3 play a central role in xenobiotics metabolism. Despite the extreme divergence in their primary sequences, the majority of CYP proteins contain a similar conserved structural fold (Graham and Peterson 1999), which generally consists of acidic residues in the N-terminus and basic residues in the C-terminus. The substrate-binding sites were identified in the vicinity of a pocket containing a molecular oxygen-associated heme moiety (Werck-Reichhart and Feyereisen 2000). The classical reaction catalyzed by CYP is monooxygenation, where one atom of oxygen is incorporated into a substrate, whereas the other oxygen atom is reduced to water by electron from  $\text{NADPH}+\text{H}^+$ . It thus introduces an OH-group into the substrates, which is the major function of phase I drug metabolism. The resulting products further undergo additional phase II reactions (e.g., glucuronidation, sulfation, acetylation and methylation), after which they are eliminated from bodies by phase III efflux transporters (Xu, Li et al. 2005).

## 1.2 Human CYP3A family

### 1.2.1 The evolutionary history of the CYP3 gene family

The evolutionary history of *CYP3* gene family has been progressively unveiled by several phylogenetic and comparative genomic analyses. Earlier studies showed that the ancestral vertebrates had a single *CYP3A* gene that underwent independent duplications in bony fishes, reptiles and mammals (McArthur, Hegelund et al. 2003). It was shown later that there has been a gene duplication in an Amniota ancestor producing *CYP3A37*- and *CYP3A80*-like genes, while both copies were preserved in *Sauropsida* (reptiles and aves). The *CYP3A80*-like was lost in an Eutheria ancestor and all Eutheria *CYP3A* genes are the descendants of the *CYP3A37* ancestral gene (Qiu, Taudien et al. 2008). In vertebrates, the highest CYP3 diversity has been achieved in fish species as evidenced by CYP3B, CYP3C and CYP3D subfamilies present only in this group of species (Nelson 2009). These fish-specific CYP3 subfamilies are the results of the fish-specific whole-genome duplication and asymmetrical accelerated evolution following gene duplication (Yan and Cai 2010). Valuable information for the redrawing of the *CYP3As* gene evolutionary

history have been gained from analyses of distantly unrelated species. The increased availability of several primate genome sequences has further illuminated the evolution of human CYP3As.

### 1.2.2 The evolution of primate CYP3A genes

Phylogenetic and comparative genomic analyses of primate CYP3A showed that gene duplications have been the major mechanism of CYP3A evolution in primates and that all extant primate CYP3A genes were originated from a single CYP3A progenitor in the primate ancestor (Fig. 1).

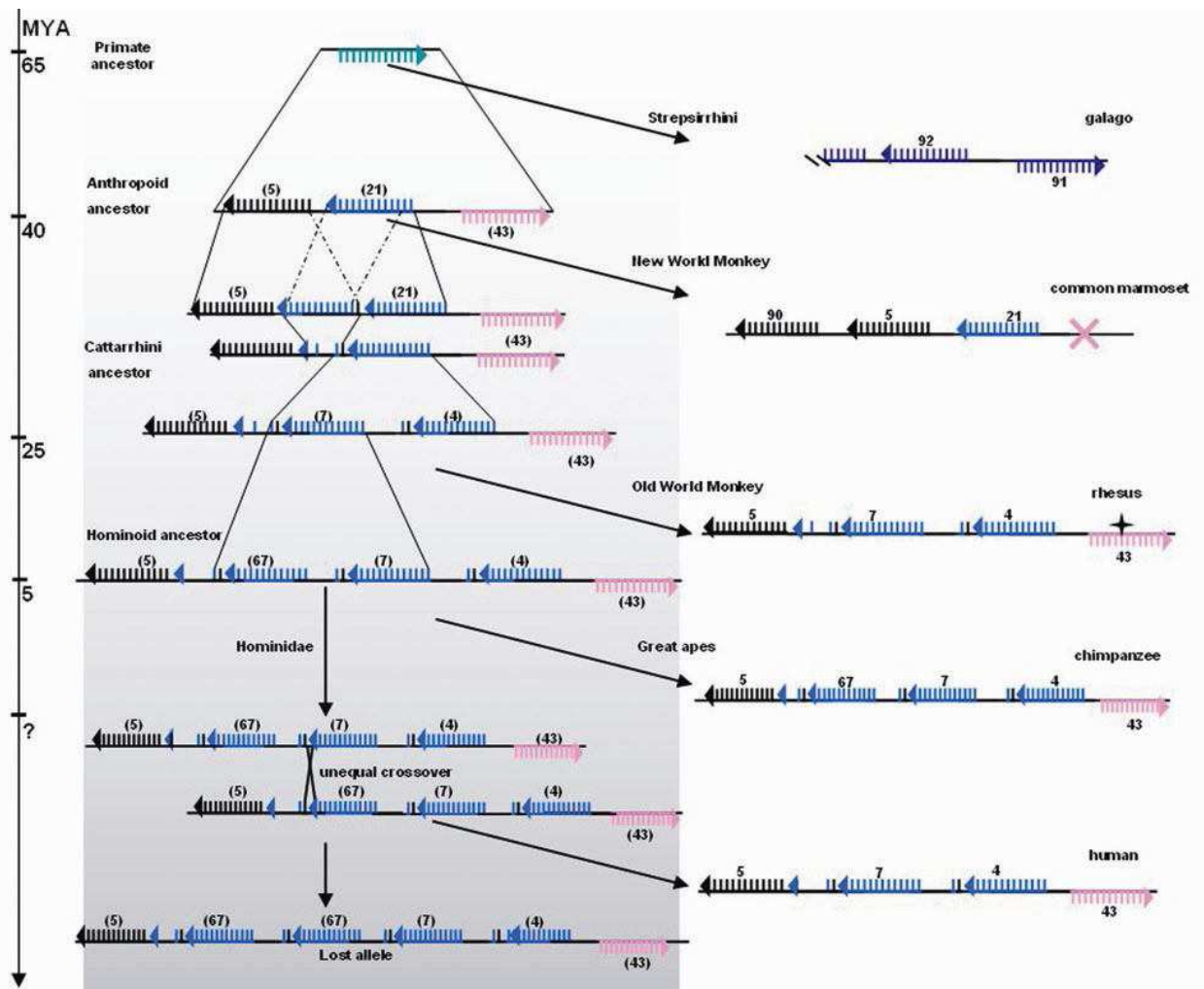


**Fig. 1. A reconstruction of the evolution of primate CYP3A loci.** Triangles represent exon 13 in functional CYP3A genes or in pseudogenes. Cross represents gene loss in common marmoset. Star represents pseudogenization of rhesus CYP3A43. Numbers indicate the gene identity (e.g. 5=CYP3A5). The left part of the figure depicts the ancestral loci, including the apparently lost 5-67-67-7-4-43 allele resulting from the unequal crossover in the human lineage. CYP3A loci in selected contemporary primates are shown on the right. Time points of divergence are shown by the y-axis on the left (MYA, million years ago). From (Qiu, Taudien et al. 2008)).

The gene duplications took place independently along lineages leading to *Strepsirrhini* and *Platyrrhini* after their divergence. In the latter lineage, two rounds of gene duplication giving rise to *CYP3A43*, 5 and 21 took place in an Anthropoid ancestor. While further duplication of *CYP3A5* gene occurred in New World monkey (marmoset), duplication of *CYP3A21* gene led to *CYP3A4* and 7 in *Catarrhini* ancestor (Qiu, Taudien et al. 2008). *CYP3A7* were further duplicated in Hominoid ancestor resulting in *CYP3A67* (Williams, Schouest et al. 2007). and 7 found in the extant chimpanzee genome (Qiu, Taudien et al. 2008). In human, however, the *CYP3A67* gene was lost during the course of Hominidae evolution. In addition to *CYP3A67*, *CYP3A43* also underwent gene losses in New World monkey and pseudogenization in Old World monkey (e.g., rhesus). In the primate *CYP3A* phylogeny, strong positive selection were detected along the lineage leading to Hominoid *CYP3A7* and to human *CYP3A4* (Qiu, Taudien et al. 2008; Chen, Wang et al. 2009). While the functional significance of the former one remains to be investigated, the latter positive selection event has led to higher activity toward lithocholic acid in human *CYP3A4* compared to that of chimpanzee, which might be implicated in the higher consumption of dietary sterols, e.g., with meat (Kumar, Qiu et al. 2009). It is evidenced that the human *CYP3A* locus was shaped by an extensive process of gene duplication of the ancestral *CYP3A* gene, conversion and deletion.

### 1.2.3 Structure of human *CYP3A* genes

The human *CYP3A* cluster spans a 231 kb region on chromosome 7q22 and contains four functional genes and two pseudogenes. As depicted in Fig. 4, these genes are arranged tandemly in the order *CYP3A5*, *CYP3A5P1*, *CYP3A7*, *CYP3A5P2*, *CYP3A4* and *CYP3A43*, from the centromere to the telomere (Finta and Zaphiropoulos 2000; Gellner, Eiselt et al. 2001). *CYP3A43* is in a head-to-head orientation to all the other *CYP3A* genes, which may have conferred higher genomic stability of the *CYP3A* locus (Graham 1995). Sequence conservation along the 14 kb of primate *CYP3A* upstream promoters is high among ortholog promoter from different species (e.g., human, chimpanzee and rhesus *CYP3A4*). Defining the *CYP3A* gene duplication boundaries indicated that the *CYP3A* locus arose through duplications of an 40-55 kb ancestral *CYP3A* gene cassette. Each intact gene is composed of 13 exons and encodes a protein consisting of 503 amino acids (Finta and Zaphiropoulos 2000). Human *CYP3A5P1* and *CYP3A5P2* pseudogenes arose from complex events of recombination between *CYP3A7* and *CYP3A5* (Finta and Zaphiropoulos 2000). The sequence conservation of the promoter across all primate *CYP3A* is restricted to the proximal 850-bp region. Because of their recent origin, human *CYP3A4* and *CYP3A7* share high sequence identity (~90%) along the proximal ~8 kb promoters. In spite of this, human *CYP3A7* promoters lacks the distal promoter, including the CLEM, found in *CYP3A4* and Old World monkey *CYP3A7* genes. This distal promoter was lost in the common ancestor of human and chimpanzee. Human

*CYP3A5* promoter shares significant sequence identity in the proximal 6.2 kb region with those of rhesus and chimpanzee, and in the proximal 2 kb region with the *CYP3A5*-related genes in New World monkey. Compared to *CYP3A5* in rhesus, a ~5.5 kb repeat element was inserted into the human and chimpanzee *CYP3A5* about 6 kb upstream of the first coding exon (Qiu, Mathas et al. 2010). Neither XREM nor CLEM is possessed by *CYP3A5* and its related genes in primates (Fig. 2). The resulting complex structure of CYP3As may be in part the reason that positions CYP3As as the most clinically important CYP family.

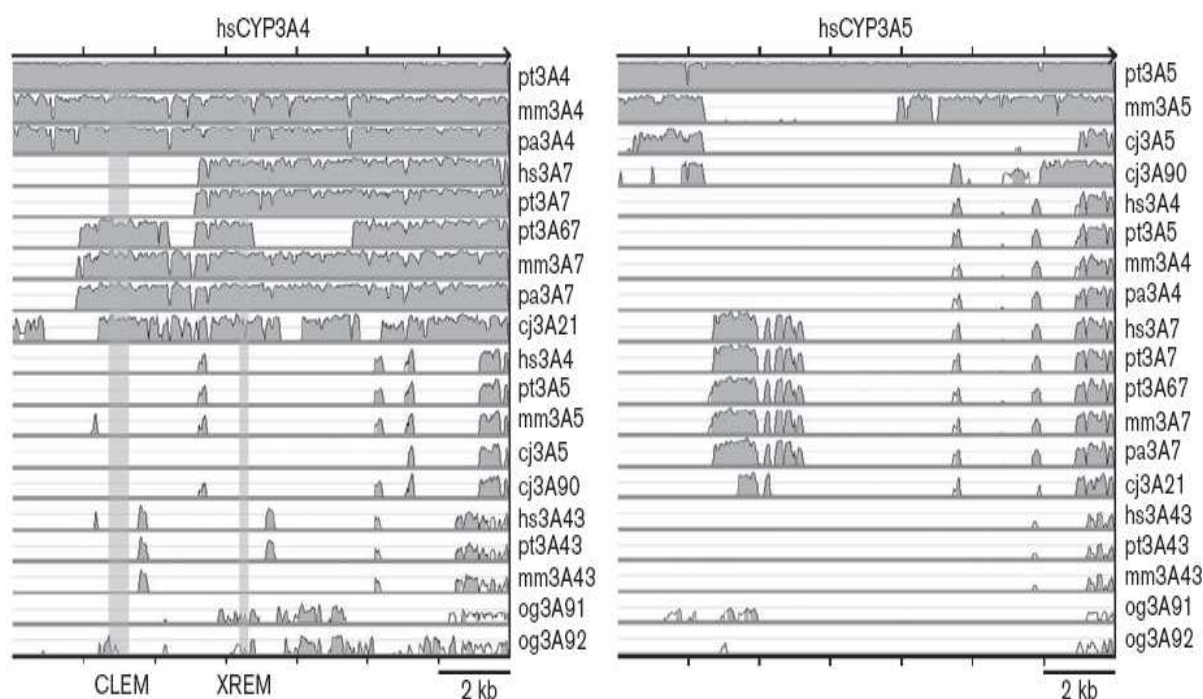


**Fig. 2. Plots of sequence identity between human *CYP3A4* (left) and *CYP3A5* (right), and all other available primate *CYP3A* promoter sequences.** The approximate locations of the CLEM (form -11.4 kb to -10.5 kb) (Matsumura et al. 2004).and XREM (form -7.8 kb to -7.2 kb) (Goodwin, Hodgson et al. 1999) modules are indicated as vertical bars. Species abbreviations: hs (human, Homo sapiens), pt (chimpanzee, Pan troglodytes), mm (rhesus, Macaca mulatta), pa (baboon, Papio anubis), cj (marmoset, Callithrix jacchus), og (galago, Otolemur garnettii). ‘Cyp’ has been removed from gene names to improve legibility (from (Qiu, Mathas et al. 2010)).

#### 1.2.4 CYP3A substrate spectrum

CYP3A enzymes metabolize about 50% of clinically used drugs (Fig. 3; (Evans and Relling 1999) and various endogenous compounds such as bile acids, steroid hormones, fatty acids, prostaglandins, leukotrienes and biogenic amines (Shimada, Yamazaki et al. 1994). In particular, CYP3A4 has the broadest catalytic spectrum. The active sites of CYP3A4 are capable of



accommodating a wide diversity of substrates (Guengerich 1999) ranging from molecules as small as benzimidazoles to substances as large as rifampicin. Moreover, the active site of CYP3A4 is able to accommodate more than one molecule of either the same or different compounds. It often leads to adverse influence on the pharmacokinetics among different drugs causing homotropic or heterotropic cooperativity (Harlow and Halpert 1998). The ligand promiscuity of CYP3A4 is the reason for its frequent involvement in clinically relevant drug-drug interactions. On the other hand, CYP3A4 can be also inhibited by a number of drugs and exogenous compounds. Selective inhibitors of CYP3A4 include azole antifungal (e.g., ketoconazole), macrolide antibiotics (e.g., erythromycin), protease inhibitors (e.g., saquinavir) and constituents of grape fruit juice such as the furanocoumarine bergamottin (Thummel and Wilkinson 1998; Evans 2000). Many of these compounds form tightly-bound or irreversible complexes with the CYP3A4 enzyme (Thummel and Wilkinson 1998) and its inhibition by affecting drug safety is in general clinically important. CYP3A4 induction is often caused by potent inducers including e.g., rifampicin, anticonvulsants such as carbamazepine, and hyperforin, a constituent of the herbal antidepressant St. John's wort (Moore, Goodwin et al. 2000; Pelkonen, Myllynen et al. 2001).

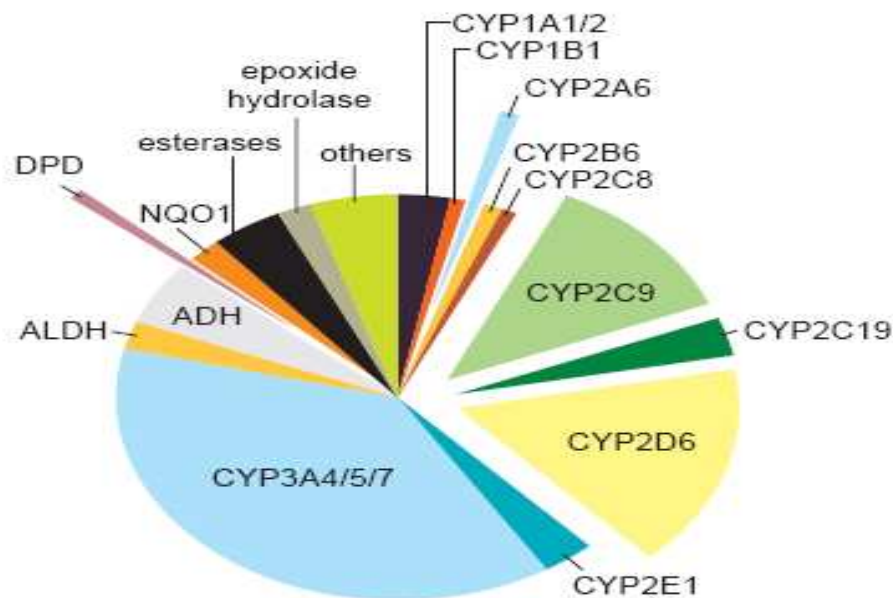


**Fig. 3. Drug metabolism by Phase I enzymes.** The portion of drugs metabolized by each enzyme is represented by the relative size of each section of the chart. (ADH, alcohol dehydrogenase; ALDH, aldehyde dehydrogenase; CYP, cytochrome P450; DPD, dihydropyrimidine dehydrogenase; NQO1, NADPH: quinone oxidoreductase (from (Evans and Relling 1999)).

The large majority of compounds metabolized by CYP3A4 can be also metabolized by CYP3A5 and CYP3A7, albeit with a weaker catalytic activity (Williams, Ring et al. 2002). However, there are some exceptions. For example, CYP3A5 metabolizes drugs with narrow therapeutic index, such as tacrolimus, the alkylating agent ifosfamide and vincristine, with higher efficiency than CYP3A4 (Kamdem, Streit et al. 2005; McCune, Risler et al. 2005; Dennison, Jones et al. 2007; Coto and Tavira 2009). CYP3A7 catalyzes the 16 $\alpha$ -hydroxylation of dehydroepiandrosterone 3-sulfate (DEHAs) and the retinoic acid metabolism more efficiently than either CYP3A4 or CYP3A5 (Kitada, Kamataki et al. 1987; Marill, Cresteil et al. 2000). CYP3A5 and CYP3A7 are less inhibited by many compounds that inhibit CYP3A4. Despite their overlapping substrate spectrum, CYP3As members are not evenly distributed in several organs. This means that their distribution may be determined by their polymorphism or/and by interaction with transcription factors present in the surrounding environment.

### **1.2.5 CYP3As genetic polymorphisms and variability of expression**

Polymorphisms have been identified throughout the *CYP3A* genes including exons, introns, upstream of the transcription start site and untranslated regions (UTRs). The major CYP3As SNPs are depicted in Fig. 4. CYP3A4 expression varies from 10- to 100-fold (Westlind, Lofberg et al. 1999; Westlind-Johnsson, Malmebo et al. 2003) with a unimodal distribution among individuals. The majority (60-90%) of variability in CYP3A4 expression and activity is supposed to have originated from genetic factors (Ozdemir, Kalow et al. 2000). Among CYP3A4 variants, CYP3A4\*1B may be involved in the progression and propensity of prostate cancer (Rebbeck, Jaffe et al. 1998; Paris, Kupelian et al. 1999). CYP3A4\*1B variant is located in the 5'-flanking region of CYP3A4, which is characterized by the A-392G transition in the putative nifedipine response element (NFSE; (Rebbeck, Jaffe et al. 1998). CYP3A4\*1B variant frequency varies among different ethnic groups ranging from 0% in Chinese, 2-9.6% in Caucasians to 35-67% in African Americans (Ball, Scatina et al. 1999).

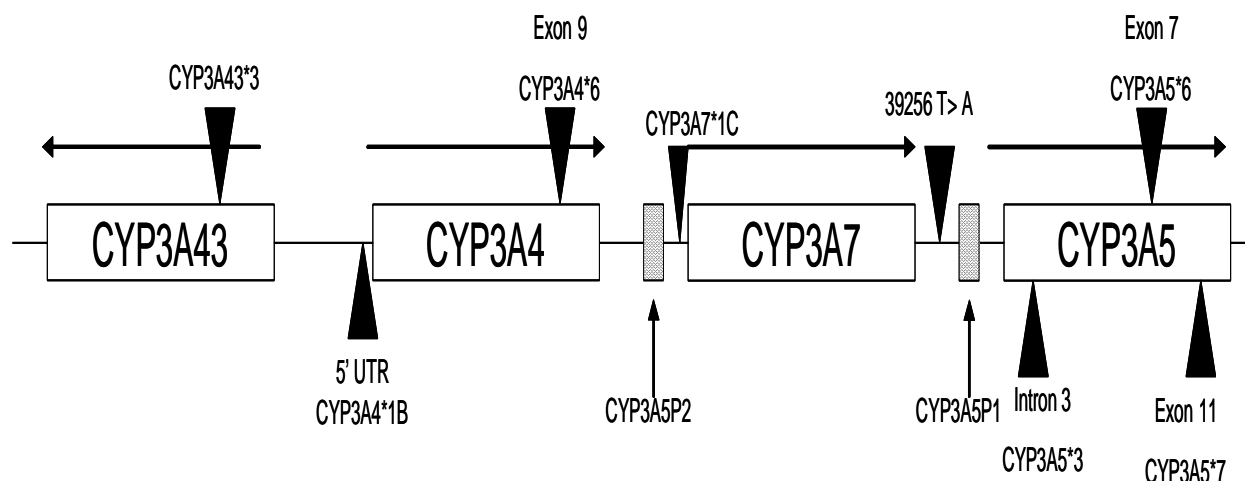


**Fig. 4. CYP3A locus.** White and grey rectangles represent complete and incomplete CYP3A genes, respectively. The horizontal arrows above each gene denote its orientation. Black triangles indicated the approximate locations of some of the important SNPs (modified from (Perera 2010)).

Comparison between CYP3A7\*1A and the wild-type genes has led to the identification of two functional major variants (\*1B and \*1C). The CYP3A7\*1B variant, a C-211T transition, affects the hepatic but not the intestinal CYP3A7 expression (Burk, Tegude et al. 2002), whereas the CYP3A7\*1C variant is associated with the expression of CYP3A7 in adults. CYP3A7\*1C is caused by the replacement of a 60 bp fragment encompassing the proximal ER6 element in CYP3A7 promoter by the corresponding part from the CYP3A4 gene (Kuehl, Zhang et al. 2001) and was reported in 3% of Caucasians (Kuehl, Zhang et al. 2001; Burk, Tegude et al. 2002) and 6% of African Americans (Kuehl, Zhang et al. 2001). Regarding CYP3A43, the missense variant CYP3A43\*3 has been associated with increased risk of prostate cancer (Rebbeck, Rennert et al. 2008).

The clinical implications for CYP3A5 polymorphic variants are more robust and unequivocal than those for CYP3A4, CYP3A7 and CYP3A43. CYP3A5 activity displays a bimodal distribution and high interindividual variation (Haehner, Gorski et al. 1996; Kuehl, Zhang et al. 2001; Koch, Weil et al. 2002). The most frequent SNP in the CYP3A5 gene is CYP3A5\*3, a A6986G transition within intron 3 (Kuehl, Zhang et al. 2001). This mutation results in a cryptic splice site leading to transcripts with premature stop codons at the junction between exons 3 and 4. The resulting mRNAs are rapidly degraded via a nonsense-mediated decay mechanism (Busi and Cresteil 2005). Another CYP3A5 variant is CYP3A5\*1, which is present in approximately 10% of Europeans, 30% of Asians, and 70% of Africans (Hustert, Haberl et al. 2001; Lin, Dowling et al. 2002;

Westlind-Johnsson, Malmebo et al. 2003). In addition, there are two other African-specific “null” CYP3A5 variants (\*6 and \*7). The CYP3A5\*6 variant results from a G14685A transition in exon 7 (Kuehl, Zhang et al. 2001), whereas the CYP3A5\*7 variant originates from a base insertion in exon 11 (27131-32 insT). Both variants result in a frameshift and truncated protein (Hustert, Haberl et al. 2001). Finally, there are some other CYP3A5 SNPs variants existing at low frequencies and thus less likely to play a major role in the CYP3A5 variable expression and activity. The effect of polymorphism on CYP3As expression and activity is generally moderate, with the exception of CYP3A5.

### 1.2.6 CYP3A genes expression

CYP3A family is predominantly expressed in the liver and the small intestine, accounting for 30% and 70% of total expressed P450 in these two organs. In particular, CYP3A4 alone accounts for most of the CYP3A protein in the adult liver and small intestine (Kolars, Schmiedlin-Ren et al. 1992; Kolars, Lown et al. 1994; Shimada, Yamazaki et al. 1994; Paine, Hart et al. 2006). The CYP3A expression follows a zonal distribution in the liver with the highest expression detected in perivenous hepatocytes (Burk and Wojnowski 2004). This expression zonation is partly due to the relative density of the smooth endoplasmic reticulum in the perivenous region and may be affected by hormones (Oinonen and Lindros 1998). Indeed, a sexually dimorphic expression of CYP3A4 has been reported in the liver of humanized transgenic mice. This expression is dictated partly by the differential growth hormone secretion (Cheung, Yu et al. 2006). While the expression of CYP3A4 is mostly undetectable in foetal livers, it increases rapidly after birth and replaces CYP3A7 in the adult liver (Lacroix, Sonnier et al. 1997; Tateishi, Nakura et al. 1997). CYP3A7 accounts for 30-50% of total CYP3A expression in foetal liver (Daly 2006) and plays a key role in the foeto-protection against the adverse effects of steroid precursors, such as the dehydroepiandrosterone-sulfate (DEHAs) during pregnancy (Lamba, Lin et al. 2002; Miller, Cai et al. 2004; Wojnowski and Kamdem 2006). In adults, CYP3A7 expression in the liver and small intestine is only restricted to the carriers of CYP3A7\*C allele (Burk, Tegude et al. 2002; Sim, Edwards et al. 2005). In addition, CYP3A7 expression has also been detected in the endometrium, placenta, adrenal gland and prostate tissues (Schuetz, Kauma et al. 1993; Koch, Weil et al. 2002; Nishimura, Naito et al. 2004). In the small intestine, CYP3A is detectable in enterocytes. Hence, CYP3A4 and CYP3A5 have their highest expression in duodenum and jejunum than tend to decrease towards the ileum (Thorn, Finnstrom et al. 2005; Berggren, Gall et al. 2007). The CYP3A5 is the universal extrahepato-intestinal CYP3A isoform.

CYP3A5 is the predominant CYP3A isoform in kidney (Koch, Weil et al. 2002; Givens, Lin et al. 2003). The renal expression of CYP3A5 is bimodal (Haehner, Gorski et al. 1996) and regiospecific, and is detected in the proximal tubule, distal tubule and the collecting duct (Murray, McFadyen et al. 1999; Joy, Hogan et al. 2007). The renal CYP3A5 is suggested to have important biological functions. For example, the renal CYP3A5 expression is thought to be associated with salt-dependent hypertension (Ho, Pinto et al. 2005; Kreutz, Zuurman et al. 2005). In support of this association, CYP3A5 expressing kidney may enhance the mineralocorticoid effect of 6 $\beta$ -hydroxylated glucocorticoids (Clore, Schoolwerth et al. 1992; Matsuzaki, Arai et al. 1995). Alternatively, renal CYP3A5 activity could regulate the glucocorticoid occupancy of mineralocorticoid receptors (Morris, Latif et al. 1998). In addition, CYP3A5 is expressed more than CYP3A4 in many other extrahepatic tissues with highest expression found in bronchial and alveolar epithelial cells, bronchial glands and alveolar macrophages tract (Anttila, Hukkanen et al. 1997; Ding and Kaminsky 2003; Raunio, Hakkola et al. 2005). CYP3A5 expression has been reported in the prostate (Yamakoshi, Kishimoto et al. 1999; Koch, Weil et al. 2002; Moilanen, Hakkola et al. 2007) and in keratinocytes (Yengi, Xiang et al. 2003; Smith, Ibbotson et al. 2006; Oesch, Fabian et al. 2007). CYP3A43 expression was detected in a variety of tissues, especially in steroidogenic organs such as prostate and testis (Domanski, Finta et al. 2001; Gellner, Eiselt et al. 2001). However, the *in vivo* expression of CYP3A43 protein and its function is doubtful, because its transcripts are mostly aberrantly-spliced and have disrupted open reading frames (Gellner, Eiselt et al. 2001). Exhaustive attempts have failed to identify a unique master factor governing the tissue-specific expression of CYP3A members. The differential expression of CYP3As in several organs may be also bound to reflect the concerted and complex interplay between *trans*- and *cis*-acting factors. Besides basic transcription factors most of the *trans*-acting factors are nuclear receptors.

## **1.2.7 CYP3As regulation**

### **1.2.7.1 Transcription regulation of CYP3As**

#### **1.2.7.1.1 Nuclear receptor superfamily**

Nuclear receptors (NR) constitute a large family of proteins found in all classes of metazoans. They are involved in a diverse array of metabolic processes, such as those of steroids, retinoids and other lipophilic ligands, through modulating expression of their target genes (Gronemeyer and Laudet 1995; Mangelsdorf, Thummel et al. 1995). The sequencing of human genome has led to the identification of 48 NRs (Germain, Staels et al. 2006). Although nuclear receptors recognize structurally distinct ligands, they share a common structural organization (Fig. 5). The N-terminal region (A/B domain) consists of a ligand-independent active transactivation region (AF-1)

followed by a DNA-binding domain (DBD, C domain). The C-terminal region is comprised of a ligand-dependent active transactivation region (AF-2) and ligand-binding domain (LBD, E domain), which is connected to DBD via a hinge region (D domain; (Giguere 1999).

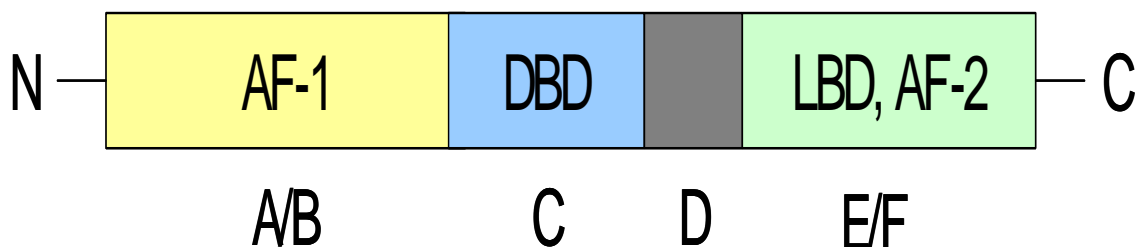


**Fig. 5. Structure of nuclear receptors. Identified domains are shown** (For the details refer to the text above).

The NRs can be broadly classified into six evolutionary sub-groups of unequal size based on their sequence alignment and phylogeny (Nuclear Receptor Nomenclature Committee (1999); (Escriva, Delaunay et al. 2000): The first group contains the receptors TRs, RARs, VDR (NR1I1), and PPARs, as well as orphan receptors such as CAR (NR1I3), PXR (NR1I2), LXRs, and others. Orphan receptors are NRs for which regulatory ligands are still unknown or may not exist (Laudet, Hanni et al. 1992; Chawla, Repa et al. 2001). The second group includes RXRs, COUP-TF, and HNF-4. The third group is that of the steroid receptors with ERs, GRs, PRs, and ARs as well as the ERRs. The fourth, fifth and sixth group comprise small number of nuclear receptors (Germain, Staels et al. 2006).

#### 1.2.7.1.2 Regulation of CYP3As by Nuclear receptors: PXR and CAR

Nuclear receptors orchestrate the process of gene transcription by recruiting a variety of coregulators to target promoters. Within the complexes, NR bind to the target DNA motif, response elements, either as monomers, homodimers or in many cases as heterodimers (Sonoda, Pei et al. 2008). Response elements are typically consist of two 6 bp half sites separated by spacer of various lengths. The sequences of the half sites are AG(G/T) TCA and two half sites form direct repeats (DR<sub>n</sub>), inverted repeats (Girnit, Webber et al. 2006) and everted repeats (ER<sub>n</sub>) by the corresponding relative orientations (Fig. 6B) (Honkakoski and Negishi 2000; Pavek and Dvorak 2008). While several nuclear receptors are involved in the transcriptional regulation of CYP3As (Table 1) CYP3As regulation is mainly regulated by pregnane X receptor (PXR; (Lehmann,

McKee et al. 1998) and constitutive androstane (CAR; (Honkakoski, Sueyoshi et al. 2003). CYP3As induction by xenobiotics is initiated by the activation of PXR and CAR upon the binding of activators, and the activated PXR or CAR heterodimerizes with the retinoid X receptor (RXR) which binds to xenobiotic response elements of the CYP3A promoter to drive transcription (Fig. 6B). (Goodwin, Hodgson et al. 1999; Tompkins and Wallace 2007).

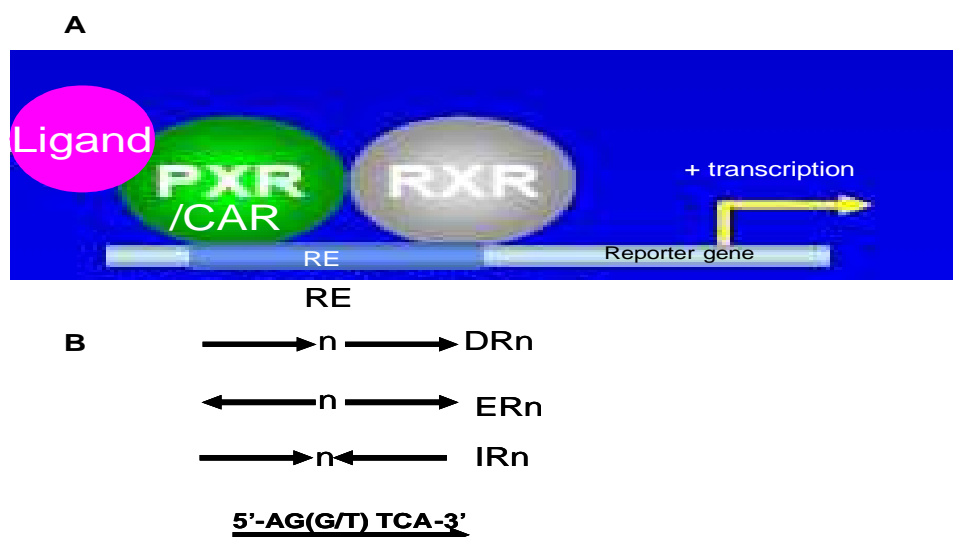


**Fig. 6. The molecular mechanism of transcriptional regulation by PXR and CAR and the structure of nuclear receptor response elements.** (A) Binding of the heterodimer PXR/RXR or CAR/RXR complex on the regulatory element on the promoter. (B) Nuclear receptor response elements DR; directed repeat, ER; everted repeat, IR; inverted repeat. n; number of nucleotides spaced between the two core elements.

Both CAR and PXR are expressed in the liver and intestine, the most important two organs for drug metabolism (Honkakoski, Sueyoshi et al. 2003; Lamba, Yasuda et al. 2004). In particular, PXR is a critical regulator of *CYP3A* gene expression and its activation is predictive of *CYP3A* induction (LeCluyse 2001). Moreover, the substrate spectrum of PXR, but not CAR, is incredibly large although the DNA binding recognitions of receptors are quite similar. PXR consists of five strands  $\beta$ -sheet with a replacement of the helix 2 by a H1-3 insert. The resulting flexible loop may therefore recognize and binds structurally variable ligands in multiple orientations at the same time (Moore, Moore et al. 2003). In contrast, the ligand binding domain of CAR lacks such a flexible loop and CAR display much narrower ligand spectrum. Determined by their LBD, PXR and CARs from different species exhibit species-specific induction of *CYP3A* gene expression (Reschly and Krasowski 2006). For example, rifampicin is the human PXR agonist, but murine PXR is activated by pregnenolone 16 $\alpha$ -carbonitrile (PCN) rather than rifampicin (Moore and Kliever

2000). Likewise, (1,4-bis-[2,-(3,5-dichloropyridyloxy)]benzene (TCPOBOP) is a murine CAR agonist (Baskin-Bey, Huang et al. 2006). It is worthy mentioning that similar to CAR and PXR, vitamin D receptor (VDR) also induces *CYP3A4* promoter (Pavek, Pospechova et al. 2010; Drocourt, Ourlin et al. 2002). However, *CYP3A* gene transcription relies not only on xenobiotic-activated nuclear receptors.

Table 1: Nuclear receptors involved in the transcriptional regulation of *CYP3As* gene (Adapted from (Tirona and Kim 2005)).

Nuclear receptor	Genomic location	Response element
Pregnane X receptor (PXR)	NR1I2; 3q13-q21	DR3, DR4, ER6 and ER8
constitutive androstane (CAR)	NR1I3; 1q23.1	DR3, DR4 and ER6
Vitamine D receptor (VDR)	NR1I1; 12q12-q14	DR3, ER6 and IR0
Hepatocyte nuclear factor 4 $\alpha$ (HNF4 $\alpha$ )	20q12-q13.1	DR1
Glucocorticoid receptor (GR)	NR3C1 5q31	GRE
Liver X receptor (LXR)	NR1H3 11p11.2	DR4
Small heterodimer partner 1(SHP-1)	NR0B2 1p36.1	Not available
Hepatocyte nuclear factor 1 $\alpha$ (HNF1 $\alpha$ )	12q24.2	TTGGC(N5)GCCAA (Gronostajski 2000)

### 1.2.7.1.3 Regulation of CYP3As by other nuclear factors

The promoters of the *CYP3A* genes contain binding sites for transcription binding sites (Hashimoto, Toide et al. 1993; Iwano, Saito et al. 2001; Saito, Takahashi et al. 2001; Matsumura, Saito et al. 2004). The most prominent is the far distal enhancer module referred to as CLEM, which mediates the constitutive *CYP3A4* expression in the liver. It appears that the constitutive expression of *CYP3A4* relies on the cooperative trans-activation through direct interactions among multiple liver-enriched factors, such as HNF1- $\alpha$ , HNF4- $\alpha$ , USF1 and AP-1 (Matsumura, Saito et al. 2004). Other factors essential for the trans-activation of the basal expression of *CYP3A4* include HNF1, HNF3- $\beta$ , HNF3- $\gamma$ , HNF4- $\alpha$  and CCAAT/enhancer binding protein (C/EBP- $\alpha$  and - $\beta$ ) (Jover, Bort et al. 2001; Martinez-Jimenez, Gomez-Lechon et al. 2005), which bind to their respective target elements within the *CYP3A4* proximal promoter.



Besides induction, repression of CYP3A4 has been proposed to be a factor underlying the unusual variability in CYP3A4 expression. For example, Johnson and colleagues (Johnson, Li et al. 2006) have demonstrated that SMRT co-repressor factor can repress CYP3A4 expression by occupying its most effective activator, e.g., PXR. Similarly, SHP-1 repressor factor also competes with HNF4- $\alpha$  and SRC-1 for the PXR-binding and thereby represses CYP3A4 expression (Li and Chiang 2006). Furthermore, a study also indicated that the decreased of CYP3A4 expression in inflammation was caused by competition between PXR and NF- $\kappa$ B for RXR (Gu, Ke et al. 2006), and by IL-6 induced repressive C/EBP $\beta$ -liver inhibitory protein (LIP; (Jover, Bort et al. 2002). CYP3A expression can be also repressed by antiglucocorticoids such as RU486 (Pariante, Pearce et al. 2001). Regardless of their chemical structures, antiglucocorticoids exert their effects by preventing the dissociation of the heterooligomeric complex of glucocorticoid receptor and a 90 kDa non-steroid-binding protein (Lefebvre, Danze et al. 1988). Paradoxically, CYP3A can be also induced by antiglucocorticoids such as PCN. Though *CYP3A4* and *CYP3A5* gene expression are both regulated by GRs (Pascussi, Drocourt et al. 2000; Hukkanen, Vaisanen et al. 2003), CYP3A4 up-regulation by GRs is not caused by a direct binding of GR to its regulatory motifs in its promoter, but via upregulation of both PXR and CAR, which in turn leads to CYP3A4 induction (Pascussi, Drocourt et al. 2001). Besides their secondary regulatory effects via nuclear receptors, basic transcription factors also play critical roles in fine-tuning the CYP3A transcription activity. Indeed, CYP3A4 and CYP3A7 expression is regulated by cooperative interaction of many ubiquitous basic transcription factors, such as, Sp1, Sp3 HNF3 $\beta$ , NF1 and upstream stimulatory factor 1. However, unlike the CYP3A7 promoter, the binding site of HNF3 $\beta$  does not overlap with the NF1 binding site in CYP3A4 promoter (Saito, Takahashi et al. 2001) and it was postulated that the increase of NF1 post-natally may underly the postnatal expression of CYP3A4. Additionally, a binding site for YY1 factor was described in *CYP3A4* promoter, though without functional verification (Saito, Takahashi et al. 2001). The basal expression of CYP3A5 was shown to be regulated by a NF-Y, in addition to Sp1 and Sp3, via a NF-Y consensus site exclusively found in CYP3A5. It is speculated that this NF-Y activity may explain, at least in part, the expression of CYP3A5 in large range of tissues (Iwano, Saito et al. 2001). A number of *in vitro* and tissue culture models are valuable tools for the study of drug metabolism and gene regulation. However, these models are incapable of fully recapitulated dynamic patterns as observed *in vivo*. Additionally, the dissection of the individual contributions of the CYP3A genes has been hampered by similarities in their sequence and function. To circumvent these limitations, transgenic mice have been increasingly used as the experimental models of choice for *in vivo* studies.

## **1.2.8 *In Vivo* known investigation of CY3As regulation and expression**

### **1.2.8.1 Molecular based-mechanism for the generation of transgenic mice**

Functional counterparts of almost all human genes exist within the murine genome (Guigo, Dermitzakis et al. 2003). The technology of introducing biological materials into fertilized mouse eggs by microinjection was first introduced by Lin when she successfully injected eggs with a bovine gamma globulin (Lin 1966). This method was further been developed to increase the efficiency of introduction of foreign DNA into mouse cells. The ability to introduce and express foreign DNA, e.g. reporter gene in mice, has opened the door to study the regulation and expression of many genes *in vivo*. Several reporter genes originating from bacteria are easily detectable by simple methodologies in transgenic mice. Reporter genes commonly used for the generation of transgenic mice include the bacterial lacZ gene, the bacterial chloramphenicol acetyltransferase (CAT) gene and the firefly luciferase gene. CAT- and luciferase-transgenes are usually used for measurements of transgene expression at the tissue level, whereas the bacterial  $\beta$ -galactosidase encoded by bacterial lacZ gene, is mostly used as *in situ* visual marker (Cui, Wani et al. 1994). The integration of DNA into mouse chromosomes can be achieved through either homology-dependent or homology-independent mechanisms (also called illegitimate integration) (Yan, Li et al. 2010). The former method makes use of the sequence homology between the incoming DNA and the targeted locus to induce homologous recombination. The resulting configuration of the modified loci is highly predictable (Fig. 7A) and has been routinely used to introduce DNA to knock-in or to knock-out genes at specific genomic loci (Babinet and Cohen-Tannoudji 2001).

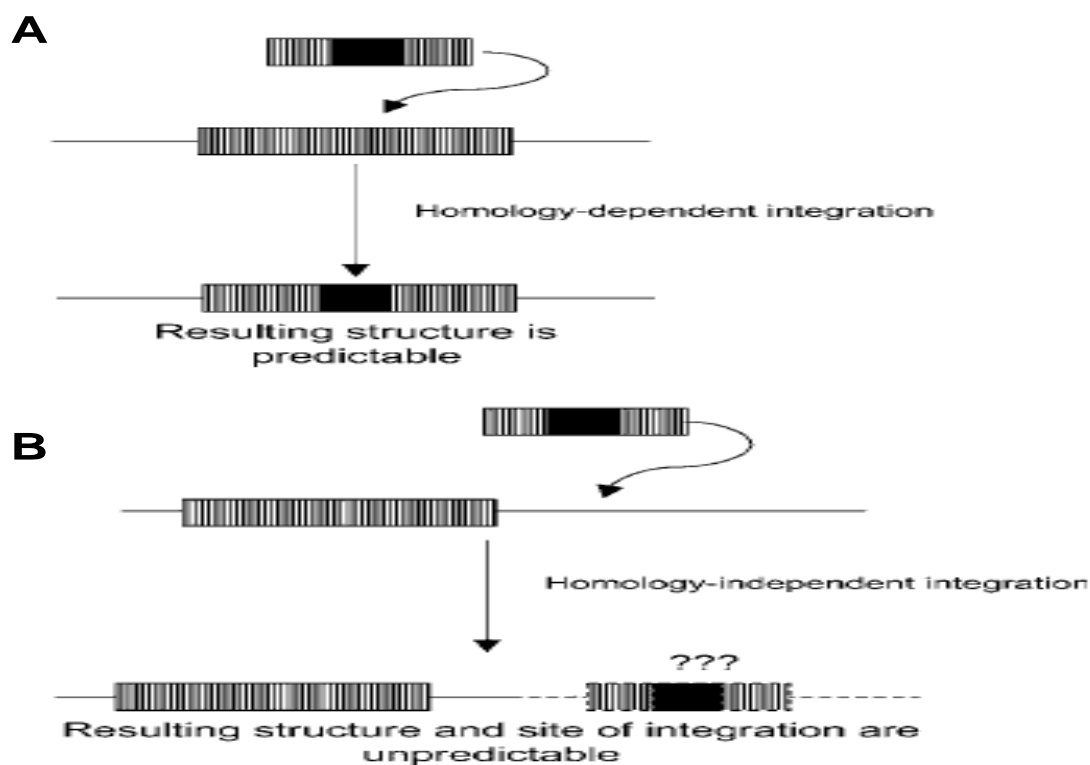


**Fig. 7. Difference between homology-directed genome modification and illegitimate DNA integration.** (A) The chromosome structure resulting from homology-directed modification is foreseeable. (B) Illegitimate DNA integration produces unexpected structures that differ in transgene copy number and endogenous integration site structure. Dashed lines represent possible degradation or rearrangements (from (Wurtele, Little et al. 2003)).

The homology-independent mechanism is characterized by much less predictable integrated structures. Following introduction into cells, exogenous DNA often forms concatamers by processes referred to as nonhomologous end joining (NHEJ). Furthermore, exogenous DNA often integrates in multiple copies (Folger, Wong et al. 1982; Merrihew, Clay et al. 2001). Thus, it is impossible to preselect the genomic site of integration and predict the resulting foreign DNA-chromosome structure (Fig. 7B). To decipher expression and regulation of *CYP3As* gene *in vivo*, both the homology-dependent and the homology-independent mechanisms have been extensively employed to generate *CYP3As* transgenic mice.

### 1.2.8.2 Known *CY3As* transgenic mice

Since 1980, microinjection of a solution of DNA into a pronucleus of fertilized eggs has been routinely utilized to generate transgenic mice. The establishments of many *CYPs* transgenic mice have been driven largely by the clinical importance of *CYP3A4* enzymes. Many *CYP3A* gene

transgenic mice have been established for the purpose of investigating CYP3A expressions *in vivo*. For example, the generation of a transgenic mouse carrying human foetus-specific CYP3A7 was first reported by (Li, Yokoi et al. 1997), followed by the establishment of a humanized CYP3A4 mouse model (Tg3A4) harboring a bacterial artificial chromosome clone containing both the genic and regulatory sequences of the human *CYP3A4* gene. Unexpectedly, the CYP3A4 gene expression of this model was restricted to the small intestine (Granvil, Yu et al. 2003). The absence of CYP3A4 expression in the liver was caused by the age-gender specific secretion of the growth hormone which suppressed CYP3A4 expression in adult male Tg3A4 mice. Consistently, later studies showed that the immature male and female mice did express the enzyme in the liver (Cheung, Yu et al. 2006). Because the above-mentioned transgenic models all possess confounding endogenous murine CYP3A genes, mice with the complete deletion of the *CYP3A* gene cluster (including catalytically active *Cyp3a13*, *Cyp3a57* and *Cyp3a59* genes) were further developed using a flipase recombinase system (van Herwaarden, Wagenaar et al. 2007). The resulting *Cyp3a*-null mice were used as background strain to generate the intestinal (CYP3A4-V) and hepatic (CYP3A4-A) humanized CYP3A4 transgenic models, both of which are able to detoxify drugs upon challenges (van Herwaarden, Wagenaar et al. 2007). These models provided effective avenues for the determination of the relative contribution of intestinal versus hepatic CYP3A4 in metabolism and bioavailability.

CYP3A4 expression is primarily regulated by PXR. Human and mouse PXR share nearly 80% and 96% identity at amino acid level across the LBD and DBD, respectively, and display similar tissue-specific expression patterns. However, the differences in the LBD sequence result in the selectivity in ligand binding of PXR (Lehmann, McKee et al. 1998). To circumvent this problem, *Pxr*-null mice were established by disrupting two exons of the mouse's *Pxr* gene (Xie, Barwick et al. 2000). The conditional PXR knock-out and the whole body hPXR humanized mice were further generated on the basis of the *Pxr*-null mice (Xie, Barwick et al. 2000). Later on, the double Tg3A4/hPXR transgenic mice were generated by crossing hPXR mouse with Tg3A4 mice (Ma, Cheung et al. 2008), which provided a valuable platform to explore drug interactions in the absence of endogenous *Pxr* functions.

Transgenic mice have been also generated for the study of the CYP3A4 transcriptional regulation, including the mice carrying the 3.2 kb and 13 kb of the human CYP3A4 promoter placed upstream of a *lacZ* coding region. Only mice carrying the 13 kb CYP3A4/*lacZ* were able to recapitulate the multifaceted patterns of CYP3A4 expression observed in humans (Robertson, Field et al. 2003). Though *lacZ* may be effectively expressed in target tissues in the embryo, its expression in adult tissues is somewhat unpredictable (Thorey, Meneses et al. 1993). Therefore, CYP3A4-*lacZ*

transgenic mouse model was later generated with the 13 kb of the human CYP3A4 promoter being placed upstream of luciferase coding region. This model allows a whole body examination of the transcriptional regulation of CYP3A4 in a non-invasive and real-time manner *in vivo* (Zhang, Purchio et al. 2003). Transgenic mice models have been established for CYP3A4 and CYP3A7. However, no such a model exists for the study of CYP3A5, the second most important CYP3A isoform. Providing the microinjection technique, the establishment of CYP3A5 transgenic models for the study of regulation of human CYP3A5 gene is feasible. Additionally, this model could also provide a model for a simultaneous analysis of CYP3A5 in many organs.

## 2. Aims of the study

CYP3A4 and CYP3A5 are the most important hepato-intestinal enzymes metabolizing natural and anthropogenic xenobiotics, including an estimated 50% of contemporary drugs (Shimada, Yamazaki et al. 1994). The hepato-intestinal expression level of CYP3A4 is tightly regulated by xenobiotics exposures (Raucy 2003) via xenosensors, such as pregnane X receptor (PXR) and constitutive androstane receptor (CAR; (Goodwin, Hodgson et al. 2002). The lack of the distal xenobiotic-responsive enhancer module (XREM) in the *CYP3A5* promoter had led to the assumption that CYP3A5 is not induced by xenobiotics. In contrast to this assumption, Burk and colleagues (2004) have reported that CYP3A agonists induced CYP3A5 in hepatic and intestinal cells via activity of the proximal xenosensing element (ER6). On the other hand, no CYP3A5 induction was reported by Busi and Cresteil (2005). Furthermore, unlike CYP3A4, CYP3A5 is expressed in several organs lacking PXR such as prostate, adrenal gland and kidney (Koch, Weil et al. 2002). The role of CYP3A5 in these organs may involve steroid metabolism. An induction of CYP3A5 in these organs could have deleterious effects on steroid homeostasis. In consequence of these considerations, the aims of this study were to:

- Clarify the induction of CYP3A5 in an *in vivo* model. To this end, transgenic mice expressing a luciferase gene under the control of a 6.2 kb human CYP3A5 were established and characterized.
- Identify the mechanism of the apparently PXR-independent expression of CYP3A5 in the kidney. This was conducted using a two-cell line model reflecting the expression relationships of CYP3A5 and CYP3A4 in the kidney and small intestine *in vivo*.

### 3. Materials and methods

#### 3.1 Materials

##### 3.1.1 Instruments

Instruments	Manufacturer
Mastercycler Gradient	Eppendorf, Hamburg, Germany
BioPhotometer	Eppendorf, Hamburg, Germany
peqLabNanoDrop (Spectrophotometer)	Peqlab Biotechnologie GmbH, Erlangen, Germany
Electrophoresis power supply E835	Consort, Belgium
Electrophoresis tank (for DNA analysis)	Bio-rad, Hamburg, Germany
INTAS-uv system (DNA analysis)	INTAS, Hamburg, Germany
Thermomixer confort Incubator (sub-culture of <i>E.coli</i> )	Eppendorf, Hamburg, Germany
Waterbath (For enzymatic reaction)	Lauda VWR International GmbH, Darmstadt, Germany
Laminar Flow Labgard class II	IBS Integra Biosciences, Fernwald, country
Vacuum-pump	IBS Integra Biosciences, Fernwald, country
CO2 tank	IBS Integra Biosciences, Fernwald
Orbital Incubator (cell culture)	Stuart, United kindom
Haemocytometer	Roth, Karlsruhe, Germany
Photonic microscope (for cell counting)	Leica, Bensheim, Germany
luminometer	Berthold Centro LB 960, Germany
Phase contrast Microscope (for the nuclear extraction)	Leica, Bensheim, Germany
Sunrise Tecan reader (for Protein concentration)	Tecan, Crailshaim, Germany
Gel caster, comb and electrophoresis thank for EMSA	Bio-rad, Hamburg, Germany
Odyssey infrared imager (For the EMSA)	LI-COR Biosciences
Microwave 800	Severin, Germany
Autoclave	Emi turbo, Germany
Centrifuge	Heraeus, Langenselbold, Germany
Microcentrifuge	Eppendorf, Hamburg, Germany
Shaking Waterbath (for DNA isolation from mice tail)	GFLLabortechnik, Burgwedel, Germany
Tissue disrupter (Ultraturrax)	Ika Labortechnik, Germany
IVIS system (mice imaging)	Xenogen Corp., Alameda, CA
pH Meter	Inolab, Weilheim, Germany
Printer	Berthol, Frankfurt, Germany
Shaver	Braum, Germany
Magnetic Shaker	Heidolph MR-Hei-Tec, Schwabach, Germany
Incubator Shaker	Innova, New Brundwick Scientific, New Jersey, USA
Hera Freeze (-80°C)	Heraeus, Langenselbold, Germany
Balance (Sartorius BL1500)	Göttingen, Germany
Balance (Kern 440-33N)	Kern and Sohn, Germany
Pipette P10, P100, P1000	Eppendorf, Hamburg, Germany
Multipipettes Matrix 10, 120, 300 µl	Biohit, Germany
Bunsen burner	Integra Biosciences, Switzerland
Ice Machine	Zeigra, Germany

### 3.1.2 Chemicals\*

Chemicals	Manufacturer
D-Luciferin (mice imaging)	BD Gentest, Woburn, MA
D-Luciferin (luciferase activity)	Sigma-Aldrich, St. Louis, MO
Ampicilin	Sigma-Aldrich, St. Louis, MO
Coelenterazine	Sigma-Aldrich, St. Louis, MO
TCPOBOP	Sigma-Aldrich, St. Louis, MO
PCN	Sigma-Aldrich, St. Louis, MO
DMSO	Sigma-Aldrich, St. Louis, MO
Ethidium Bromide	Applichem, Darmstadt, Germany
BSA (For the standard curve)	Applichem, Darmstadt, Germany
Agar	Applichem, Darmstadt, Germany
Agarose	SeaKem Agarose, Lonza, Rockland, USA
Bacto-yeast extract	Roth, Karlsruhe, Germany
Bacto-Tryptone	Applichem, Darmstadt, Germany
Glycerine	Applichem, Darmstadt, Germany
Tris base	Applichem, Darmstadt, Germany
NaCl	Applichem, Darmstadt, Germany
EDTA	Applichem, Darmstadt, Germany
HEPES	Roth, Karlsruhe, Germany
EGTA	Applichem, Darmstadt, Germany
benzoase	Novagen, USA
IGEPAL	Sigma-Aldrich, St. Louis, MO
EDTA-free protease inhibitor cocktail	Calbiochem, Darmstadt, Germany
DTT	Applichem, Darmstadt, Germany
TEMED	Applichem, Darmstadt, Germany
Ammonium persulfate (APS)	Applichem, Darmstadt, Germany
Sodium Dodecyl Sulfate (SDS)	Applichem, Darmstadt, Germany
30% (w/v) Acrylamid-/Methylenbisacrylamid (37,5:1)	BioRad, München, Germany
Dulbecco's Modified Eagle Medium with/without phenol red (DMEM)	Invitrogen/GIBCO BRL
Foetal bovine serum	FBS GOLD, PAA, Pasching
Non-essential amino acids	Invitrogen/GIBCO BRL
Minimal Eagle Medium (MEM)	Invitrogen/GIBCO BRL
Natrium-pyruvate	PAA, Pasching, Austria
25 mM HEPES	PAA, Pasching, Austria
Penicillin-Streptomycin (10000 U/ml – 10000 µg/ml)	Invitrogen/GIBCO BRL
Trypsin-EDTA 1× (0,25% Trypsin, 1mM EDTA×4 Na)	Invitrogen/GIBCO BRL

\*All other chemicals used in this study were of commercially available molecular biology grade

### 3.1.3 Reagents/Kits/enzymes/Antibodies/solvents

Reagents	Manufacturer
Bradford reagent	Biorad, München, German
Gene Juice transfection reagent	Novagen, USA
5×Passive Lysis Buffer	Promega, Madison, USA
5×Cell Lysis Buffer	Promega, Madison, USA
<b>Kits</b>	
PCR Purification Kit	Fermentas
Plasmid Miniprep Kit II	PEQLAB Biotechnologie
Gene Jet gel extraction kit	Fermentas
QuikChange® Site-Directed Mutagenesis Kit	Stratagene, Darmstadt, Germany



DNA Markers (Low, middle and high range)	Fermentas FastRuler TM
DNA loading buffer (6x)	Fermentas FastRuler TM
RNA isolation Kit	PEQLAB Biotechnologie
<b>Enzymes</b>	
High Fidelity Taq polymerase	Bioline
Taq polymerase	PEQLAB Biotechnologie
Mung Bean exonuclease	New England Biolabs
T4 ligase	New England Biolabs
<i>DpnI</i> exonuclease	Fermentas
Other restriction enzymes used in this study	New England Biolabs
Proteinase K	Roth, Karlsruhe, Germany
<b>Antibodies</b>	
Anti-YY1 (sc-7341x)	Santa Cruz Biotechnology
anti-PXR (sc-7737)	Santa Cruz Biotechnology

### 3.1. 4 Solvents

Solvents	Manufacturer
Isopropanol	WWW international Prolabo, leuven, Belgium
Ethanol	Roth, Karlsruhe, Germany
Chloroform	Roth, Karlsruhe, Germany
Formaldehyde	Merck, Darmstadt, Germany
1×PBS	Invitrogen/GIBCO BRL

### 3.1.5 Tools data analysis

#### 3.1.5.1 Local software

Software	
GraphPad Prism V3.0	GraphPad San Diego, CA, USA
Base ImagIR Image Analysis LI-COR	Lincoln, NE, USA
Mikrowin 2000 V4 Program (luciferase)	Microtek Laborsystem, Overath, Germany
Magellan V6.4 Program (Protein)	Austria
Biophotometer PC-online v1.00	Eppendorf, Hamburg, Germany
INTAS GDS	INTAS, Hamburg, Germany
LivingImage	Xenogen Corp., Alameda, CA

### 3.1.5.2 Online data banks and software

Data bank and programm	
UCSC genome browsers	(Hinrichs, Karolchik et al. 2006)
ENSEMBL genome browsers	
NCBI Genbank database	(Johnson, Zaretskaya et al. 2008)
<i>Multi-LAGAN</i> programm	(Brudno, Do et al. 2003)
<i>BIOEDIT</i> programm	(Hall 1999)
P-Match programm	(Chekmenev, Haid et al. 2005)

### 3.1.6 Consumable materials\*

Products	Manufacturer
Liquid Nitrogen	Tec-lab, Königstein, Germany
Adhesive PCR film	ABgene, Hamburg, Germany
25 ml three division	WWW international West chester, PA, USA
Whatman filter	Dassel, Germany
20G, 27G needles	Braum, Germany
Syringe 1ml, 10 ml	Terumo, Leuven, Belgium
Pasteur Pipettes	Roth, Karlsruhe, Germany
24-, 48-, 96-well plates	Greiner Bio-one, Germany
Tissue culture dishes and flasks	Frickenhausen, Germany
Tubes 0.5-, -1.5, -2, -15 and 50 ml	Frickenhausen and Eppendorf, Germany
Cuvette	Eppendorf, Germany
Disposable gloves	Kimberly Clark, Belgium
Microscope slides	WWW international, China
Cover glasses 20x26 ml	Roth, Braunschweig, Germany

\*All other consumable materials used in this project were commercially available. They were purchased from the following companies: Biozym (Germany), Roth (Germany), Calbiochem (Germany), Greiner Bio-one (Germany), Eppendorf (Germany), Starstedt (Germany), Nalgene (USA), Schott Duran (Germany).

### 3.1.7 Oligonucleotides

The oligonucleotides used in this project are listed in table 2 to 5.

Table 2: Primers used for cloning of the 370 bp, 990 bp, 1.35 kb, 2.0 kb and 6.2 kb *CYP3A5* proximal promoter constructs.

Primer name	Sequence (5' to 3')*
CYP3A370-Fw	GGCAGCCATGGAGGGGCAGGTGAGAGG
CYP3A370-Rv	ATGGGCGCC GGCCTTTCTTTATG
CYP3A5 <sub>5,4</sub> -Fw	CACAACATCACAAACGCGTTGCGAAACC
CYP3A5 <sub>5,4</sub> -Rv	CCTCTCACCTGCCCCCTCCATGGCTGCC
CYP3A5 <sub>6,2</sub> -Fw	GGCACAAAATGTATCCTAGGCTTATC
CYP3A5 <sub>6,2</sub> -Rv	GTGAGATGAACCCGGTACCTCAGATG
CYP3A5-Fw 990	TCGGGGTACCCCAAGTACTGGGAGCACAGC
CYP3A5-Fw 1.35	TCGGGGTACCTCCAGAAATCCCCATGCTG
CYP3A5-Fw2.0	TCGGGGTACCTGAAATCTGAGACCTCAAACG
CYP3A5-Rv	ACCTAGATCTGAGTGCTGCTGTTTGCTGG
CYP3A5-XREM-Fw	GTAACGCGTGAGATGGTTCATTCT
CYP3A5-XREM-Rv	ATGCCATGGCGTCAACAGGTTAAAG
TgCYP3A5-Fw	GCCACCCCTAGTTAGCACC
TgCYP3A5-Rv	CTCGAACTCCTGACCTCAGG

\* Restriction enzyme cutting sites within primers are underlined.

Table 3: Primers used for insertions and deletions of the 370 bp *CYP3A5* (1-4) proximal promoter construct and of the 374 bp *CYP3A4* (5-8) promoter construct.

	Primer name	Sequence (5' to 3') <sup>#</sup>
1	CYP3A5-57ins-Fw	tgactactccaactgcaggcagagcacaggtggcccTGCTATTGGCTGCAGC TATAGCCCTGCC
2	CYP3A5-57ins-Rv	aggettctccaccttgaagtggCAAAGAATCGCACACACCCCTTTG CTGACCTCTTTTGA
3	CYP3A5-57SP-Fw	cgaacgaacgaacgaacgaacgaacgaacgTGCTATTGGCTGCAGCTAT AGCCCTGCC
4	CYP3A5-57SP-Rv	ttcgttcggttcggttcggttcggttcGCAAAGAATCGCACACACCCCTTT GCTGACC
5	CYP3A4-57del/SPins-Fw	cgaacgaacgaacgaacgaacgaacgaacgTGCTACTGGCTGCAGCTCC AGCC
6	CYP3A4-57del/SPins-Rv	ttcgttcggttcggttcggttcggttcAGTTGGCAAAGAATCACACACACA CCTACTC
7	CYP3A4-57del-Fw	TGCTACTGGCTGCAGCTCCAGCCCTGCCTCCTTCTCTAGC (Biggs, Wan et al. 2007)
8	CYP3A4-57del-Rv	GTTGGCAAAGAATCACACACACACCACTCACTGACCTCC (Biggs, Wan et al. 2007)

<sup>#</sup> Nucleotides complementary to the respective promoter sequence are capitalized in each primer pair. The circularization of the resulting PCR products by ligation was improved by phosphorylation of oligonucleotides.

Table 4: Primers sequences used for site-directed mutagenesis of nuclear factor binding sites.

Primer name	Sequence (5' to 3') <sup>**</sup>
Canonical YY1 binding site	(C/g/a)(G/t)(C/t/a) <u>CATN(T/a)(T/g/c)</u>
CYP3A5-57insM1/ CYP3A4M1	GTTGGAAGAGGCTT <u>CTCCATCT</u> TGGAAGTTGGCAAAG
CYP3A5-57insM2	GTTGGAAGAGGCTT <u>CTCAACCT</u> TGGAAGTTGGC
CYP3A5-57insM3	GGAAGAGGCTT <u>CTCCACCCT</u> TGGAAGTTGG
CYP3A5-57insM4	GAGGCTT <u>CTCCACCGAG</u> GGAAGTTGGCAAAG
CYP3A5-57insM5	GGAAGAGGCTT <u>CTCAGCCT</u> TGGAAGTTGGC
CYP3A5-57insM6	GGAAGAGGCTT <u>TTGCACCCT</u> TGGAAGTTGG
CYP3A5- 57insM7/CYP3A4M7	GTTGGAAGAGGCTT <u>CTCAGCCGAG</u> GGAAGTTGGCAAAG
CYP3A4-NF1M	GGTGTGTG <u>CAAATCTTTGTAGT</u> CTTCCAAGGTGGAGAAGC

<sup>\*\*</sup> Nucleotides corresponding to the canonical YY1-binding and NF1-binding sites are underlined. Mutated nucleotides are shown in bold type.

Table 5: Primers used for RT-PCR quantification of YY1 (1-2), NF1 (3-4) and internal standard 18SRNA (5-6). And for the EMSA analysis, IRDye-800 labeled YY1 CYP3A4-derived probe (7-8) and YY1 positive control (9-10).

	Primer name	Sequence (5' to 3') <sup>##</sup>
1	YY1-RTFw	CATGTGGTCCCTCAGATGAAAAAAAAAGATATTG
2	YY1-RTRv	CAGCCTTCGAACGTGCACTGAAAGGGCTTCTC
3	NF1-RTFw	CATCCAAGTGTCCCGGACACCCGTGGTGACTG
4	NF1-RTFw	CGGGGACGAGATGCCTCCTTCCATGTCC
5	18SRNA-Fw	GCTGCTGGCACCAGACTT
6	18SRNA-Rv	CGGCTACCACATCCAAGG
7	YY1-CYP3A4-IRDye-800 Fw	TGCCAACTTCCA <u>AAGGTGGAGAAGCCTCTTCCAA</u>
8	YY1-CYP3A4-IRDye-800 Rv	TTGGAAGAGGCTT <u>CTCCACCTT</u> GGAAGTTGGCA
9	YY1-IRDye-800-Fw	CGCTCCGCGGCCATCTTGGCGGCTGGT
10	YY1-IRDye-800-Rv	ACCAGCCGCCAAGATGGCCGCGGAGCG

<sup>##</sup> YY1 binding sites located within primers are underlined.

## 3.2 Methods

### 3.2.1 CYP3A promoter sequence analysis

The sequences of proximal promoter around 1 kb upstream of the first exon *CYP3A* genes from human (*Homo sapiens*), chimpanzee (*Pan troglodytes*) and rhesus (*Macaca mulatta*), were downloaded from either ENSEMBL genome browser or NCBI Genbank. The corresponding sequences from marmoset (*Callithrix jacchus*) *CYP3A5*, *CYP3A21* and *CYP3A90*, and the galago (*Otolemur garnetti*) *CYP3A91* and *CYP3A92* genes were obtained from BAC sequences (CH259-48H24 and CH256-241K21), respectively (Qiu, Taudien et al. 2008). Tarsier (*Tarsius syrichta*) sequences were identified from the whole-genome shotgun sequence database in NCBI using BLASTn (Johnson, Zaretskaya et al. 2008). Sequences were aligned using Multi-LAGAN (Brudno, Do et al. 2003) and visualized in BIOEDIT (Hall 1999). P-Match (Chekmenev, Haid et al. 2005) was used for the identification and scoring of YY1 DNA response elements. Matching was performed to predefine vertebrate matrices in a liver-specific profile.

### 3.2.2 Construction of *CYP3A5* reporter gene constructs

The 370 bp *CYP3A5* proximal promoter was amplified from the BAC clone 22300 (Gellner, Eiselt et al. 2001) with *NcoI*- and *NarI*-extended primers (Table 2). The PCR products were digested, gel-extracted (Gene Jet gel extraction kit, Fermentas) and ligated to the analogously digested pGL3-Basic vector (Promega). To generate the 6.2 kb *CYP3A5* promoter construct, a 5.4 kb *MluI/NcoI* and a 555 bp *KpnI/AvrII* *CYP3A5* promoter fragments were amplified from the BAC 22300 clone using primers (Table 2). The resulting 5.4 kb *MluI/NcoI* and 555 bp *KpnI/AvrII* fragments were sequentially sub-cloned into the *CYP3A5*-370 construct. The *CYP3A5*-688 has been described previously (Burk, Koch et al. 2004). Various lengths of the human *CYP3A5* upstream 5'- promoter were generated via PCR using the *CYP3A5*-6.2 kb plasmid as a template and a common reverse primer and different forward primers. All forward primers were extended with *BglII* site and the reverse primer with *KpnI* (Table 2). The 374 bp *CYP3A4* promoter construct and the chimerical XREM-*CYP3A4* construct were from previous studies (Hustert, Zibat et al. 2001; Tegude, Schnabel et al. 2007). To generate the chimeric XREM-*CYP3A5*-370 and XREM-*CYP3A5*-57ins constructs, the *CYP3A4* distal enhancer module XREM was amplified by PCR from the XREM-*CYP3A4* plasmid using the primers extended with *MluI* and *NcoI* sites (Table 2). The resulting products were double digested using *MluI* and *NcoI* and cloned into the corresponding sites of the *CYP3A5*-370 and *CYP3A5*-57ins construct. The sequences of all constructs generated and used in the present study were confirmed by sequencing (GENterprise GENOMICS, Mainz, Germany).

### 3.2.3 Generation of CYP3A5-luc transgenic mice

CYP3A5-luc transgenic mice were established by pronuclear injection of the *CYP3A5*-6.2 kb plasmid, which expresses firefly luciferase under the control of the proximal 6.2 kb of the human *CYP3A5* gene promoter (see above). Briefly, the plasmid was linearized and purified by gel-extraction (Gene Jet gel extraction kit, Fermentas). The solution of the linear transgene (5 ng/μl in 10mM Tris, 0.1mM EDTA, pH 7.4) was microinjected into the male C57BL/6N mouse pronucleus of fertilized mouse eggs. The embryos were then transferred into pseudopregnant C57BL/6N mice. The CYP3A5-luc transgenic founders were identified by PCR amplification of genomic DNA isolated from mice tail tips. The transgene was maintained in the original genetic background C57BL/6N by breeding heterozygous carriers with wild-type C57BL/6N mice. CYP3A5-luc transgenic and wild-type mice were housed in our animal facility and maintained under the controlled environmental conditions with a 12/12 hours light/dark cycle. Food and water were available *ad libitum*. All animals experiment and the protocol described in this study were approved by the Regional Committee on the Ethics of Animal Experiments of Koblenz, Germany (Permit Number: 23 177-07/G 10-1-045).

#### 3.2.3.1 Isolation of genomic tail-tip DNA

Genomic DNA was extracted from tail biopsies of 3 weeks old mice. Briefly, tail biopsies about 0.5 cm were removed with sterile scalpel and placed into a 1.5 ml microfuge tubes, after which 500 μl of tail lysis buffer and 25 μl proteinase K (10 mg/ml) (Roth) were added. The tail lysates were fairly vortex and subsequently incubated overnight at 55°C with gentle shaking. The digested tail mixture was thereafter centrifuged for 10 minutes at room temperature at 14000g to pellet debris. The supernatants were transferred to new tubes, filled with 1 ml cold 100% Ethanol and mixed by inversion until DNA was precipitated. After centrifugation at 14000g for 20 minutes (at 4°C) and removing the supernatants, the pellets were washed with 1 ml cold 70% Ethanol, followed by centrifugation at 14000g for 20 minutes (at 4°C). The supernatants were carefully removed and the pellets were air-dried for 10 minutes at room temperature. Finally, the DNA was resuspended in 100 μl TE 10 mM, pH 8.0. The DNA concentration was determined using a spectrophotometer (Eppendorf). DNA aliquots were stored at -20°C until used.

#### 3.2.3.2 PCR genotyping of CYP3A5-luc transgenic mice

Transgenic mice were identified by PCR screening of the genomic DNA isolated from mice tail tips using the TgCYP3A5-Fw and TgCYP3A5-Rv primers (Table 1). The reaction mixtures (25 μl) contain 60 ng of genomic DNA, 0.25 μM each oligonucleotide, 200 μM dNTPs, and 1 U Taq

Polymerase (PeQlab). The PCR program consists of an initial denaturing step at 94°C for 3 minutes, 35 cycles of amplifications (45 seconds denaturation at 94°C, 30 seconds annealing at 58°C and 1 minute extension at 72°C) and a final extension at 72°C for 10 minutes. The ~500 bp PCR amplicons were separated by gel electrophoresis on a 1.5% agarose gel. CYP3A5-luc transgenic mice from the F1 progeny were further crossed with wild-type mice to generate F2 offsprings. Mice from the F1 to F5 at age of 6 to 8 weeks, weighing 20 to 29 g were used in this study.

### **3.2.3.3 Determination of the tissue distribution of CYP3A5-luc transgene**

CYP3A5-luc transgenic mice (n = 4 per group) were used for the determination of the tissue distribution of CYP3A5-luc transgene. The small intestine was divided into eight successive segments from the duodenum to the ileum. In addition, adrenal gland, spleen, liver, kidney, prostate, testis, ovary, heart, lung, oesophagus, forestomach and the colon were rapidly excised, snap-frozen in liquid nitrogen and stored at -80°C until used. Cell lysis buffer (Promega) was diluted 1:4 with 100mM Tris pH 7.4 and the organs were homogenized in 200 or 500 µl cell lysis buffer by at least ten strokes of a tissue disrupter (Ultraturrax) on ice. The homogenates were shocked frozen in liquid nitrogen, thawed and subsequently centrifuged at 5000g for 5 minutes at 4°C. Then the supernatants were collected and used for luciferase activity measurement using the luciferase reporter assay system (Promega). The measurements were performed in triplicates for 10 sec integration with a luminometer (Berthold Centro LB 96). The concentrations of protein were determined by the Bradford method (Bradford 1976) (see Appendix). Luciferase activity is normalized to relative light units (RLU)/µg of total protein in the homogenates.

### **3.2.3.4 Animal treatment with PCN and TCPOBOP agonists**

For the induction assay, CYP3A5-luc transgenic mice (n = 3 per group) were injected i.p. with PCN (50 or 100 mg/kg) for murine PXR induction and with TCPOBOP (6 mg/kg) for the murine CAR induction, both dissolved in DMSO. Control mice were injected with DMSO only. Mice were sacrificed by cervical dislocation 6 hours and 24 hours after treatments and organs of interests were removed, washed in ice cool 1x PBS, snap-frozen in liquid nitrogen and stored at -80°C until used.

### **3.2.3.5 Transgenic mice bioluminescent imaging assay**

The CYP3A5-luc transgenic mice were imaged *in vivo* using a non-invasive method that allows screening of living animals as describe previously (Zhang, Purchio et al. 2003). Briefly, abdominal shaved mice were anesthetized with (isofuran/oxygen) and injected i.p. with an aqueous substrate

D-luciferin (150 mg/kg) 5 minutes prior to imaging. The imaging was conducted for 5 minutes using the IVIS system (Xenogen Corp). Bioluminescent activities were quantified using LivingImage software (Xenogen Corp). For the induction analysis, CYP3A5-luc transgenic mice were treated with PCN (100 mg/kg) or DMSO as described above 24 hours prior to imaging. For the *ex-vivo* bioluminescent imaging assay, female CYP3A5-luc transgenic mice and wild-type littermates were sacrificed and the gastrointestinal tract, kidney and lung were harvested. Organs were soaked for 10 minutes into an aqueous substrate D-luciferin protected from light and imaged as described above.

### **3.2.4 *In vitro* analyses of the human CYP3A4 and CYP3A5 promoters**

#### **3.2.4.1 Inverted PCR-based mutagenesis**

To insert (or delete) desired DNA fragments into (or from) the wild-type *CYP3A5* and *CYP3A4* promoter constructs, we used inverted PCR-based method described previously (Biggs, Wan et al. 2007) with primers listed in Table 2. The primers used for insertion comprise the sequence to be inserted at 5'-halves and the sequences reverse-complement to those flanking the insertion sites in the template plasmid at 3'-halves. The primers used for the deletion are homologous to the 5' and 3' upstream boundaries of the region to be deleted. PCR products amplified using the High Fidelity Taq polymerase (Bioline) were pooled and subjected to *DnpI* digestion (Fermentas) to remove the dam-methylated parental DNA templates. The resulting products were purified using a PCR Purification kit (Fermentas) and were further digested with Mung Bean exonuclease (New England Biolabs) for 90 minutes to ensure blunt ends for the circularization using T4 ligase (New England Biolabs).

#### **3.2.4.2 Site-directed mutagenesis of the YY1 and NF1 binding sites**

All mutations introduced into the *CYP3A5-57ins* and *CYP3A4-374* constructs were achieved using the QuikChange site-directed mutagenesis kit (Stratagene). Sites important for the YY1 binding and specificity were mutated in *CYP3A5-57ins* and *CYP3A4-374* constructs, respectively with primers listed in Table 3. Both half sites of NF1 binding site in *CYP3A4* were mutated using primers listed in Table 3. To generate mutants, PCR was carried out in a total mixture of 50  $\mu$ l containing 5  $\mu$ l of 10x reaction buffer, 50 ng of dsDNA template, 125 ng of each primer, 1  $\mu$ l of dNTP and 2.5 U of PfuTurbo DNA polymerase (Stratagene). The PCR program consisted of an initial denaturing step at 95°C for 30 seconds followed by 18 cycles of amplification (30 seconds at 95°C for denaturation, 30 seconds at 55°C for annealing and 1 minute at 68°C for extension). PCR



products were subjected for 1 hour *DnpI* digestion at 37°C to remove parental DNA templates and transformed into *E.coli*. All clones carrying desired mutations were confirmed by sequencing.

### 3.2.4.3 Expression vector constructs

The human PXR (pcDhPXR) and the renilla luciferase (pRL-EF-1 $\alpha$ ) expression vectors have been described previously (Geick, Eichelbaum et al. 2001). The wild-type CMV-YY1 expression vector was kindly provided by Dr. Noako Tanese (Department of Microbiology and NYU cancer Institute, New York University School of Medicine, New York) (Lieberthal, Kaminsky et al. 2009). The YY1 mutant expression vectors (CMVYY1 $\Delta$ GA, CMVYY1 $\Delta$ 296–331, and CMVYY1 $\Delta$ 399–414) were provided by Prof. Bernhard Lüscher (Institute of Biochemistry and Molecular Biology, Medical Faculty RWTH Aachen University, Germany) (Austen, Cerni et al. 1998). The pCH-NF1A1.1 expression vector was kindly provided by Dr. Richard Gronostajski (State University of New York at Buffalo, Buffalo, NY) (Gronostajski 2000).

### 3.2.4.4 Bacterial cell transformation and plasmid isolation

The NEB 10-beta competent *E. coli* cells (New England Biolabs) were thawed on ice for 10 minutes. Plasmid DNA (50-100 ng) was incubated with competent *E. coli* cells on ice for 30 minutes, followed by heat shock at 42°C for 32 seconds and further incubated on ice for 5 minutes. After that, 475  $\mu$ l room temperature NZY+broth medium was added to the cells and the mixtures were incubated at 37°C with shaking for 1 hour. The resulting cell cultures (100-150  $\mu$ l) were spreaded on a pre-heated LB agar plates supplemented with 100  $\mu$ g/ml ampicilin (Sigma). The plates were incubated upside down overnight at 37°C and colonies were picked afterwards and inoculated in 100 ml of LB medium with 100  $\mu$ g/ml ampicillin (Sigma) for over-night incubation at 37°C. The same protocol was applied to constructs with site-directed mutagenesis, except that the super-competent *E. coli* strain was used instead of NEB 10-beta competent cells and that heat shock at 42°C was operated for 45 seconds. The cell cultures were then used for plasmids isolation using Plasmid Miniprep Kit II (Fermentas). The quality and concentration of plasmid DNA were determined using a spectrophotometer (Eppendorf). DNA aliquots were stored at -20°C until used.

### 3.2.4.5 Cell Culture

Human colon carcinoma cells namely LS174T (Tom, Rutzky et al. 1976), canine kidney derived-cells MDCK.2 (Cedrone, Reid et al. 2009), and human hepatocarcinoma cells HepG2 were obtained from American Type Culture Collection. LS174T and MDCK.2 Cells were maintained in

Dulbecco's Modified Eagle Medium (DMEM) (Invitrogen) and HepG2 in Minimal Eagle Medium (MEM) (Invitrogen) supplemented with 25 mM HEPES, 100 units/ml penicillin and 100 mg/ml streptomycin (Invitrogen), 1 mM sodium pyruvate (Invitrogen), and 10% heat inactivated foetal bovine serum (PAA). Culture medium for LS174T was further supplemented with 1% nonessential amino acids (Invitrogen). All cells were grown at 37°C in humidified conditions with 8% CO<sub>2</sub>.

#### **3.2.4.6 Transient transfection and luciferase assays**

LS174T and MDCK.2 cells were plated onto a 24 and 48-well plates one day prior to the transfection. At 70-80% confluence, reporter gene plasmids and internal standard (renilla luciferase, pRL-EF-1 $\alpha$  plasmid) were transfected into cells using the Gene Juice transfection reagent (Novagen). For experiments in 48-well plates cell number, reagent and transfected DNA content were downscaled proportionally. For the co-transfection experiments, 10 ng transactivator pcDhuPXR or 20 ng of CMV-YY1/mutant YY1 or pCH-NF1A1.1 expression vectors were added. Luciferase activities were measured as described (Gödtel-Armbrust, Metzger et al. 2007). Briefly, Cells were harvested 40 hours after the transfections, washed with 1x PBS, lysed using passive lysis buffer (Promega) and incubated 15 minutes at room temperature. The lysates (40  $\mu$ l for each sample) were subjected to a dual luciferase assay (Promega) using a luminometer (Berthold Centro LB 960). Luciferase activity is normalized to Renilla luciferase activity.

#### **3.2.4.7 *In vitro* transcription and translation**

The synthesis of the YY1 wild-type protein was performed using TNT Quick Coupled Transcription/Translation System (Promega). Briefly, the wild-type CMV-YY1 expression vector under the control of T7 promoter (1  $\mu$ g) was added to reaction mixtures of 50  $\mu$ l containing 40  $\mu$ l TNT quick Master mix, 1  $\mu$ l Methionine, 1 mM and 2  $\mu$ l Transcend Biotinylated-Lysine-tRNA. The reaction mixtures were incubated at 30°C for 90 minutes. The human PXR expression vector (pcDhPXR) was included as a positive control. Protein synthesis was confirmed by Western Blot according to the supplier's instruction (Promega). The concentration of protein was determined using the Bradford method.

#### **3.2.4.8 RNA isolation and cDNAs synthesis**

RNA isolation and cDNAs synthesis were performed as previously described (Wadman, Osada et al. 1997) with minor modifications. Briefly, Total RNA from renal, intestinal and hepatic cells was isolated respectively using TriFast reagent (Peqlab). RNA quality and concentration were

determined spectrophotometrically. cDNA was synthesized using 1 µg of total RNA, random hexamer primers (0.1 A260 units), dNTPs (0.3 mM), and 50 U SuperScript reverse transcriptase (Invitrogen) in total volume of 30 µl reaction as instructed by the manufacturer. RNA and cDNA concentrations were determined using a Nanodrop spectrophotometer (Peqlab). cDNA samples were diluted to a final concentration of 10 ng/µl and stored in aliquots at -80°C.

#### **3.2.4.9 RT-PCR and amplification of the YY1 and NF1 cDNAs**

cDNAs prepared from LS174T, MDCK.2 and HepG2 cells were used as templates. The expression of the 18S RNA was included as an internal control. Briefly, a second PCR was performed in a total reaction mixture (50µl) containing: (3µl) cDNA, 0.2 mM dNTPs, 50 pmol of each primer, 2.5 U Taq polymerase (Bioline) and 5x Taq reaction bufferMgSO<sub>4</sub> (5 µl). The reaction was performed for 25 cycles with respect to the exponential phase of the synthesis. The PCR profile is as follows: an initial denaturing step at 94°C for 45 seconds, 25 cycles of amplification (denaturing: 45seconds at 94°C for denaturation, annealing: 45seconds at 55°C for annealing, and 1 minute at 72°C for extension). The PCR products were separated by electrophoresis on a 1.5% agarose gel. YY1 and NF1 primers are designed to encompass two exons boundaries to avoid amplification of residual genomic DNA. Additionally, the specificity of the primers was confirmed by BLAST searches against NCBI nucleotide databases. The sequences of primers used for the RT-PCR are listed in Table 5.

#### **3.2.4.10 Nuclear extract preparation**

For the EMSA analysis, nuclear extracts were prepared from MDCK.2 cells as described previously with slight modifications (Wadman, Osada et al. 1997). Briefly, the confluent MDCK.2 cells were washed twice with ice-cold 1xPBS and detached using cell scrapers in 1 ml of hypotonic buffer A. Cells were pelleted at 750g for 5 minutes, resuspended in 1 ml of buffer A with 0.4% IGEPAL (Sigma) and kept on ice for 15 minutes for cell swelling and membrane lysis. After a brief centrifugation, the nuclear pellet was resuspended in 100 µl of ice-cold hypertonic buffer B and vigorously mixed for 60 minutes at 4°C to disrupt the nuclear membranes. This was followed by centrifugation at 7,500g for 15 minutes at 4°C to remove the nuclear debris. The supernatants (nuclear extract) were collected and stored in aliquots at -80°C. The protein concentrations were determined using the Bradford method. The enrichment of nuclear proteins was confirmed by Western blot using antibodies against nucleus-specific (lamin B) and a cytosol-specific (GADPH) protein (data not shown).

### 3.2.4.11 Annealing of labeled oligonucleotides

we used the nucleotide containing the YY1 consensus binding site from the *CYP3A4* promoter and a positive YY1 control. The positive control contains a previously reported YY1-binding site (Hariharan, Kelley et al. 1991). The oligonucleotides were 5'-labeled with IRDye-800 (Metabion). Equimolar amounts of complementary oligonucleotides were annealed by boiling for 5 minutes at 100°C followed by slowly cooling down to room temperature. The obtained double-stranded labeled probes were diluted with double-desalted water and stored in aliquots at -20°C in light-protected tubes until used in EMSA. Sequences of labeled oligonucleotides are listed in Table 5.

### 3.2.4.12 Electrophoretic mobility gel shift assay (EMSA) and supershift assay

EMSA reactions contained binding buffer mixed with 20 µg of nuclear extract, 50 fmol of a ID800-labeled probe in a total volume of 10 µl. For the confirmation of the specificity of binding 1 µg of an anti-YY1 antibody was added to the mixture. The anti-YY1 antibody is raised against amino acids 1-414 representing full length YY1 of human origin. This antibody is therefore able to either supershift a YY1-DNA complex or to immunodeplete YY1 protein present in the mixture. Similarly, 300 ng of an anti-PXR antibody was added as a negative control. Reaction mixtures were pre-incubated 15 minutes or, for supershift/immunodepletion, 30 minutes at room temperature and further incubated for 20 minutes after the addition of the labeled probes in a volume of 2.5 µl. The resulting products were subsequently resolved by native PAGE in a pre-run 4% minigel in 0.5x TBE at 100 V for 60 minutes at 4°C and visualized using an Odyssey infrared imager (LI-COR Biosciences) with focus offset at 0.375 mm.

### 3.2.5 Statistical analyses

Statistically significant differences of the mean values were determined with Mann-Whitney U test or one-way analysis of variance following a Dunnett's post test, if applicable, using GraphPad Prism version 5.0 (GraphPad Software, San Diego, CA). Differences were considered to be statistically significant if the resulting *P* values <0.05.

## 4. Results

### 4.1 In vivo analysis of *CYP3A5* promoter activity

#### 4.1.1 Generation and identification of the *CYP3A5*-luc mice

Transgenic mice were generated using the *CYP3A5*-luc-6.2 kb plasmid as described in Methods (Fig. 8A). Six founders were identified by PCR genotyping using the genomic DNA isolated from mice tip tails. One founder died prematurely. Two founders designated as Founder A and Founder C were used to pass the *CYP3A5*-luc transgene to the progenies by backcrossing with C57BL/6N wild-type mice. Offsprings carrying the desired transgene were identified by PCR screening. The used primers led to ~500 bp PCR amplicons from the carriers (Fig. 8B).

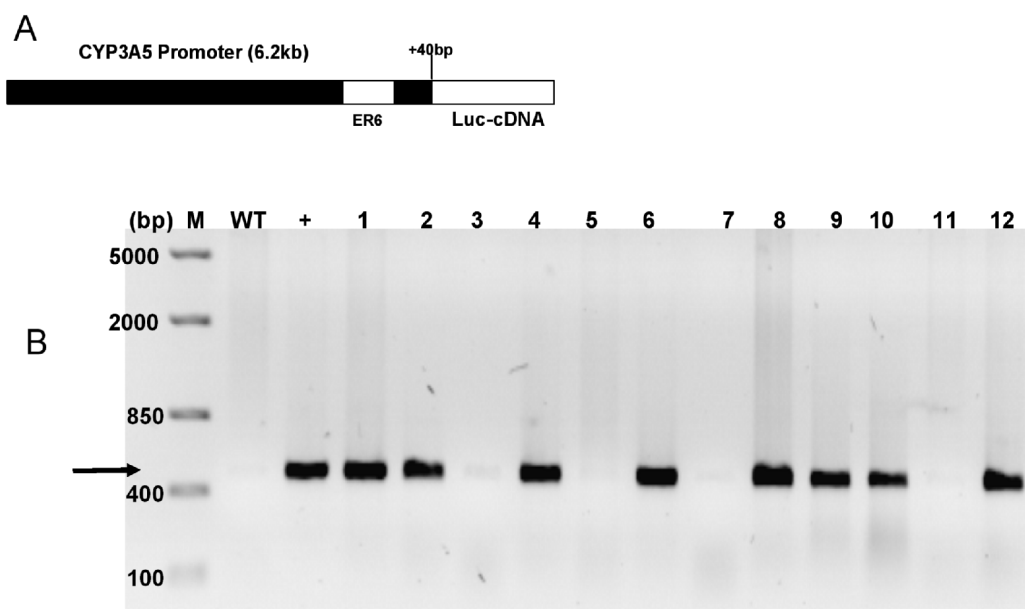


**Fig. 8. PCR screening of *CYP3A5*-luc mice.** (A) The schematic representation of the *CYP3A5*-6.2 construct used for *CYP3A5*-luc transgenic mice, which contains a 6.2 kb of *CYP3A5* proximal promoter sequence inserted upstream of firefly luciferase cDNA. (B) Eletrophoresis of PCR screening products on 1.5% agarose gel. The expected location of PCR amplicons is indicated by the left arrow. WT: Wild-type, “+”: positive control.

#### 4.1.2 *In vivo* determination of the basal activity of the *CYP3A5* transgene

To determine the expression pattern of the transgene *in vivo*, the transgenic mice were subjected to bioluminescent imaging together with the wide-type mice as negative controls. Mice of both genders were injected i.p. with D-luciferin solution and the ventral images were collected.

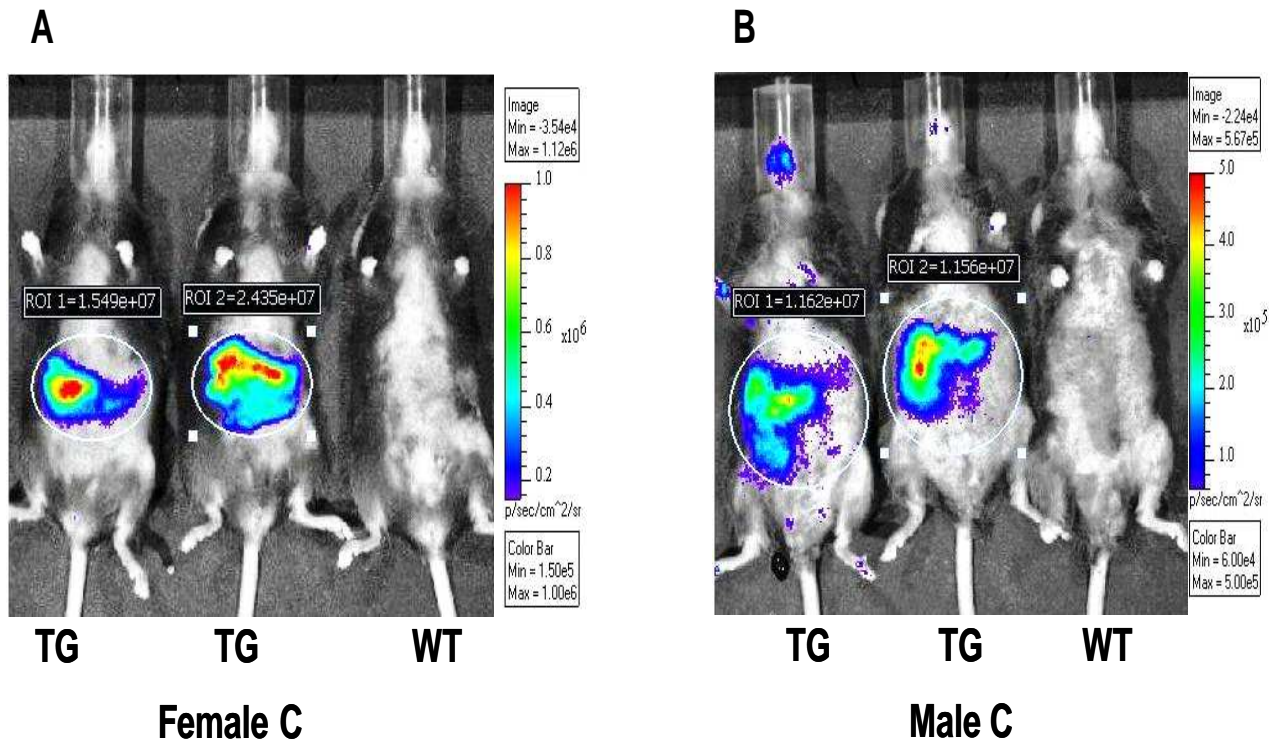


**Fig. 9. Bioluminescent images of basal CYP3A5-luc transgene activity *in vivo*.** The *in vivo* bioluminescent activity of the CYP3A5-luc transgene was quantified in both female (A) and male (B). CYP3A5-luc transgenic and wild-type mice were injected i.p. with a single dose of an aqueous D-luciferin substrate (150mg/kg body weight) 5 minutes prior to imaging. The photoluminescent activity was quantified with the LivingImage software (Xenogen Corp.) program. A ventral view of three representative mice is depicted for each gender. The colour scales next to the images indicate the signal intensities at the different regions of the animals in photons per second. WT: Wild-type; TG: transgenic mice.

Hot spots of the light emission of luciferase activity were detected exclusively from the lower abdomen of both female ((Fig. 9A) and male (Fig. 9B) transgenic mice, which correspond to the position of gastrointestinal tract. No signals were detected from the upper abdomen and the position of the kidney. Occasionally, we also detected very weak signals from the feet, the tail and ears of transgenic mice in both sexes (Fig. 9B and data not shown). As expected, no light emission was detected from the wild-type mice. Thus, the CYP3A5-luc transgenic mice did express the transgene *in vivo*. The transgene signals restricted in the gastrointestinal tract indicates that the transgene may be not expressed in other organs or that expression in other organs was too weak to be detected.

### 4.1.3 *In vitro* determination of the tissue distribution of CYP3A5 transgene activity

In order to verify the results from *in vivo* bioluminescent imaging, we examined the basal expression pattern of the transgenic luciferase activity *in vitro*. Homogenates were prepared from twelve organs of transgenic mice line A and line C and they were assayed for the luciferase activity using a luminometer. As shown in Fig 10 (A and B), the pattern of luciferase activities across different organs were highly similar in both lines and with comparable expression levels.

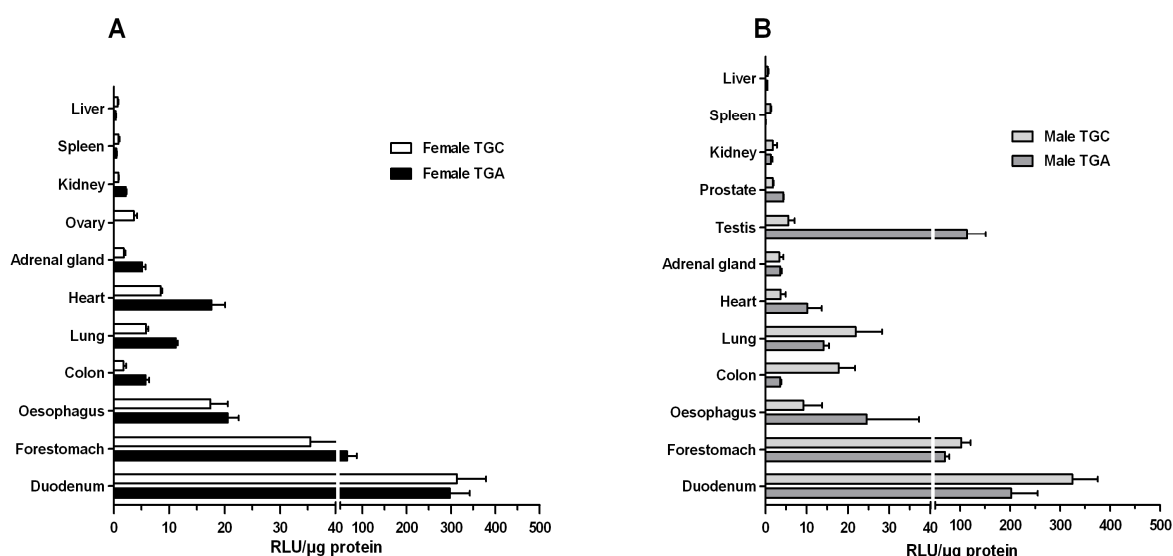


**Fig. 10. The expression of the CYP3A5-luc transgene in different organs.** Twelve organs were isolated from transgenic mice ( $n = 4$  per group) from line A (TGA) and line C (TGC). Data are represented as relative light units (RLU)/ $\mu\text{g}$  protein shown as mean values ( $\pm\text{SEM}$ ).

The highest luciferase activities were detected in the small intestine, followed by oesophagus, testis, lung, adrenal gland, ovary, prostate and kidney. In addition, luciferase activities were detected in the forestomach, a structure lacking in humans, and in the adjacent oesophagus. Most strikingly, no luciferase activities were detected in the liver, which is consistent with the restricted transgene expression in lower abdomen *in vivo*. Taken together, the pattern of CYP3A5-luc transgene activity expression *in vivo* and *in vitro* largely reflects that of CYP3A5 in human (Koch, Weil et al. 2002). In the following, we used the line C for further characterization of the CYP3A5-luc transgenic mice models.

#### 4.1.4 Photonic localisation and segmental determination of the CYP3A5-luc activity along the small intestine

The above bioluminescent data (Fig. 9) indicated that the abdominal signal may originate from the gastrointestinal tract. To further localize the origin of the abdominal signal, *ex vivo* imaging of the gastrointestinal tract was performed together with the kidney and lung isolated from both transgenic and wild-type female mice. These organs were soaked into a solution of D-luciferin protected from light for 10 minutes and imaged.

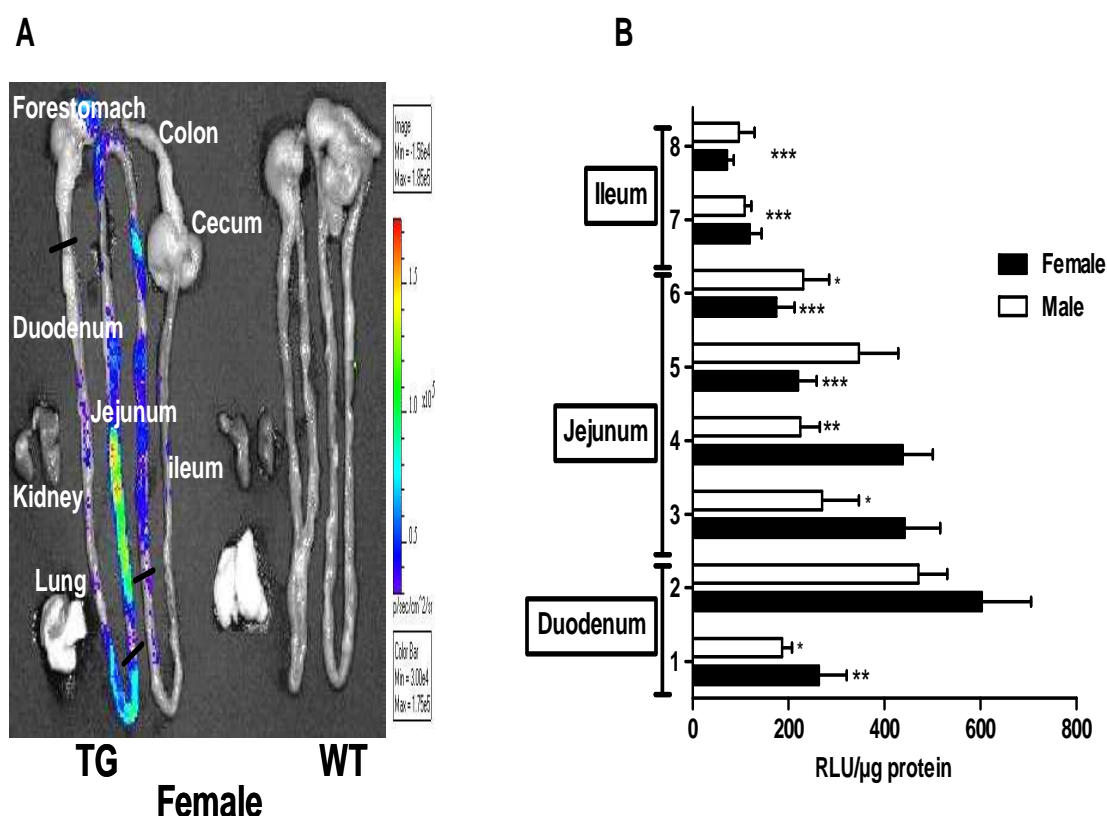


**Fig. 11. Determination of the CYP3A5-luc transgene activity along the small intestine.** (A) Representative photonic localisation of the CYP3A5-luc transgene activity. The gastro-intestinal tract, lung and kidney were isolated from CYP3A5-luc transgenic and wild-type (WT) mice and soaked into an aqueous D-luciferin substrate for 10 minutes prior to imaging. The imaging was conducted as described in Fig. 8 legend. (B) The small intestine from both male and female transgenic mice (n = 3 per group) was divided into eight segments (1 to 8), starting from the proximal duodenum to the distal ileum. Homogenate from each segment was assayed for the luciferase activity using a luminometer. Data are represented as relative light unit (RLU)/μg protein shown as mean values ( $\pm$ SEM) and compared with the segment 2. \* p < 0.05, \*\* p < 0.01, \*\*\* p < 0.001.



The light emission originated exclusively from the small intestine and the forestomach of the transgenic mice, with the strongest signals located in the middle of the small intestine (Fig. 11A). No signals were detected from kidney and lung and in all organs from wild-type mice. Additionally, the luciferase activity was determined along the small intestine from both male and female transgenic mice. To further define the expression of the transgene along the length of the small intestine, we divided this organ into one-eighth segments from the proximal duodenum to the distal ileum. Luciferase activities were detected in all segments, with the strongest signals in the distal duodenum (segment 2) and middle small intestine (jejunum) and significantly lower in the distal intestine (ileum) (Fig. 11B). This pattern of CYP3A5 luciferase transgene expression is consistent with those of human CYP3A along the gastrointestinal tract (McKinnon, Burgess et al. 1995), indicating that the CYP3A5-luc transgenic model is suitable for the study of CYP3A5 induction in the small intestine.

#### 4.1.5 The dose-effect on the PXR-driven CYP3A5-luc transgene activity in the small intestine and kidney

For the dose-response analysis, transgenic mice of both genders were injected i. p. with PCN (50 or 100 mg/kg) for 24 hours and the wide-type mice were injected with DMSO as control. Thereafter, luciferase activities were assayed in the duodenum (segment 2) and in kidney homogenates. As shown in Fig. 12A, the CYP3A5 transgene was induced in a dose-dependent manner in the duodenum, with the induction of 3~4 -fold by 50 mg/kg PCN and 6~8 -fold by 100 mg/kg PCN. The expression of the transgene was not induced in kidneys in both sexes (Fig.12B).

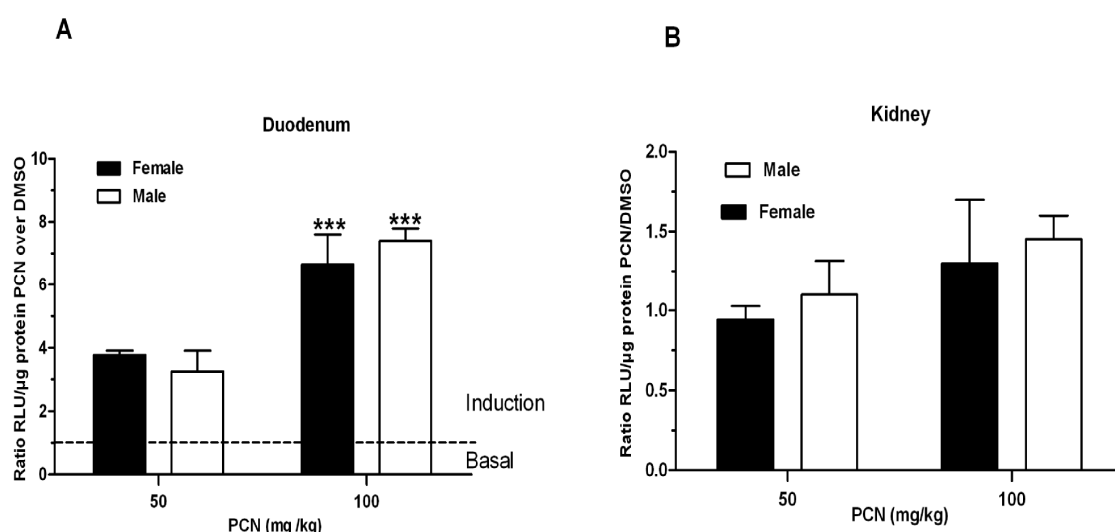


**Fig. 12. The dose- and sex- effect on the PCN induction of the CYP3A5-luc transgene activity in the duodenum (A) and kidney (B).** Transgenic mice (n =3 per group) were injected i.p. with PCN (50 mg/kg) and (100 mg/kg) or DMSO for control. Homogenates from the duodenum and kidney were

assayed for the luciferase activity using a luminometer. Data are shown as mean ratios ( $\pm$ SEM) relative light units (RLU)/ $\mu$ g protein PCN vs. DMSO. \*\*\*  $p < 0.001$ .

#### 4.1.6 The time-effect on the PXR- or CAR-driven CYP3A5-luc transgene induction in the small intestine

Transgenic mice were injected i.p. with either PCN (100 mg/kg) or TCPOBOP (6 mg/kg). The duodenum was isolated 6 hours and 24 hours after treatments and the homogenates were assayed for the luciferase activity. As shown in Fig. 13, similar levels of induction (6-fold for males and 8-fold for females) were detected at 6 hours and 24 hours by PCN treatments. Similarly, no difference in the induction level was detected between 6 hours and 24 hours by TCPOBOP in females. In contrast, the induction by TCPOBOP in males decreased from 7-fold at 6 hours to 4-fold at 24 hours. As expected, no induction of CYP3A5-luc transgene was observed at any time points neither with PCN nor TCPOBOP in wild-type mice (data not shown).

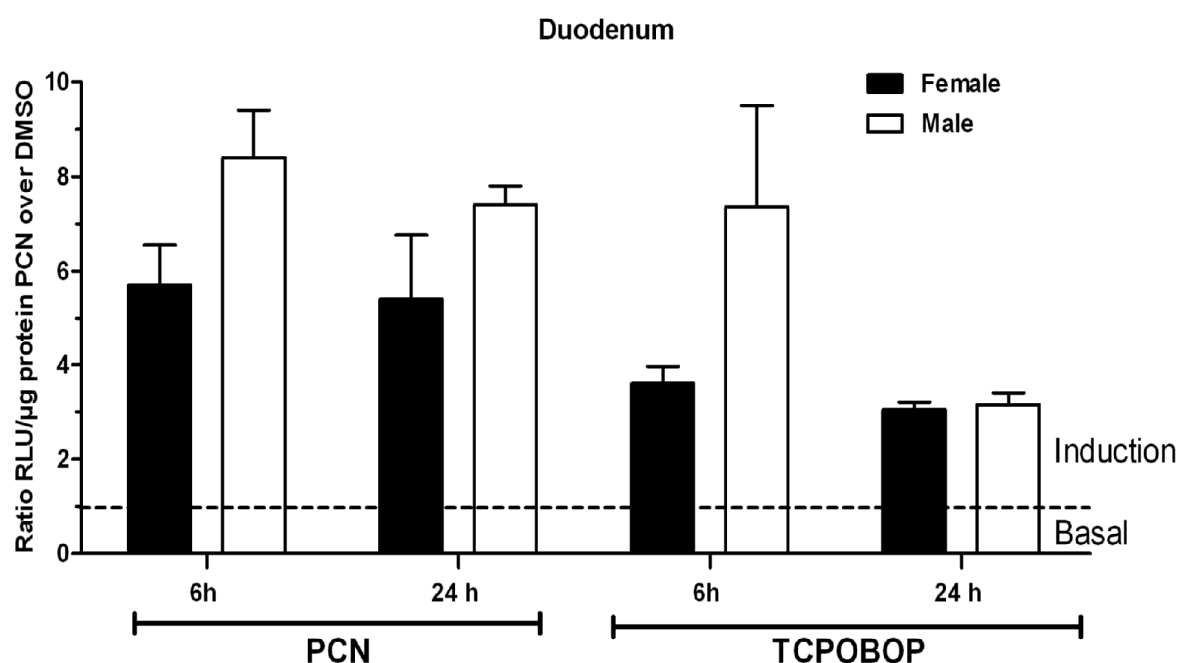


**Fig. 13. The time- and sex-effect on the induction of the CYP3A5-luc transgene activity in the duodenum.** Transgenic mice ( $n = 3$  per group) were injected i.p. with PCN (100 mg/kg) or TCPOBOP (6 mg/kg). DMSO treated mice were included as controls. Six hours and 24 hours after treatments, homogenates from duodenum were assayed for the luciferase activity using a luminometer. Data are shown as mean ratios ( $\pm$ SEM) relative light units (RLU)/ $\mu$ g protein PCN vs. DMSO.

#### 4.1.7 Induction activity of the CYP3A5-luc transgene along the small intestine

Our results on the basal activity of the transgene in the small intestine (Fig. 11) indicate that the transgene basal activity decreases with the distance to the duodenum. We further addressed the extents of transgene induction in each of segments of the small intestine. To this end, a whole body bioluminescent imaging of 24 hours PCN (100 mg/kg) or DMSO treated transgenic mice was performed. As shown in Fig. 14A, the hot spots of the light emission of the transgene were stronger in PCN treated mice as compared with the DMSO treated ones. Furthermore, the small intestine from 24 hours PCN or DMSO treated transgenic mice ( $n = 3$  per group) was divided into eight segments. Later on, mean values of luciferase activity were determined for the duodenum, the jejunum and ileum as indicated in Fig. 11B legend.

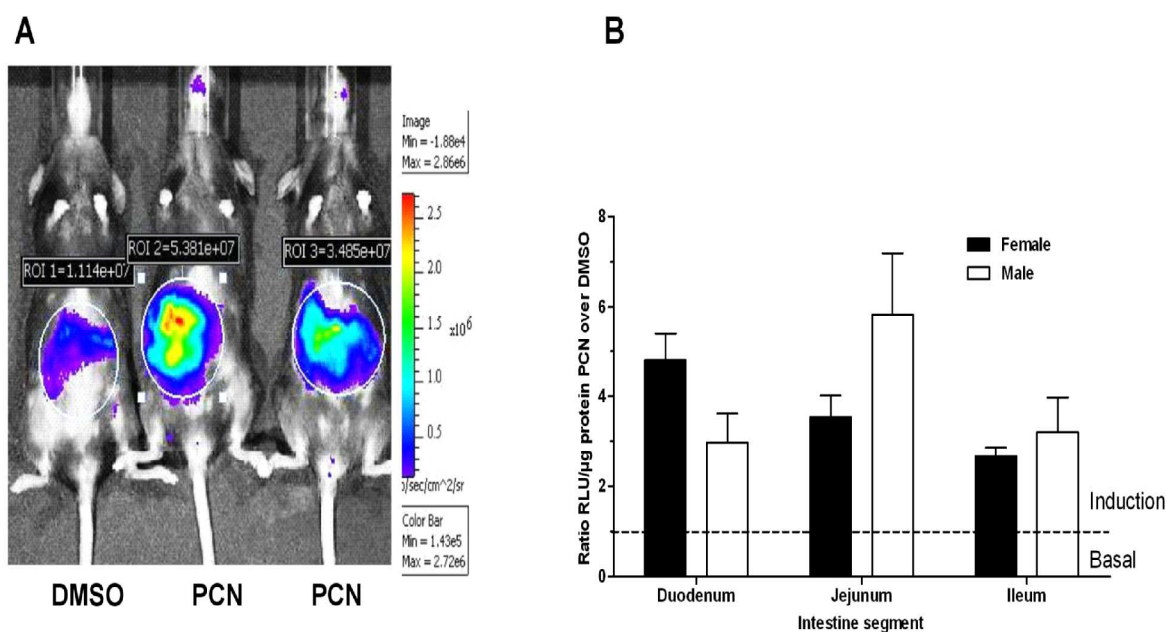


**Fig. 14. The effect of the PCN on the CYP3A5-luc transgene induction in different parts of the small intestine.** (A) Representative whole body bioluminescent *in vivo* imaging induction. 24 hours PCN (100 mg/kg) or DMSO treated female mice were injected with an aqueous substrate D-luciferin (150 mg/kg) and imaged as described in the Fig. 9 legend. (B) The small intestine from 24 hours PCN (100 mg/kg) or DMSO treated transgenic mice ( $n = 3$  per group) was divided into eight segments. Homogenate from each segment was assayed for the luciferase activity using a luminometer. Data are shown as mean ratios ( $\pm$ SEM) relative light units (RLU)/ $\mu\text{g}$  protein PCN vs. DMSO.

As shown in Fig. 14B, PCN induced all intestinal segments in both sexes. As a whole, the small intestine was induced 4- and 3.7-fold in female and males, respectively. On average, the CYP3A5-luc transgene was induced in the small intestine without significant difference between females and males. Taken together, these results indicate that CYP3A5 is activated *in vivo* by xenobiotics throughout the small intestine.

## **4.2 In vitro evaluation of the determinants of the differential tissue-specific activity of CYP3A4/CYP3A5 promoters**

### **4.2.1 Identification of the minimal CYP3A5 promoter**

The above studies of CYP3A5-luc transgenic mice models indicated that the human 6.2 kb upstream *CYP3A5* promoter recapitulates the observed broad tissue-specific and intestinal activation of *CYP3A5* promoter *in vivo*. However, it was still unclear which parts of the 5' upstream sequence of the *CYP3A5* underlined this regulatory feature of the *CYP3A5* gene. Comparisons of the *CYP3A4* and *CYP3A5* promoter sequences showed that they share similarity within the 1.5 kb proximal region (Fig. 2). Thus, to identify the minimal CYP3A5 promoter region required for the broad tissue expression of *CYP3A5* gene, we further made deletion constructs analysis in cell-based models (i.e, small intestine-derived LS174T cells and the kidney-derived MDCK.2 cells). The LS174T cells have been repeatedly validated as a faithful model for the basal and drug-induced CYP3A expression in the small intestine (Cervený, Svecová et al. 2007; Novotná, Doricáková et al. 2010; Qiu, Mathas et al. 2010). On the other hand, MDCK.2 cells exhibit many characteristics of tubular and collecting ducts cells (Verkoelen, van der Boom et al. 1999; Arthur 2000), which are the sites of CYP3A5 expression in humans (Aleksa, Matsell et al. 2005; Joy, Hogan et al. 2007). The reporter gene constructs containing various lengths of *CYP3A5* promoter sequences were transfected into LS174T and MDCK.2 cells. A similar high luciferase activity was detected from the shortest *CYP3A5*-370 construct in LS174T and MDCK.2 cells (Fig. 15A), suggesting that important elements for the *CYP3A5* basal promoter activity are located within the proximal 370 bp region.

### **4.2.2 Comparative analysis of CYP3A5-6.2 and chimeric XREM-CYP3A5 constructs in LS174T cells**

In the following, we also examined whether any other putative PXR regulatory element is localized in the distal *CYP3A5* promoter and may contributed to the intestinal induction of CYP3A5 as observed *in vivo*.

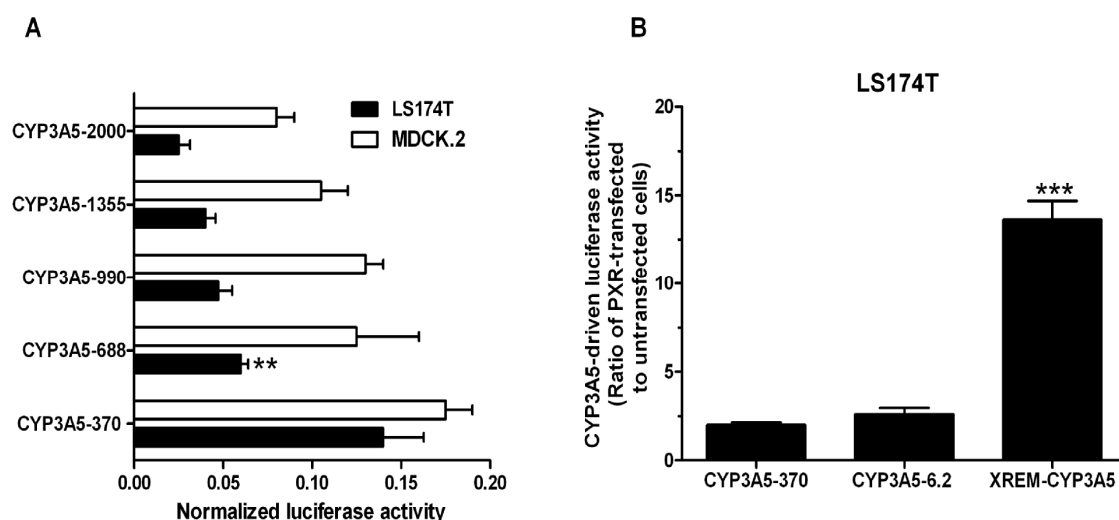


**Fig. 15. Induction conferred by *CYP3A5* promoter with serial of deletions.** (A) Determination of the minimal *CYP3A5* promoter. Deletion constructs of the *CYP3A5* upstream promoter were transiently transfected in LS174T and MDCK.2 cells. The numbers on the left of each promoter deletion construct refer to the beginning of the promoter fragments relative negatively to the transcription start site (TST). Data are expressed as mean values ( $\pm$ SEM) of four to six independent experiments conducted as triplicates (B) The effect of PXR on the proximal *CYP3A5-370* promoter the *CYP3A5-6.2* and the *XREM-CYP3A5* constructs in LS174T cells. Data are expressed as mean ratios ( $\pm$ SEM) of firefly luciferase activity of PXR-transfected vs. untransfected cells. Firefly luciferase activities in the individual well were normalized using activities of the co-transfected renilla luciferase driven by a constitutive promoter. \*\*  $P < 0.01$ , \*\*\*  $P < 0.001$ .

To this purpose, the *CYP3A5-370*, the *CYP3A5-6.2*, the chimeric *XREM-CYP3A5* constructs and PXR expression vector were transiently co-transfected into LS174T cells. As shown in Fig. 15B, the chimeric *XREM-CYP3A5* construct was 13-fold induced, while the *CYP3A5-370* proximal and *CYP3A5-6.2* distal promoter were similarly induced 3-fold, indicating that no additional important functional PXR regulatory elements likely reside in the distal sequence of the human *CYP3A5* promoter.

#### 4.2.3 Evaluation of *CYP3A5* and *CYP3A4* proximal promoter activities in renal and intestinal cells

The sequence conservation between the primate *CYP3A5* and *CYP3A4* promoters is limited to their most proximal parts (Qiu, Mathas et al. 2010). We investigated if these parts are sufficient to confer the previously reported differential expression of these genes in renal cells (Koch, Weil et al. 2002), using the *CYP3A5-370* and *CYP3A4-374* minimal promoters, which are referred to in the following as *CYP3A5* and *CYP3A4* promoters.

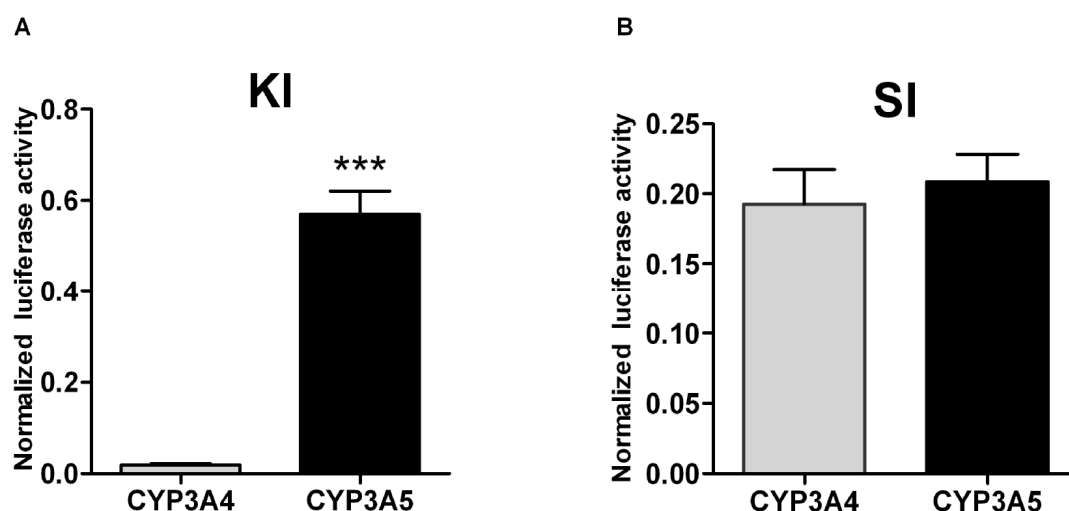


**Fig. 16. The activities of proximal *CYP3A4* and *CYP3A5* promoters in kidney-derived MDCK.2 and in small intestine-derived LS174T cells.** (A) *CYP3A4* and *CYP3A5* promoter activities in kidney-derived MDCK.2 cells; KI. (B). *CYP3A4* and *CYP3A5* promoters activities in small intestine-derived LS174T cells; SI. Data are expressed as mean values ( $\pm$ SEM) of six independent experiments conducted as triplicates. Promoter-driven firefly luciferase activities in the individual wells were normalized using activities of the co-transfected renilla luciferase driven by a constitutive promoter. \*\*\* $p < 0.001$ .

These plasmids were transiently transfected into MDCK.2 and LS174T cells. The *CYP3A5* promoter was robustly expressed, whereas the expression of *CYP3A4* was 31-fold lower in renal cells (Fig. 16A). On the other hand, the activities of these two promoters were similar in the small intestine-derived cell line LS174T (Fig. 16B). These findings were fully compatible with the differential expression of *CYP3A4* and *CYP3A5* in the human kidney and in the small intestine *in vivo* (Koch, Weil et al. 2002). Therefore, these two cell lines were taken as a model for more detailed investigations of the determinants of the differential renal and intestinal *CYP3A4* and *CYP3A5* expression.

#### **4.2.4 Function of the 57 bp promoter fragment in *CYP3A4/5* expression and comparison of the proximal *CYP3A5* and *CYP3A4* promoters**

The most prominent difference between the proximal *CYP3A5* and *CYP3A4* promoter sequences is the presence of a 57 bp fragment in *CYP3A4* which is absent from *CYP3A5*.

```

CCAAT-box-262-257 (-213-208)
CYP3A4 -275 TAATAGATTTTAT GCCAATGGCTCCACTTGAGTTTCTGATAAGAACCCAGAACCCTTGGA
CYP3A5 -226 TAATAGATTTTCATGCCAATGGCTCCACTTGAGTTTCTGATAAGAACCCAGAACCCTTGGA
*****

ER6-169-152 (-120-103)
-215 CTCCCCAGTAACATTGATTGAGTTGTTTATGATACCTCATAGAATA TGAACTCAAAGGAG
-166 CTCCCCGATAAACACTGATTAAGCTTTTCATGATTCCTCATAGAACATGAACTCAAAGAG
*****

NF1-134-122 YY1-116-106
CCAAT-box E-box
-155 GTCAGTGAGTGGTGTGTGTGATTTGCCAACTTCCCAAGGTGGAGAAGCCTCTTCCA
-106 GTCAG-CAAAGGGGTGTGTGCGATTCTTT -----
*****

E-box-80-73 BTE-52-36 (-61-45)
-95 ACTGCAGGCAGAGCA CAGGTGGCCCTGCTACTGGCTGCAGCTC CAGCCCTGCCTCCTTCT
-78 ----- GCTATTGGCTGCAGCTATAGCCCTGCCTCCTTCT
*****

CCAAT-box (-76-71)

TATA-box-29-24 (-38-33) +1 →
CYP3A4 -35 CTAGCATTATAACAATCCAACAGCCTCACTGAATC ACTG +1 →
CYP3A5 -44 CCAGCACATAAATCTTTCAGCAGCTTGGCTGAAGACTGCTGTGC AGGG
* ***** * ** ***** * *****

```

**Fig. 17. Sequence identity and distribution of regulatory elements in the proximal promoters of human *CYP3A4* and *CYP3A5*.** Identical nucleotides are denoted by asterisks. The 57 bp region absent from the *CYP3A5* promoter is represented as a stretch of hyphens. The transcription start sites (Hashimoto, Toide et al. 1993; Iwano, Saito et al. 2001; Saito, Takahashi et al. 2001) are indicated by arrows. The sequence is numbered relative to the transcription start site taken as +1. The binding sites for previously characterized transcriptional regulators CCAAT-box, ER6, BTE and TATA-box and NF1 are underlined (Saito, Takahashi et al. 2001; Biggs, Wan et al. 2007). The portion of the NF1 binding site described to constitute a CCAAT box, the YY1 site, and the two E-box motifs (Saito, Takahashi et al. 2001), all contained in the 57 bp region, are boxed. The positions of binding sites are shown separately for *CYP3A4* and, if applicable, in brackets for *CYP3A5*.

This region is localized upstream of the basic regulatory elements, i.e., CCAAT-box, BTE and TATA-box and downstream of the ER6 and NF1 enhancer elements (Fig. 17). Except NF1 element, all these elements are conserved between the *CYP3A4* and *CYP3A5* promoters. To determine the role of the 57 bp fragment in the apparent suppression of renal *CYP3A4* expression,

reporter gene construct were made with its region deleted from the proximal *CYP3A4* promoter. In parallel, this sequence was replaced by one of identical length but with no apparent transcriptional activity (“spacer”, SP in Fig. 18). The use of spacer allows to detect activity changes independent from the content of the 57 bp fragment, but caused by any altered spatial interactions among surrounding *cis*-acting elements following its deletion. Conversely, the *CYP3A4*-derived 57 bp region, or alternatively the spacer, were inserted into the corresponding location in the *CYP3A5* promoter.

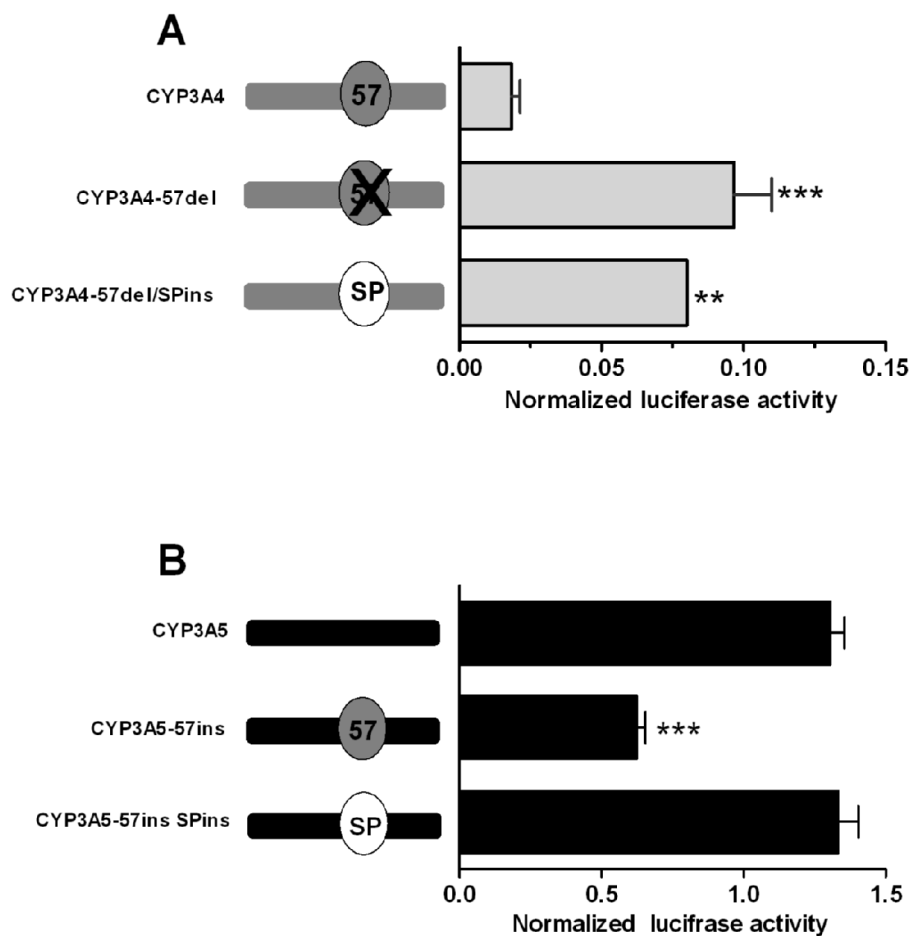


**Fig. 18. The effect of the *CYP3A4*-derived 57 bp region on the activities of the proximal *CYP3A4* and *CYP3A5* promoters in MDCK.2 cells.** (A) The effect of a deletion of the 57 bp region from the proximal *CYP3A4* promoter, or of its replacement with an unrelated “spacer” (SP) sequence of an identical length. (B) The effect of the insertion of the 57 bp region, or of the “spacer” into the *CYP3A5* promoter. Data are expressed as mean values ( $\pm$ SEM) of six independent experiments conducted as triplicates. Promoter-driven firefly luciferase activities in the individual wells were normalized using



activities of the co-transfected renilla luciferase driven by a constitutive promoter.  
\*\*p<0.01,\*\*\*p<0.001.

The resulting constructs (*CYP3A4-57del*, *CYP3A4-57del/SPins*, *CYP3A5-57ins*, and *CYP3A5-SPins*, respectively) were assessed for activity in MDCK.2 cells in parallel with the corresponding wild-type promoters. The deletion of the 57 bp element led to 4-fold increase in the activity of the *CYP3A4* promoter (Fig. 18A) and its replacement by the 57 bp spacer (*CYP3A4-57del/SPins* construct) displayed a similar effect (Fig. 18A). Conversely, the *CYP3A5-57ins* construct exhibited a ~2/3 decrease in the luciferase activity in comparison to the wild-type *CYP3A5* promoter, whereas no such effect was observed for the spacer insertion (Fig. 18B).

#### 4.2.5 Evolutionary history of the 57 bp region in primates

The above data demonstrated that the 57 bp fragment contains elements responsible for the repression of the *CYP3A4* promoter activity in renal cells. In order to identify the responsible mechanism, the 57 bp region was investigated in more detail *in silico* and *in vitro*. The evolutionary history of the 57 bp fragment was further illuminated to increase the specificity of the regulatory elements prediction. To this end, we first searched for its homolog sequences from all the other available primate species. The 57 bp homolog sequences were found in both galago *CYP3A* genes (*CYP3A91* and *CYP3A92*), in both tarsier *CYP3A* genes, provisionally designated as gene A and B (in cont323625 and contig840032 of the assembly tarSyr1, respectively), in the *CYP3A21* of the marmoset, as well as in *CYP3A4*, *CYP3A7*, and *CYP3A43* genes from rhesus, chimpanzee, and human (Fig. 19A). Furthermore, sequences ortholog to the 57 bp fragment were identified in many non-primate mammalian *CYP3A* genes (data not shown). In contrast, we found the 57 bp fragment fully deleted from the promoters of all primate *CYP3A5* genes. In addition, a partial deletion of a distal 25 bp within the 57 bp was found in the tarsier gene B (Fig. 19A).

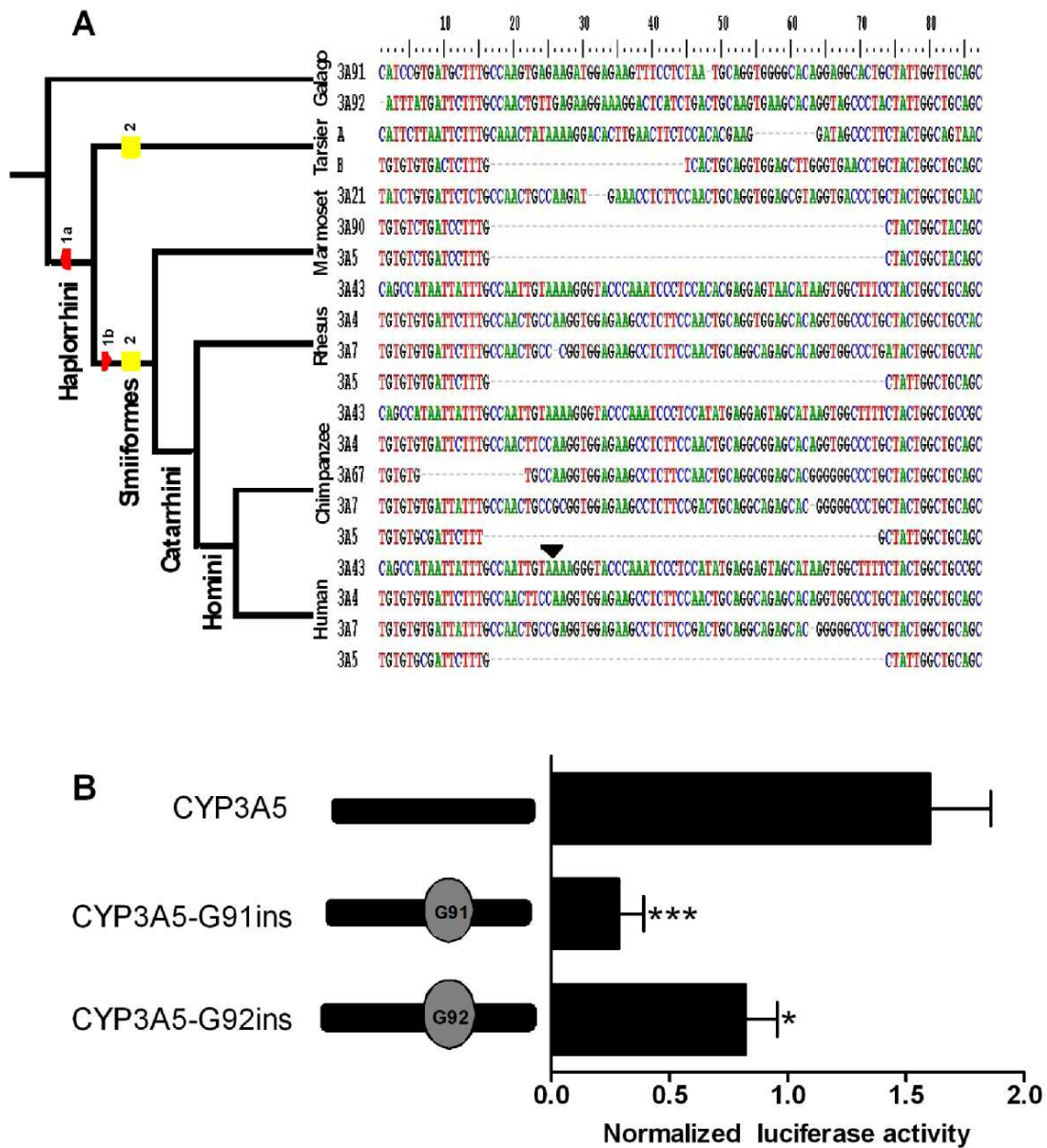


**Fig. 19. Genomic and functional conservation of the 57 bp *CYP3A* promoter region in primates.**

(A) Representation of the evolution of the 57 bp region. Deletions are shown as stretch of hyphens, with the widest one corresponding to the deletion of the entire 57 bp region. 1a-b and 2 indicate the two alternative scenarios of the 57 bp deletion. A 7 bp fragment present only in all *CYP3A43* genes has been removed for clarity and its position in the human *CYP3A43* gene is indicated by an arrow. “*CYP*” has been removed from gene names to improve legibility. (B) The effect of galago *CYP3A91*- and *CYP3A92*-derived 57 bp fragment on the human *CYP3A5* promoter activity in MDCK.2 cells. Data are expressed as mean values ( $\pm$ SEM) of five independent experiments conducted as triplicates. Promoter-driven firefly luciferase activities in the individual wells were normalized using activities of the co-transfected renilla luciferase driven by a constitutive promoter. \* $p < 0.05$ , \*\*\* $p < 0.001$ .

These results indicated that the 57 bp fragment was present in at least the promoter of the ancestral primate *CYP3A* gene, but was lost along the *CYP3A5* gene lineage via one of the two alternative scenarios (Fig. 18A) described in detail in the Discussion. To verify if the repressive effect of the 57 bp region is conserved in primates, orthologous sequences derived from the galago genes *CYP3A91* and *CYP3A92* were inserted into the human *CYP3A5* proximal promoter. Sequence from either gene repressed the luciferase activity in renal cells, whereby the effect of that derived from *CYP3A91* was stronger (Fig. 19B).

#### 4.2.6 The 57 bp region contains conserved regulatory elements

Besides a portion of the NF1 binding site and a E-box motif, the 57 bp fragment contains, on the anti-parallel strand, a binding site for a dual-function transcriptional regulator YY1 (Fig. 20A). YY1 binding to this element in the human *CYP3A4* promoter has been reported previously (Saito, Takahashi et al. 2001), but its functional significance remains unknown. YY1 binds to a highly degenerated consensus sequence 5'-VKH**C**ATNWB-3' (5'-(C/g/a)(G/t)(C/t/a)**CAT**N(T/a)(T/g/c)-3'). Uppercase and lowercase letters represent preferred nucleotides and tolerated ones respectively. The bolded tri-nucleotide **CAT** constitutes the YY1 binding core motif (Hyde-DeRuyscher, Jennings et al. 1995). In contrast, all human, chimpanzee, and rhesus *CYP3A4* and *CYP3A7* promoters, as well as the promoter of the chimpanzee-specific *CYP3A67* gene and of the tarsier gene A contain the mismatch T>C in the core motif CAT which is accompanied by decreased core d-scores (Fig. 20A). In the 57 bp fragment, the NF1 binding site and the E-box motif are present on the leading strand as compared with YY1 binding site. Moreover, the NF1 binding site is conserved across all primate *CYP3A* promoters except chimpanzee *CYP3A67*. Meanwhile, the putative E-box motif (CANNTG) is well conserved within *CYP3A4* genes but not in all other primate *CYP3A* homologous sequences (Fig. 20B). Notably, interaction of the E-box motif with factors of basic loop-helix family could either activate or repress gene expression (Yang, Freeman et al. 2002; Salero, Gimenez et al. 2003).

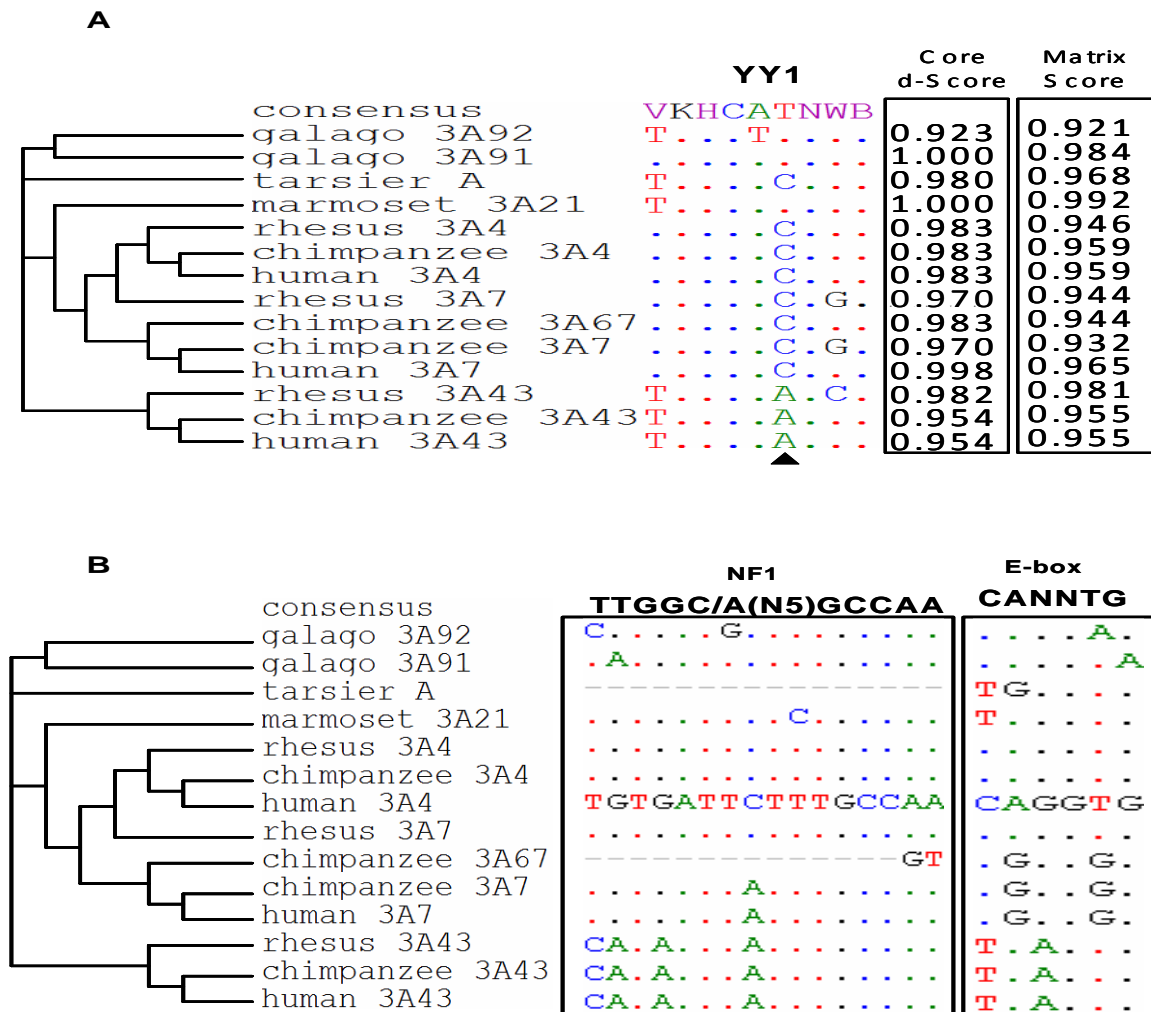


**Fig. 20. Conservation of the regulatory elements in the 57 bp region.** (A) Conservation and P-Match scores of the YY1 site. The arrowhead (on the bottom) indicates the T>C mutation in the YY1 core motif. (B) conservation of NF1 and E-box in the 57 bp region. Identical nucleotides are denoted by dots. Absence of nucleotides is represented as a stretch of hyphens. Consensus sequence for YY1, NF1 and E-box are depicted on top of sequences. The phylogenetic tree of selected primate *CYP3A* genes represented on the left was adopted from previous study (Qiu 2008). “*CYP*” has been removed from gene names to improve legibility.

#### 4.2.7 The effect of the mutation of the NF1 and the E-box on *CYP3A4* and *CYP3A5-57ins* activities

We first confirmed the reported functions of the NF1 and E-box binding sites (Saito, Takahashi et al. 2001) in MDCK.2 cells, by introducing mutations into the *CYP3A4* and *CYP3A5-57ins* constructs. The mutation of the E-box or NF1 sites affected promoter activities in neither *CYP3A4* (Fig. 21A) nor *CYP3A5-57ins* (Fig. 21B) constructs. Since the insertion of the 57 bp region in *CYP3A5* restores the NF1 binding site, we also determined whether the restoration of the NF1 binding site would lead to the suppression on the promoter activities. To this end, the *CYP3A5-*

*57NF1/SP* construct was made, which harbors the full length of the NF1 binding site extended with a spacer “SP”. As depicted in Fig. 21B, the luciferase activity produced by this construct was similar to that by the wild-type *CYP3A5* promoter. These results indicate that neither the NF1 binding site nor the E-box motif are the causes of the repressive effect of the 57 bp region in renal cells.

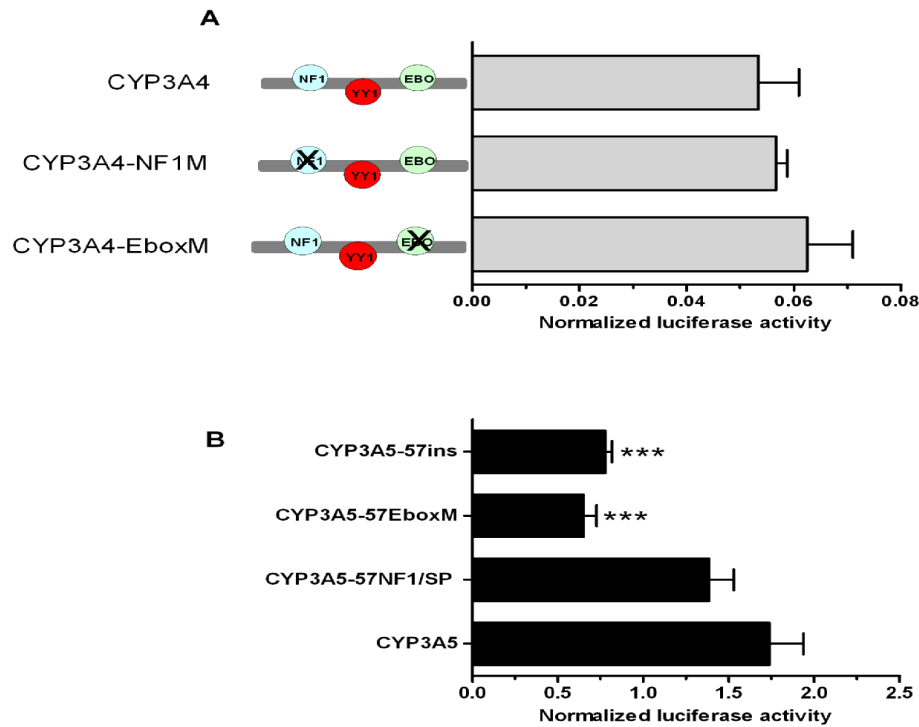


**Fig. 21. Mutational analysis of the NF1 and the E-box in *CYP3A4* and *CYP3A5-57ins* constructs in MDCK.2 cells.** The mutations either restore the NF1 consensus core motif (*CYP3A5-ins57NF1/SP*) or disrupt the NF1 (*CYP3A4-NF1M*), the E-box site (*CYP3A4-EboxM* and *CYP3A5-57insEboxM*). Mutants, wild-type *CYP3A4* and *CYP3A5* promoter constructs were transiently transfected in MDCK.2 cells. Promoter-driven firefly luciferase activities were normalized using activities of the co-transfected renilla luciferase driven by a constitutive promoter and compared to that of the wild-type construct. Data are expressed as mean values ( $\pm$ SEM) of four independent experiments conducted as triplicates. \*\*\* $p < 0.001$ .

## 4.2.8 Functional characterization of the human *CYP3A4* YY1 binding site

### 4.2.8.1 Determination of the tissue expression of YY1

Considering the established role of YY1 as a transcriptional repressor, we concentrated on the binding site for this protein. Firstly, we tested the expression of YY1 in our cell-based models using RT-PCR. As expected, the reference HepG2 cells express high level of YY1 mRNA, in agreement with the high YY1 protein expression reported in this cell line (Begon, Delacroix et al.

2005). Consistent with the previously reported ubiquitous expression of YY1 (Shi, Lee et al. 1997), its transcripts were also detected both in LS174T and MDCK.2 cell lines (Fig. 22), though the level of expression in LS174T cells was slightly lower as compared to both the reference HepG2 and MDCK.2 cells.

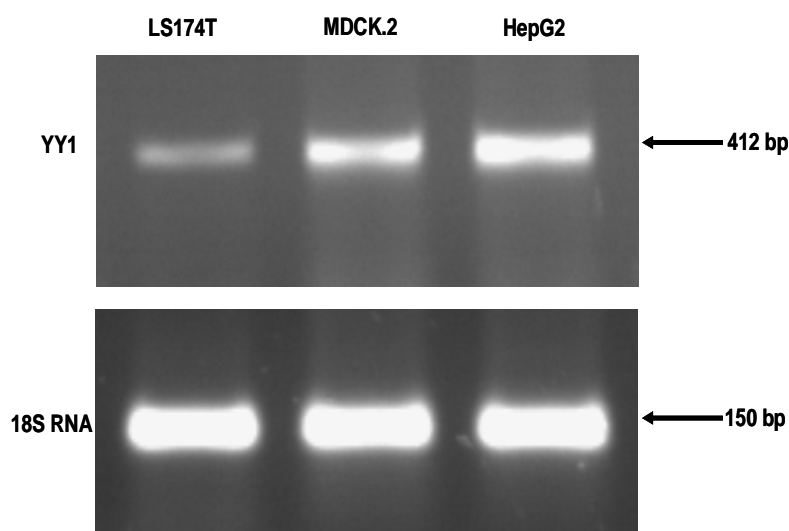


**Fig. 22. The determination of the YY1 expression in LS174T, MDCK.2 and HepG2 cells.** RT-PCR analysis of the endogenous level of YY1 mRNA in LS174T, MDCK.2 and HepG2 cells. The expression of 18S RNA was measured in parallel as an internal control. PCR products were separated by electrophoresis on a 1.5% agarose gel. Numbers on the right indicate the lengths of the amplicons.

#### 4.2.8.2 EMSA analysis of the CYP3A4 YY1 binding

We further confirmed the reported YY1 binding to its consensus target site within the 57 bp fragment in *CYP3A4* promoter using an electrophoretic mobility shift assay (EMSA). The IRDye800-labeled oligonucleotides encompassing the *CYP3A4*-YY1 binding site were used as probes. A previously described YY1 binding sequence from the promoter of an unrelated gene, *rpL30* was included as a positive control (Hariharan, Kelley et al. 1991). A shifted complex was obtained for the *CYP3A4* YY1 region-derived oligonucleotide with MDCK.2 cell-derived nuclear extract (Fig. 23). The complex migrated at the same level as the YY1-DNA positive control one. The identity of the shift was confirmed with an anti-YY1 antibody, which resulted in an immunodepletion. In contrast, an anti-PXR antibody, included as a negative control, had no effect. Consistent with the low level of YY1 in LS174T cells, we did not observe a YY1 shifted complex with the corresponding nuclear extract (data not shown).

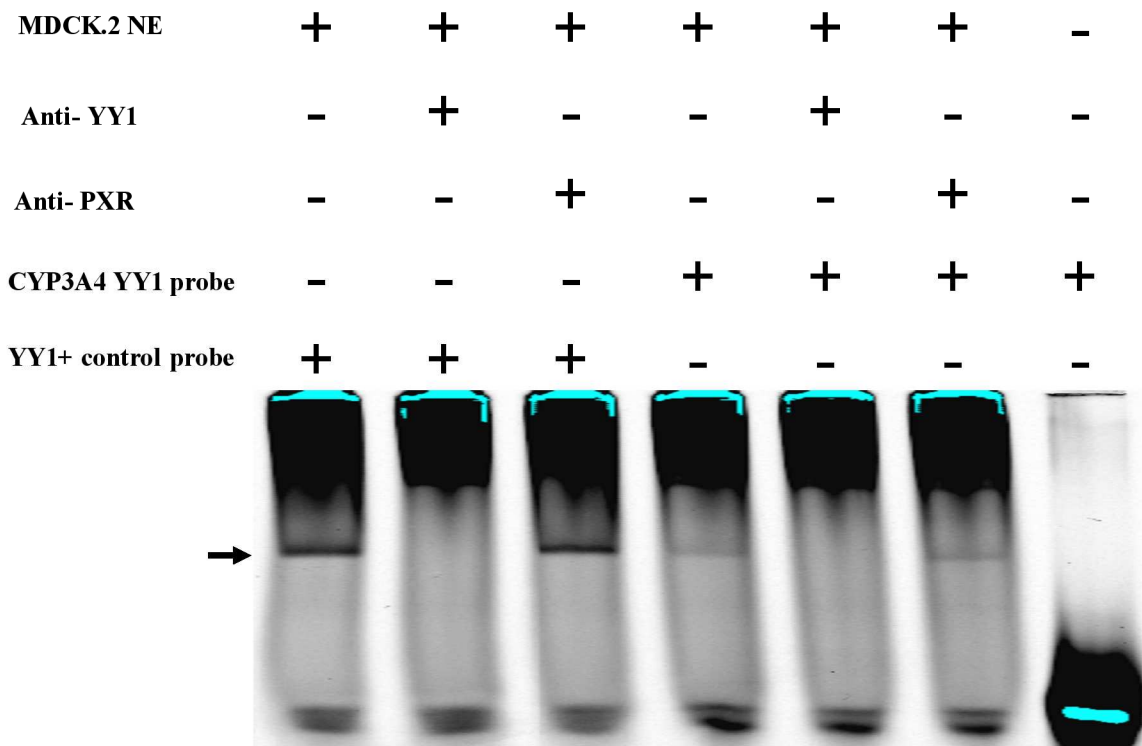


**Fig. 23. Binding of YY1 to the 57 bp element of the *CYP3A4* promoter.** Electrophoretic mobility shift assay of oligonucleotides containing the *CYP3A4*-derived YY1 binding sequence incubated with MDCK.2 cell-derived nuclear extract (NE). The rpL30 gene-derived oligonucleotide containing an unrelated, previously described (Hariharan, Kelley et al. 1991) YY1 binding site was used as a positive control. The arrow points to the YY1-DNA-binding complex. The super-shift /immunodepletion assays was performed with an anti-YY1 antibody. An anti-PXR antibody was used as a negative control. FP: free probe.

#### 4.2.8.3 Mutational analysis of the YY1 binding site in MDCK.2 cells in the *CYP3A5-57ins* construct

The functional importance of the *CYP3A4*-derived YY1 binding site was then investigated in the *CYP3A5* promoter context (*CYP3A5-57ins* construct) using mutagenesis followed by transfection into MDCK.2 cells. Statistically significant effects were observed with two mutants. The *CYP3A5-57insM1* mutant converts the imperfect YY1 core motif CAC into a consensus motif CAT such as seen in galago *CYP3A91* and marmoset *CYP3A21*. This enhanced the repression of the promoter activity conferred by the 57 bp fragment (Fig. 24). In the *CYP3A5-57insM7*, the core motif consensus dinucleotide CA was replaced with the non-consensus dinucleotide AG. Simultaneously, the dinucleotide TT outside the binding core motif, implicated in the specificity of YY1 binding (Weill, Shestakova et al. 2003), was replaced by the dinucleotide GA. This mutant not only fully abolished the repressive effect of the 57 bp region on the *CYP3A5*-driven luciferase but increased

its activity 5-fold in comparison to the wild-type CYP3A5 promoter (Figure 24). As no such excessive activity was observed with the “spacer” sequence (*CYP3A5-SPins*, Figure 18B), this suggested the existence within the 57 bp fragment of additional, as yet unidentified transcriptional enhancers which come to light after the removal of the YY1-mediated repression. In contrast, mutant *CYP3A5-57insM6*, generated to inactivate a putative E-box-like binding site (Biggs, Wan et al. 2007), overlapping with the YY1 binding site (Fig. 17), had no effect on activity. Taken together with the EMSA results, these observations demonstrated the existence within the 57 bp sequence of a transcriptionally repressive YY1 binding site.

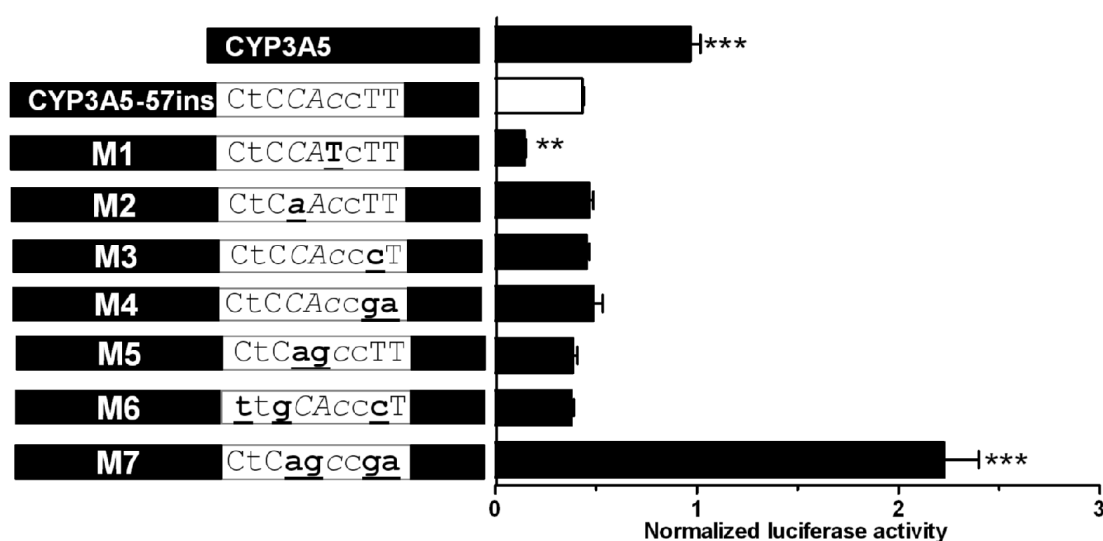


**Fig. 24. Mutational analysis of the *CYP3A4*-derived YY1 binding site in the *CYP3A5-57ins* construct.** The uppercase and lowercase letters represent preferred and tolerated nucleotides, respectively. The core motif is italicized. The bolded and underlined letters indicate the mutated nucleotides. The mutations either restore the consensus core motif (*CYP3A5-ins57M1*), or progressively disrupt the YY1 binding site (*CYP3A5-57ins*: M2 to M7). Mutants and the wild-type *CYP3A5* promoter construct were transiently transfected in MDCK.2 cells; KI. Promoter-driven firefly luciferase activities were normalized using activities of the co-transfected renilla luciferase driven by a constitutive promoter and compared to that of the *CYP3A5-ins57* construct. Data are expressed as mean values ( $\pm$ SEM) of six independent experiments conducted as triplicates. \*\* $p < 0.01$ , \*\*\* $p < 0.001$ .

#### 4.2.8.4 The effect of overexpression of YY1 on CYP3A4 promoter in LS174T and MDCK.2 cells

The above results were consistent with a role of YY1 in the suppression of the renal CYP3A4 expression. In contrast, they provided no explanation for the virtually identical activities of



*CYP3A4* and *CYP3A5* proximal promoters measured in the small intestine-derived cells LS174T (Fig. 16B). We reasoned that the discrepancy between *CYP3A4* and *CYP3A5* activities in renal and intestinal cells is bound to reflect differences in *trans*-acting factors between these cells such as the expression of transcription factors or the chromatin structure. In the most parsimonious scenario, the difference in YY1 expression in intestinal cells would suffice to abolish the effect of the YY1 binding site in the *CYP3A4* promoter. Considering the reproducibly lower mRNA YY1 level in LS174T cells in comparison to MDCK.2 cells, we tested the effect of an YY1 overexpression in both cell lines. To determine whether the putative transcriptional factor YY1 could regulate *CYP3A4* promoter activity, CMV-YY1 expression vector and *CYP3A4* promoter construct were co-transfected into LS174T and MDCK.2 cells, followed by luciferase assay. The *CYP3A4* promoter activity was significantly repressed with an overexpression of CMV-YY1 construct in LS174T cells but not in MDCK.2 cells (Fig. 25A). No such repression was observed with *CYP3A5* promoter lacking a YY1 binding site (data not shown). As shown in Fig. 25B, the *in vitro* expression of the CMV-YY1 vector suggests that this result do not reflect a lack of CMV-YY1 vector expression in the cells. Therefore, we posit that the YY1 level might be not sufficient in LS174T cells, whereas the threshold by which YY1 represses *CYP3A4* promoter in MDCK.2 may be already reached. Thus, YY1 expression level may play a role in the differential expression of *CYP3A4* promoter in LS174T and MDCK.2 cells.

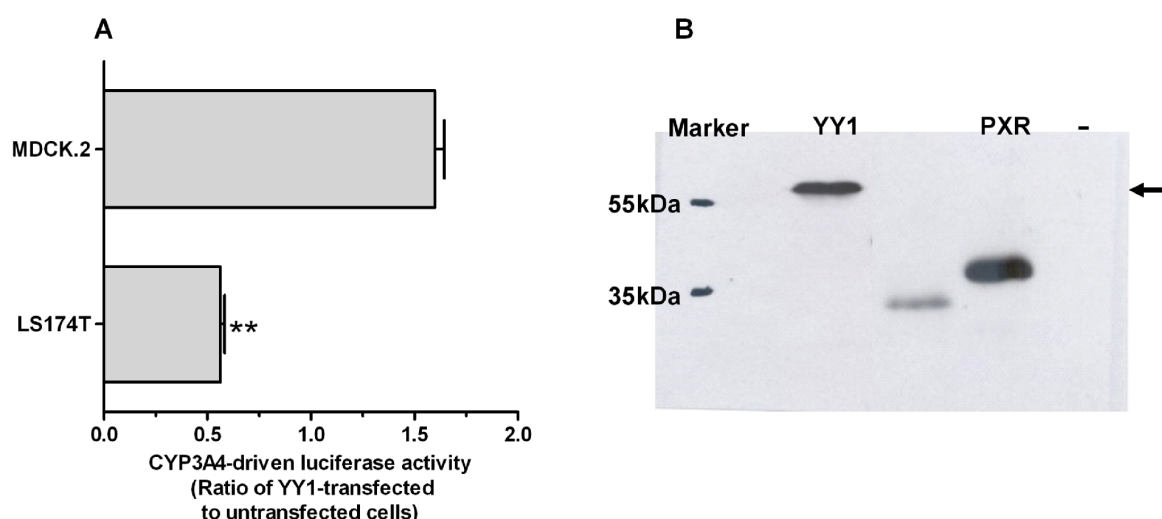


**Fig. 25. The effect of YY1 overexpression in LS174T and MDCK.2 cells.** (A) The effect of the overexpression of YY1 on the wild-type *CYP3A4* promoter construct in LS174T and in MDCK.2 cells. Promoter-driven firefly luciferase activities were normalized using activities of the co-transfected renilla luciferase driven by a constitutive promoter and compared to that of the

untransfected cells. Data are expressed as mean values ( $\pm$ SEM) of six independent experiments conducted as triplicates. **\*\*p<0.01.** (B) *In vitro* TNT expression analysis of YY1 and PXR protein.

#### 4.2.8.5 Identification of YY1 domain(s ) required for the CYP3A4 promoter inhibition

Next, we wished to determine which domain of YY1 protein is required for the repression on the *CYP3A4* promoter. YY1 consists of two acidic regions (amino acids 1-54 and 80-154) on the N-terminus separated by a histidine cluster domain (amino acids 54-80). A glycine-alanine (GA)-rich region (amino acids 154-198) is present in the middle and links to the C-terminus (amino acids 296-414) by a spacer (Fig. 26).

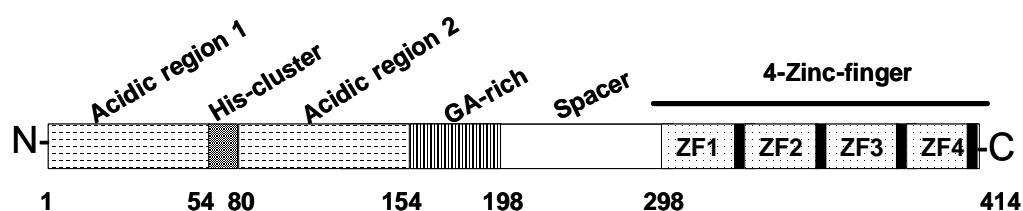


**Fig. 26. Structure of the YY1 transcription factor. Functional domains are shown.** The numbers above represent amino acid from the N-terminus to the C-terminus (from (Natesan and Gilman 1993)).

The acidic regions act as activating domains (Austen, Cerni et al. 1998). The DNA-binding domain contains four C2H2-type zinc-finger motifs that have been conserved without any amino acid changes in the past 600 million years. This feature of YY1 structure represents one of the most extreme cases for functional selection imposed on eukaryote genes (Kim, Faulk et al. 2007). Notably, previous studies indicated that the binding domain near the carboxyl terminus; including zinc finger 3 and 4 is involved in repression (Bushmeyer, Park et al. 1995). Furthermore, the Gly/Ala-rich region also represses gene via a protein-protein interaction mechanism (Lewis, Tullis et al. 1995; Yang, Inouye et al. 1996; Weill, Shestakova et al. 2003). Consistent with the well-recognized function of YY1 as transcription repressor factor, we tested the YY1 domains required for the YY1 repression on the *CYP3A4* promoter. To this end, we transiently transfected YY1 wild-type, YY1 deletion mutants (Fig. 27A) and *CYP3A4* promoter into LS174T cells.

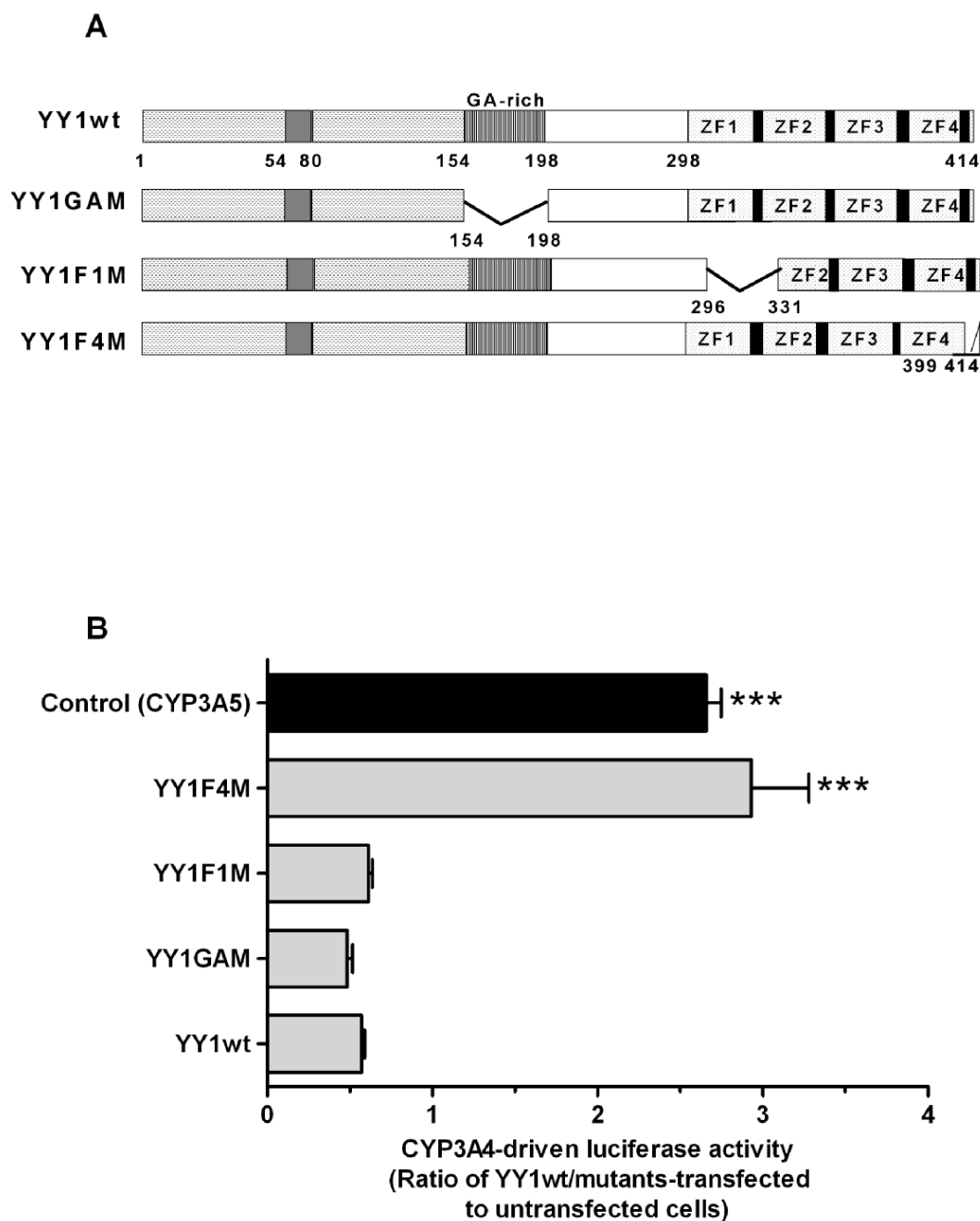


**Fig. 27. The effect of the wild-type and mutated YY1 proteins on the *CYP3A4*-driven luciferase construct.** (A) Illustration of mutants and wild-type YY1 constructs. (B) Mutants and the wild-type YY1 expression construct were transiently co-transfected with the wild-type *CYP3A4* promoter construct in LS174T cells. Data are shown as mean ratios ( $\pm$ SEM) of firefly luciferase activity in YY1/mutants-transfected vs. untransfected cells. Firefly luciferase activities in the individual wells were normalized using activities of the co-transfected renilla luciferase driven by a constitutive promoter. \*\*\*  $P < 0.001$ .

As shown in Fig. 27B, comparable activities were obtained between the YY1GAM mutant and the YY1wt. The deletion of the Gly/Ala-rich region did not alter the repressive effect of YY1 on the *CYP3A4* promoter. The same result was observed with the mutation of the first zinc-finger (YY1F1M). Notably, the Gly/Ala-rich region lies outside of the DNA binding domain and generates protein still able to bind DNA (Austen, Cerni et al. 1998). Therefore, in this context, YY1 does not require this region or any cell-specific interaction of YY1 with other proteins for the transcriptional repression of *CYP3A4* promoter. However, deletion affecting Zn-Finger 4 (YY1F4M mutant) and carboxyl terminus region abolish repressive effect of YY1. These results indicated that the distal DNA binding domain is required for binding and repression of the *CYP3A4* promoter by YY1.

#### 4.2.8.6 Mutational analysis of the YY1 binding site in LS174T cells in the *CYP3A4* construct

We showed above that repression by YY1 requires an intact distal DNA binding domain. Next, we verified whether any repression could be observed in the context of basal expression of YY1 in LS174T cells. Indeed, mutations of the YY1 site tested previously in MDCK.2 cells in a *CYP3A5* promoter context (Fig. 24), showed an identical response profile in the *CYP3A4* promoter tested in intestinal cells (Fig. 28 and data not shown).

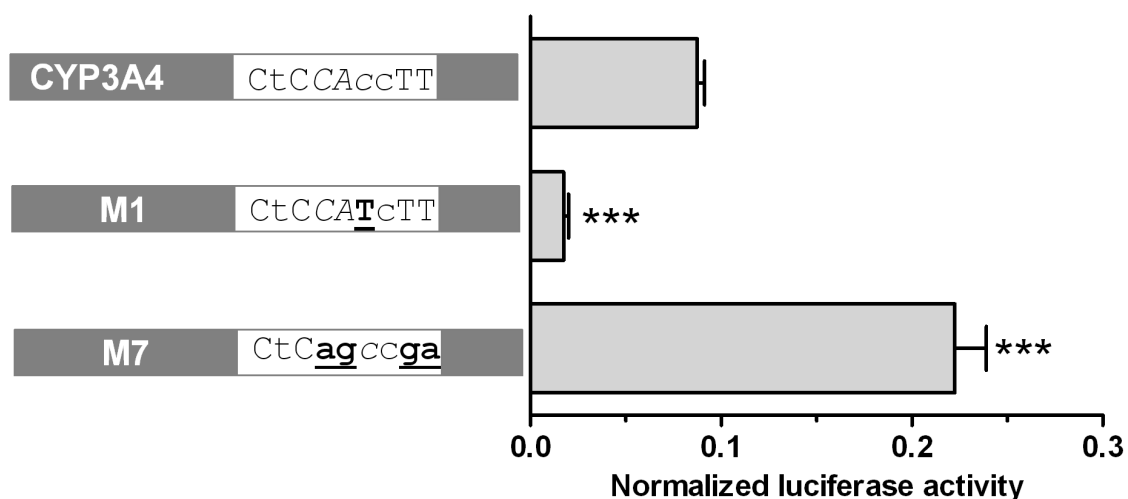


**Fig. 28. Mutational analysis of the YY1 binding site within the human *CYP3A4* promoter.** The uppercase and lowercase letters represent preferred and tolerated nucleotides, respectively. The core motif is italicized. The bolded and underlined letters indicate the mutated nucleotides. The mutations either restore the consensus core motif (*CYP3A4-M1* construct), or disrupt the YY1 binding site (*CYP3A4-M7*). Mutants and the wild-type *CYP3A4* promoter construct were transiently transfected in

LS174T cells. Promoter-driven firefly luciferase activities were normalized using activities of the co-transfected renilla luciferase driven by a constitutive promoter and compared to that of the wild-type *CYP3A4* construct. Data are expressed as mean values ( $\pm$ SEM) of four to eight independent experiments conducted as triplicates. \*\*\* $p < 0.001$ .

Thus, the restoration of the consensus YY1 core motif (*CYP3A4-M1*) significantly reduced, whereas the disruption of the site (*CYP3A4-M7*) increased the *CYP3A4* promoter activity. Taken together with the YY1 overexpression analysis (Fig. 25), these results suggest similar effects of YY1 in renal and intestinal cells, arguing against the importance of this factor in the differential expression of *CYP3A4* in the kidney and small intestine. Therefore, we addressed the importance of the transcriptional CYP3A regulator PXR, which is expressed in the small intestine, but not in the kidney (Koch, Weil et al. 2002; Lamba, Yasuda et al. 2004; Nishimura, Naito et al. 2004). We speculated that PXR may offset the inhibitory effect of YY1 on the *CYP3A4* expression in the small intestine. In this case, a similar effect could reasonably be expected from renal cells transfected with PXR.

#### **4.2.9 The Effect of PXR on the differential activity of CYP3A4 and CYP3A5 promoters**

The importance of the endogenous PXR activity was investigated with *CYP3A4* promoter and chimeric *XREM-CYP3A4* construct. As shown in Fig. 29A, the co-transfection of a PXR-expressing construct had only a weak (two-fold increase) and statistically not significant effect on the activity of the proximal *CYP3A4* promoter. We therefore co-transfected into MDCK.2 cells PXR together with the proximal *CYP3A4* promoter extended by the PXR-responsive enhancer XREM present in the *CYP3A4*, but not in the *CYP3A5* distal promoter. In this case, PXR resulted in a 13-fold increase in the luciferase activity (Fig. 29A). Notably, the XREM inclusion had no effect on the luciferase activity in the absence of PXR co-transfection.

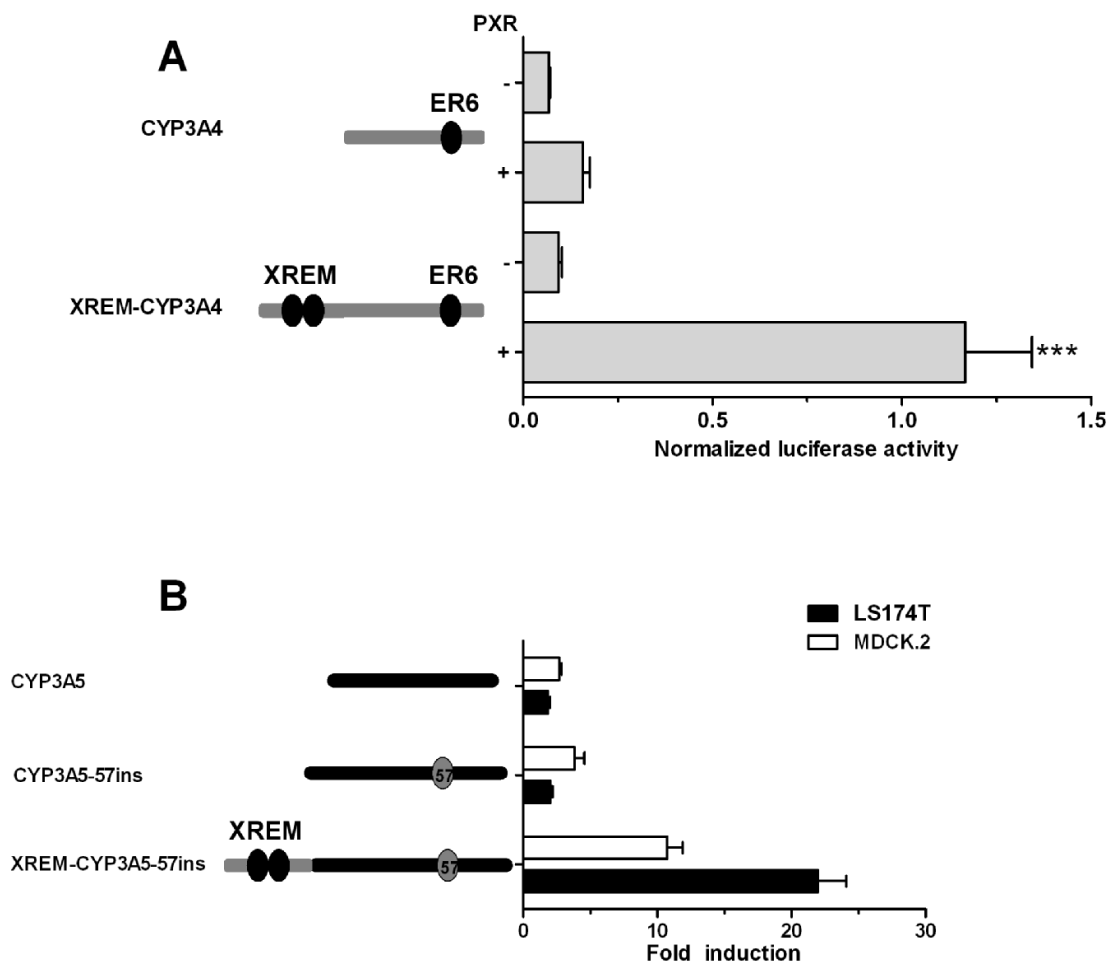


**Fig. 29. The effect of PXR overexpression on the *XREM-CYP3A4*- and *XREM-CYP3A5-57ins*-driven luciferase activity.** (A) The wild-type *CYP3A4* and the chimeric *XREM-CYP3A4* promoter constructs were transiently co-transfected with the PXR expression vector in LS174T cells. (B) The wild-type *CYP3A5*, the *CYP3A5-57ins* and the chimeric *XREM-CYP3A5-57ins* promoter constructs were transiently co-transfected with the PXR expression vector in either LS174T or MDCK.2 cells. Promoter-driven firefly luciferase activities were normalized using activities of the co-transfected renilla luciferase driven by a constitutive promoter and compared to that of the *CYP3A4* construct. Data are expressed as mean values or fold induction ( $\pm$ SEM) of four independent experiments conducted as triplicates. \*\*\* $p < 0.001$ .

This demonstrated that PXR may indeed override the inhibitory effect of YY1 on the *CYP3A4* expression and that this effect is mostly mediated by the enhancer XREM rather than by the PXR-responsive elements of the proximal promoter such as ER6. In addition, we evaluated the role of the deletion of both XREM and the 57 bp fragment from *CYP3A5* promoter in both MDCK.2 and LS174T cells. A previous study indicated that deletion of XREM and the 57 bp fragment

containing YY1 repressive system from the *CYP3A5* gene lineage had occurred simultaneously in evolutionary terms (Fig. 2). By using the chimeric *XREM-CYP3A5-57ins*, we wished to mimic the putative original scheme of *CYP3A5* promoter, containing both the XREM and the 57 bp fragment. As shown in Fig. 29B, similarly to the chimeric *XREM-CYP3A4*, the chimeric *XREM-CYP3A5-57ins* construct was induced 10-fold in MDCK.2 cells. A 22-fold activation was observed in LS174T cells. The relatively high PXR induction of the chimeric construct *XREM-CYP3A5-57ins* in LS174T cells reflects its endogenous PXR expression (Burk, Koch et al. 2004). Therefore, the putative “ancestral primate *CYP3A5*” may have been potentially able to elicit a stronger PXR activation similar to that of the contemporary *CYP3A4* promoter.

#### **4.2.10 Functional characterization of the human *CYP3A4*-NF1 binding site**

Our data indicated that other factors different from PXR may activate *CYP3A4* regardless cell lines. In agreement with our hypothesis, we first observed that deletion of the 57 bp fragment from the wild-type *CYP3A4* increased activity of the resultant *CYP3A4-57del* construct by 4-fold in renal cells (Fig. 18A) which are known to do not express PXR. Secondly, a complete disruption of the YY1 binding site in the context of *CYP3A5-57ins* increased activity by 5-fold in renal cells (Fig. 24). Together, these results indicated existence of activating element (s) different from PXR element (s) within or/and upstream of the 57 bp fragment. Therefore, we reasoned that YY1 may repress also other activating factors in renal cells. One of our serious candidate for *CYP3A4* activation seems to be the NF1 element which is adjacent to the YY1 binding site (Fig. 17) and well conserved within all primate *CYP3A4* genes (Fig. 20B). Interestingly, it has been demonstrated that among NF1 isoforms, NF1A1.1, NF1B2, NF1C1, NF1C2 and NF1X1 *trans*-activated the *CYP3A4* promoter (Riffel, Schuenemann et al. 2009). NF1 is a basic transcription factor involved in the *trans*-activation of many genes. The NF1 isoforms are generated through alternative splicing of the four NF1 genes (NF1-A, -B, -C, and -X). They are ubiquitously expressed in most tissue types (Chikhirzhina, Al'-Shekadat et al. 2008). NF1 may also play a role in the system that overrides the repressive effect of YY1 on the *CYP3A4* promoter in intestinal cells. Therefore, we focused on the putative function of the NF1 on intestinal and renal activity of *CYP3A4* promoter.

#### 4.2.10.1 Endogenous and overexpression analysis of NF1 in LS174T and MDCK.2 cells

In spite of the reported ubiquitous expression of NF1 (Gronostajski 2000), we evaluated the expression of NF1 in LS174T and MDCK.2 cells. A concomitant expression of NF1 at the level of mRNA and protein in a related intestinal epithelial cells has been established (Xu, Uno et al. 2005). Therefore, the expression of NF1 was examined only at the level of mRNA by RT-PCR, using specific NF1 primers. Similar NF1 mRNA levels were obtained in both LS174T and MDCK.2 cells (Fig. 30A). This result prompted verification of the transcriptional *trans*-activation of *CYP3A4* promoter by NF1 in both cell lines. We tested the effect of an NF1 overexpression in LS174T and MDCK.2 cell lines using an NF1A1.1 expression vector. A co-transfection of the NF1A1.1 expression vector in LS174T and MDCK.2 cells increased significantly the *CYP3A4*-driven luciferase activity both cell lines (Fig. 30B), whereas no such effect was observed with *CYP3A5* lacking a NF1 binding site. This result suggests similar *trans*-activation effects of NF1 in renal and intestinal cells.

#### 4.2.10.2 Mutational analysis of the NF1 binding site

It is well known that NF1 stimulates transcription by maintaining a specific chromatin structure open to render the gene competent for transcription and by transmitting the regulatory signal to the transcription machinery (Gronostajski 2000). NF1 binds as a dimer to a dyad symmetric motif TTGGC(N<sub>5</sub>)GCCAA or its variants on DNA duplex (Gronostajski 2000). NF1 factor has been shown to recognise specifically the *CYP3A4-NF1* derived binding site within the *CYP3A4* promoter (Saito, Takahashi et al. 2001; Riffel, Schuenemann et al. 2009). To confirm the putative activating role for NF1, mutation analysis of the NF1 binding site was performed with the wild-type *CYP3A4* and the *CYP3A4-57del*. Specific mutations that abolish completely the NF1 binding were also introduced in both half-sites of NF1 within the wild-type *CYP3A4* promoter using mutagenesis. The resulting *CYP3A4-NF1M* mutant, the *CYP3A4-57del* and the *CYP3A4* wild-type were transiently transfected into LS174T and MDCK.2 cells. In LS174T cells, the *CYP3A4-57del* luciferase activity was significantly reduced by 50%. This result indicates that putative activating element (s) within the 57 bp fragment is required for intestinal activation of *CYP3A4* promoter.



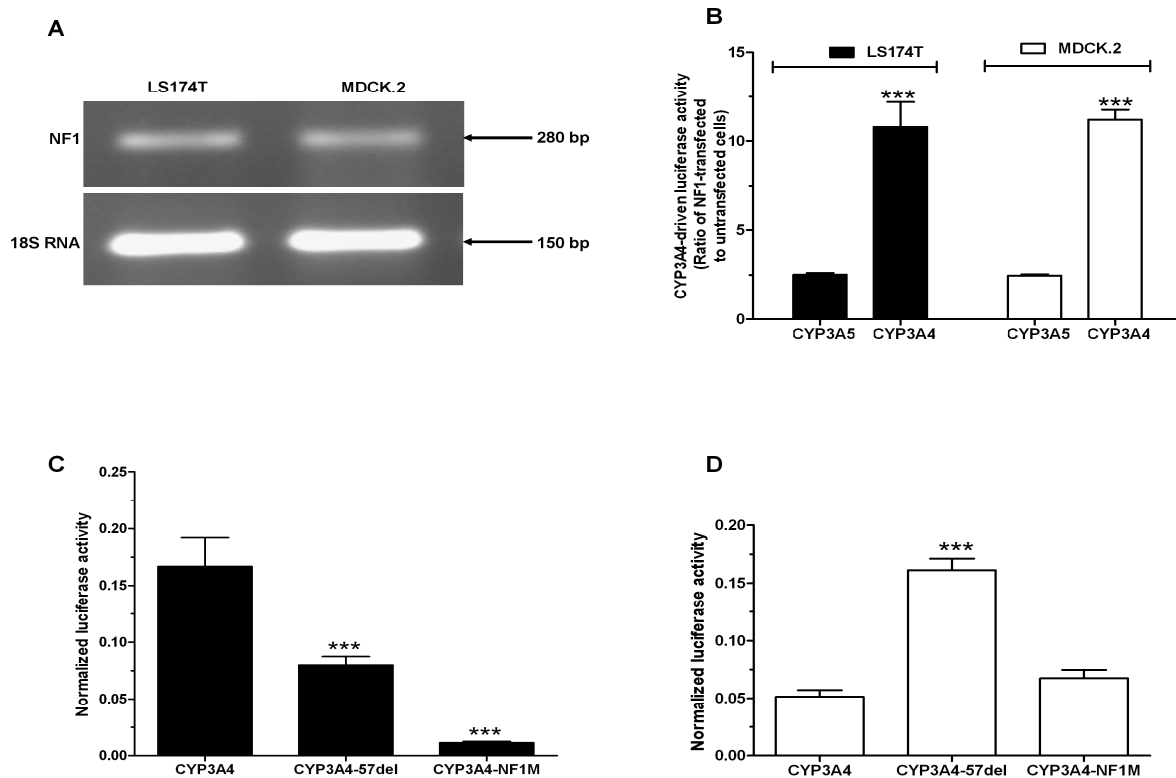


**Fig. 30. Functional analysis of the NF1 binding site within the wild-type *CYP3A4* construct.**

(A) RT-PCR analysis of the endogenous level of NF1 mRNA in LS174T and MDCK.2 cells. The expression of 18S RNA was measured in parallel as an internal control. PCR products were separated by electrophoresis on a 1.5% agarose gel. Numbers on the right indicate the lengths of the amplicons. (B) The effect of NF1 overexpression on the *CYP3A4*-driven luciferase activity in LS174T and MDCK.2 cells. LS174T and MDCK.2 cells were co-transfected with the wild-type *CYP3A4*, the NF1 (NF1A.1 isoform) expression vector and the control (*CYP3A5* promoter) constructs. Data are shown as mean ratios ( $\pm$ SEM) of firefly luciferase activity in NF1A.1-transfected vs. untransfected cells. (C and D) Mutational analysis of the NF1 binding site within the human *CYP3A4* promoter (C) in LS174T and (D) in MDCK.2 cells. Mutants (the *CYP3A4-57del* and the *CYP3A4-NF1M*) and wild-type *CYP3A4* constructs were transiently transfected in LS174T cells. Promoter-driven firefly luciferase activities were normalized using activities of the co-transfected renilla luciferase driven by a constitutive promoter and compared to that of the *CYP3A4* construct. Data are expressed as mean values ( $\pm$ SEM) of four independent experiments conducted as triplicates. Firefly luciferase activities in the individual wells were normalized using activities of the co-transfected renilla luciferase driven by a constitutive promoter. \*\*\* $p < 0.001$ .

Our data are also consistent with the observation showing that NF1 may retain the capability to activate transcription by interacting with either half binding site, although with lower affinity (Meisterernst, Gander et al. 1988). Importantly, the *CYP3A4*-NF1M mutant (with both NF1 halves site mutated) activity was sharply lowered by about 93% as compared with the wild-type *CYP3A4* promoter (Fig. 30C). In MDCK.2 cells, the YY1 repression system may inhibit the NF1 *trans*-activation by further lowers *CYP3A4* promoter activity. In support of this hypothesis, the deletion of the 57 bp containing YY1 repression system led to 4-fold increase of the *CYP3A4*-57del activity and argue in favour of a free *trans*-activation by the NF1. While no change in activity was observed with the *CYP3A4*-NF1M mutant, whereby YY1 binding site is intact but the NF1 binding site completely destroyed (Fig. 30D). Together, the NF1 activity is essential for the basal activity of *CYP3A4* promoter in both intestinal and renal cells.

## 5. Discussion

### 5.1 *In vivo* regulation of CYP3A5 promoter in the small intestine

Considering the expression of CYP3A5 in several steroidogenic organs, reports of its induction by PXR seemed paradoxical, as enhanced CYP3A5 activity could affect the steroid homeostasis. Admittedly, it has been noticed that aside from liver and small intestine, CYP3A5 is expressed exclusively in organs devoid of PXR expression (Koch, Weil et al. 2002), so that induction could be restricted to the former two organs. However, this in turn raises questions about the mechanism of CYP3A5 expression outside liver and small intestine, as the importance of PXR in CYP3A regulation is paramount. In the present work we illuminate these issues by demonstrating that the expression of CYP3A5 in most organs expressing this enzyme is indeed independent from PXR and in consequence irresponsive to the latter one's ligands, at least in transgenic mice. This constitutes a first description of uncoupling induction from constitutive expression for a major detoxifying enzyme, and of the underlying mechanism.

We have first established two strains of mice transgenic for a plasmid expressing firefly luciferase driven by a 6.2 kb of the human *CYP3A5* promoter to investigate the regulation of the human *CYP3A5* promoter *in vivo*. The two strains of the *CYP3A5*-luc mice exhibited similar tissue distribution of the *CYP3A5* transgene activity, suggesting the negligible confounding effects by the random insertion on our results. Contrary to the transgenic *CYP3A4* mice (Zhang, Purchio et al. 2003), no gender-specific effects were observed on the transgene expression. These mice appear to be good models for the wide tissue expression of CYP3A5, in that the 6.2 kb promoter driven reporter gene expression in almost all examined tissues, especially in the small intestine. The only major difference is the absence of luciferase expression in the liver, which suggests the existence of a liver-specific enhancer outside the promoter fragment used for transgenesis. There is increasing evidence that gene clusters are co-regulated (Singer, Lloyd et al. 2005) and it is tempting to speculate that the liver expression of CYP3A5 may require an enhancer shared with the other *CYP3A* genes, which form a cluster on chromosome 7 (Fig. 4). This possibility is consistent with the existence of the functional liver-specific enhancer CLEM identified only in the distal region of *CYP3A4* upstream promoter (Fig. 2). This module mediates the constitutive expression of *CYP3A4* by cooperating with multiple liver-enriched factors, such as HNF1- $\alpha$ , HNF4- $\alpha$ , USF1 and AP-1 (Matsumura, Saito et al. 2004). The transgenic mice carrying a *CYP3A4* promoter encompassing this region exhibited activity of *CYP3A4* in the liver (Robertson, Field et al. 2003; Zhang, Purchio et al. 2003). It is not known whether this module also determined the postulated common

regulatory pathway for the constitutive expression of *CYP3A4* and *CYP3A5* genes in liver (Lin, Dowling et al. 2002). Alternatively, some DNA segments within the 6.2 kb fragment of the human *CYP3A5* promoter might mediate a hepatic-repression in the mouse. Such effects resulting from heterologous expression of human *CYP3A4* promoter has been observed in the kidney by Zhang and colleagues (2003). In any case, further investigations of the *CYP3A5* are needed to explain why *CYP3A5* transgene activity is not observed in mouse livers. Due to the overlapping expression of *CYP3A5* and *CYP3A4* in small intestine, there is increased need for animal models that allow investigation of the relative contribution of *CYP3A5* in xenobiotic induction in the small intestine *in vivo*. The distribution of the transgene activity along the small intestine of *CYP3A5*-luc transgenic mice models we have established reflects that of *CYP3A* expression along the human gastrointestinal tract (McKinnon, Burgess et al. 1995). These models are therefore considered suitable for the study of *in vivo* induction of *CYP3A5* in the small intestine.

Hepatic and intestinal *CYP3A5* induction is considered to be mediated by PXR and CAR via a mechanism similar to that of *CYP3A4* induction (Burk, Koch et al. 2004). In addition, the host cellular factors determine in part gene expression (Barwick, Quattrochi et al. 1996). Therefore, *CYP3A5*-luc mice were injected i.p. with either PCN (a murine PXR) or TCPOBOP (a murine CAR) inducers to investigate the induction of *CYP3A5* promoter *in vivo*. Besides induction of the *CYP3A5* transgene in all parts of the small intestine, we observed that *CYP3A5* promoter was activated in dose-dependent but not in time-dependent manner. However no induction was observed in kidney. The differential changes in luciferase activity in the kidney and small intestine in response to the mouse PXR agonist PCN is in agreement with the observations by Cheng and Klaassen, who detected an intestinal, but not renal, induction of the mouse gene *Cyp3a11* in response to the same compound (Cheng and Klaassen 2006). Since the PXR expression in human kidneys is either non-detectable or at least much lower than in mouse kidneys, we infer that *CYP3A5* in human kidneys is similarly irresponsive to PXR activators. This is consistent with the failure of the agonist of the human PXR rifampicin to affect the renal activity of the PXR target P-glycoprotein in human subjects (Greiner, Eichelbaum et al. 1999). In turn, the small-intestinal induction of *CYP3A5* in our transgenic mice in response to PCN is in agreement with the upregulation of this gene in small intestines of humans treated with the agonist of the human PXR rifampicin (Burk, Koch et al. 2004). Besides the kidney, *CYP3A5* induction was also absent from the adrenal gland and lung (data not shown), i.e. tissues, which in humans and mice exhibit none or at best a very low level of PXR (Bertilsson, Heidrich et al. 1998; Blumberg, Sabbagh et al. 1998; Kliewer, Moore et al. 1998; Lehmann, McKee et al. 1998; Koch, Weil et al. 2002; Lamba, Yasuda et al. 2004; Nishimura, Naito et al. 2004; Su, Wiltshire et al. 2004). This suggests that the *CYP3A5*

expression in human organs unrelated to xenobiotic response (i.e. other than small intestine and liver) may be generally unresponsive to PXR-mediated induction, as already demonstrated for the kidney (Greiner, Eichelbaum et al. 1999). Regardless polymorphism of CYP3A5, we confirm that *CYP3A5* promoter is induced *in vivo* in the small intestine of transgenic mice. The discrepancy observed by Busi and Creistel (2005) may reflect the effect of a faster mRNA decay in *CYP3A5*\*3/\*3 carriers than in *CYP3A5*\*1 carriers. Even if caution should be taken when extrapolating from transgenic mice to the human situation. The present report provides once more evidence for the *in vivo* induction of the *CYP3A5* in the small intestine.

## **5.2 Differential regulation of the human CYP3A4 and CYP3A5 proximal promoters in renal and intestinal cells**

*CYP3A5* exhibits an organ expression and activities overlapping, but also different from the other major postnatal CYP3A isoform, *CYP3A4*. Most strikingly, *CYP3A5* is expressed in several organs beyond *CYP3A4*. From a medical point of view, the broader *CYP3A5* expression, especially in the kidney, could be relevant to side effects of drugs metabolized by *CYP3A5*, and as a risk factor for hypertension. These considerations warranted a detailed study of the determinants of the differential expression of *CYP3A5* and *CYP3A4* in this organ. To this end, we first established a two-cell line model comprising the small intestine-derived LS174T cells and the kidney-derived MDCK.2 cells. The LS174T cells have been repeatedly validated as a faithful model of the basal and drug-induced CYP3A expression in the small intestine (Cervený, Svecová et al. 2007; Novotná, Doricáková et al. 2010; Qiu, Mathas et al. 2010). The MDCK.2 cells exhibit many characteristics of the collecting duct cells, a principal site of *CYP3A5* expression in the kidney (Aleksa, Matsell et al. 2005). Transfected with *CYP3A4* and *CYP3A5* promoter constructs, these cell lines fully reflected the expression relationships between these genes in the kidney and small intestine (Koch, Weil et al. 2002), with both genes expressed at similar levels in small intestinal, and *CYP3A5* only in renal cells.

## **5.3 Evolution of the YY1 binding site within the CYP3As promoters**

YY1 is a ubiquitously expressed and evolutionary conserved member of the GLI-krüppel family of zinc finger transcription factors (Shi, Lee et al. 1997), which have been implicated in the transcriptional regulation of numerous genes important for cell proliferation, differentiation, and

metabolism (Luke, Sui et al. 2006). YY1 gene is localized in the telomere region of human chromosome 14 at segment q32.2 (Yao, Dupont et al. 1998). Depending upon the promoter context, YY1 can function either as a transcriptional activator or repressor (Shi, Lee et al. 1997), with the latter function apparently applying to CYP3A. The CYP3A YY1 binding site predates primate origin and its suppressing function seems to be conserved across primates, as demonstrated by a comparison of the ortholog elements from the human and galago. It is tempting to speculate that this genomic element originally may have helped to restrict the tissue spectrum of CYP3A expression. This may have been important for the homeostasis of endobiotics such as steroid hormones, some of which are CYP3A substrates (e.g., testosterone, corticosterone, progesterone and androstenedione) (Morris, Latif et al. 1998; Yamakoshi, Kishimoto et al. 1999; Henshall, Galetin et al. 2008).

The deletion of the 57 bp element from the CYP3A5 gene lineage occurred early in *Haplorrhini* following the separation from *Strepsirrhini* via one of two alternative two-step scenarios. In one scenario, the first step comprises the more distal 25 bp and occurs in the common ancestor of *Tarsiiformes* and *Simiiformes* (before 57 MYA), as indicated by a 25 bp deletion found in one of the two tarsier genes. Following the separation of *Tarsiiformes* and *Simiiformes*, the more proximal part was subsequently lost in a common ancestor of the latter infraorder. This occurred not later than 40 MYA, since the 57 bp deletion is detected in both parvorders of *Simiiformes*, i.e. in Old World monkeys (human, chimpanzee, rhesus), and in New World monkeys represented by the marmoset. The second scenario comprises two independent deletions of different lengths, but of the same distal boundary occurring in *Tarsiiformes* and *Simiiformes* following their separation (Fig. 19A). In either case, the 57 bp fragment was lost from the entire CYP3A5 gene repertoire and not inserted into the human CYP3A4 promoter, as suggested previously by a comparison of exclusively human CYP3A4 and CYP3A5 sequences (Lin, Dowling et al. 2002; Biggs, Wan et al. 2007).

#### **5.4 The CYP3A5 proximal promoter had acquired an altered ancestral function**

Gene duplications constitute an important source of innovation and adaptation. Novel gene function associated with gene duplication can arise from either neofunctionalization (NEO-F) or escape from adaptative conflict (Schuetz, Beach et al. 1994). In the NEO-F, after the gene duplication one copy maintain ancestral function, whereas the other undergoes directional selection to perform a novel function. Alternatively, in the EAC, a single copy of the gene is selected to improve either novel or ancestral function (Des Marais and Rausher 2008). Functional analyses of

closely related sequences to the ancestral could help illuminating the evolution of an ancestral gene expression (Gu, Zhang et al. 2005). Analysis of chimeric *XREM-CYP3A5-57ins* (Fig. 27B), *CYP3A5-G91ins* and *CYP3A5-G92ins* (Fig. 19B) indicated that the ancestral *CYP3A5* was potentially able to function like *CYP3A4* promoter. Following the deletion of the 57 bp fragment from *CYP3A5* a sequence rearrangement had led to the generation of a NF-Y binding site unique to *CYP3A5* proximal promoter. Introduction of mutation in this site caused 96% and 80% decrease of activity in HepG2 (Iwano, Saito et al. 2001) and lung A549 cells (Biggs, Wan et al. 2007), respectively. The ubiquitously expressed NF-Y was then suggested to be required for the constitutive expression of *CYP3A5* especially in extrahepato-intestinal organs lacking PXR. We also observed such decrease in activities in either renal or intestinal cells (data not shown). Together, the generation of a functional NF-Y binding site, the deletion of XREM and the 57 bp fragment may have conferred *CYP3A5* with a fitness advantage of tissue expression.

## 5.5 Identification of factors overriding YY1 inhibitory effect in *CYP3A4*-expressing organs

Although this work focuses on *CYP3A5*, some of our observations illuminate the regulation of *CYP3A4*, which is expressed concomitantly with *CYP3A5* in the liver and small intestine. Considering the ubiquitous expression of YY1, the presence of a transcriptionally repressive YY1 element in the *CYP3A4* promoter seemed to be at odds with the expression of *CYP3A4* in these organs. Subsequent experiments designed to resolve this contradiction suggest that the inhibitory effect of YY1 on *CYP3A4* promoter activity is overridden, at least in small-intestinal cells, by the concerted action of one *trans*- and one *cis*-acting factor. We have identified these factors using MDCK.2 cells, which normally do not support *CYP3A4* expression, due to the inhibitory effect of the YY1 on its promoter, demonstrated above. Through expression of the transcriptional *CYP3A* regulator and xenobiotic sensor PXR, we conferred onto these cells a capability to express *CYP3A4*. PXR is normally expressed in the small intestine, but not in the kidney (Koch, Weil et al. 2002; Lamba, Yasuda et al. 2004; Nishimura, Naito et al. 2004). Besides PXR, the expression of *CYP3A4* in MDCK.2 cells required the presence of the PXR-responsive, *cis*-acting element XREM, located in the distal part of the *CYP3A4* promoter. Together with the proximal ER6 (Fig. 16) and the far-distal CLEM, XREM represents the original scheme of *CYP3A* regulation by nuclear receptors such as PXR in placental mammals (Qiu, Mathas et al. 2010).

The need to offset the inhibitory effect of YY1 may have been the force driving both the conservation of XREM and the origin of novel PXR-responsive elements outside XREM in the

*CYP3A4* gene lineage (Qiu, Mathas et al. 2010). Conversely, the loss of XREM from the *CYP3A5* gene lineage (Qiu, Mathas et al. 2010) may reflect reduced negative selection acting on XREM, conferred by the loss of YY1.

The XREM-mediated, *CYP3A4* expression-promoting effect of PXR may have been additionally facilitated by the apparent attenuation of the YY1 inhibitory effect. This attenuation is conferred by the mutation of the YY1 consensus site core sequence CAT->CAC, which is present in all *Haplorrhini CYP3A* genes containing this element, except the pseudogene *CYP3A43*. The importance of this mutation was suggested by the diminished score values and confirmed by mutagenesis. The results of this latter experiment suggest that the sequence change in the YY1 core sequence may contribute to the high expression level of *CYP3A4* in humans. The differential expression of *CYP3A4* and *CYP3A5* in the small intestine and kidney represents the combined effect of the loss of the YY1 binding element from the *CYP3A5* promoter together with the differential organ expression of PXR and the higher accumulation of ancestral PXR response elements in *CYP3A4*. The identification of the advantage conferred by this mechanism requires a better characterization of its applicability to other *CYP3A5*-expressing organs and of the physiological *CYP3A5* function outside the hepato-intestinal system.

The expression of PXR, acting in *trans*, thus appears to be an indispensable determinant of the *CYP3A4* expression in organs such as small intestine. However, PXR expression alone might be not the reason explaining higher basal *CYP3A4* expression in intestinal cells as well as the repression activity of YY1 on *CYP3A4* promoter in renal cells. The specific distribution of receptor elements within the *CYP3A4* promoter indicates their importance in the transcriptional regulation. Due to the well-recognized function and ubiquitous expression of NF1, we assumed that NF1 might be another strong candidate for the basal activation of the *CYP3A4* promoter in LS174T cells. NF1 stimulates transcription by maintaining a specific chromatin structure open to render the gene competent for transcription and by transmitting the regulatory signal to the transcription machinery (Chikhirzhina, Al'-Shekadat et al. 2008). Similar to Riffel and colleagues (2009), NF1A1.1 *trans*-activates *CYP3A4* promoter in both LS174T and MDCK.2 cells. Additionally, introduction of a mutation in the NF1 binding site in the *CYP3A4* promoter indicates that NF1 is vital for the *CYP3A4* activity in LS174T cells. It appears also that inhibition of the NF1 activity by the YY1 repressing mechanism might be the reason for the repression of *CYP3A4* activity in renal cells. Together, the basal intestinal *CYP3A4* activity is under the net control of several transcription factors as opposed to a single transcription factor.



## 5.6 The physiological significance of the YY1 binding site from the *CYP3A5* proximal promoter

In the light of our data, the differential expression of *CYP3A5* and *CYP3A4* in renal cells appears to be primarily enabled by the deletion from the *CYP3A5* promoter of an element binding the transcriptional regulator YY1. This is supported by several lines of complementary evidence. Thus, the 57 bp fragment comprising a consensus YY1-binding site suppresses the activity of *CYP3A4* in renal cells, as evidenced by *CYP3A4* derepression following its deletion. Conversely, the same genomic fragment inserted into the *CYP3A5* promoter can inhibit its transcriptional activity. The specific involvement of YY1 in these effects is evidenced by the effects of its mutagenesis, which mimic the transcriptional effects of the entire 57 bp fragment. Thus, mutations designed to disrupt the YY1-binding site increase the activities of the *CYP3A4* and *CYP3A5* promoters, whereas optimizing the core sequence of the YY1 site has an opposite effect. Lastly, this sequence binds YY1 (Saito, Takahashi et al. 2001), as confirmed in our study. We speculate that the loss of the YY1-mediated transcriptional repression may have enabled the constitutive *CYP3A5* expression in all organs expressing this enzyme aside from liver and small intestine. This speculation is strongly supported by the findings by Biggs and colleagues (2007), which provided one of the starting points and many experimental ideas for our investigation. These workers demonstrated a derepression of a *CYP3A5* promoter activity in a lung-derived cell line upon deletion of the same 57 bp fragment as in our study. Likewise, our results from transgenic mice do not formally prove the role of YY1 in the differential expression of *CYP3A4* and *CYP3A5* in human organs. They were conducted primarily to test the prediction of the differential organ induction of *CYP3A5*. However, this role is strongly suggested by the accumulating data on the effects of the YY1 site on promoter activity in cell lines derived from three relevant human organs (lung (Biggs, Wan et al. 2007), small intestine, and kidney). Taken together, YY1 formally affects the activity of *CYP3A* promoters analyzed in cell lines. However, its effects are fully consistent with the available information on the differential organ expression and induction of *CYP3A5* and *CYP3A4* *in vivo*. The loss of the YY1-mediated transcriptional repression may have thus allowed for the widening of the *CYP3A5* tissue expression in the absence of induction. This has allowed on the one hand, for avoiding the deleterious effects of *CYP3A5* induction on the homeostasis of any endogenous substrates of the *CYP3A5* protein, such as steroids. On the other hand, the *CYP3A5* expression outside the liver and small intestine must have conferred fitness advantages, which remain to be identified. Renal *CYP3A5* expression may have enhanced salt and water retention mediated by *CYP3A5*-catalyzed 6 $\beta$ -hydroxycortisol, which may have been advantageous in a hot climate. This mechanism has been suggested to be responsible for the high prevalence of the gene

polymorphism-driven CYP3A5 expression in Africans, most of which express CYP3A5 in the kidney, perhaps at the expense of an increased risk of salt-dependent hypertension (Thompson, Kuttab-Boulos et al. 2004). Several lines of evidence and clinical observation also indicated that activation of PXR is involved in disruption of steroid metabolism. For example, the PXR-activating of VP-Human (h)PXR transgenic mice was followed by hypertrophy of the adrenal cortex, loss of glucocorticoid circadian rhythm, and lack of glucocorticoid responses to psychogenic stress (Zhai, Pai et al. 2007). Furthermore, carbamazepine a PXR agonist which is known to induce steatosis (Grieco, Forgione et al. 2005) is also metabolized by CYP3A5. This enzyme is largely heteroactivated in the presence of heteroactivators such as endogenous steroids and flavonoids (Henshall, Galetin et al. 2008).

## **5.7 Molecular mechanism of the differential renal and intestinal expression of CYP3A5 and CYP3A4**

Several explanations could explain the differential expression of *CYP3A4* and *CYP3A5* promoter in renal and intestinal cells. Firstly, the transcriptional repression of *CYP3A4* in MDCK.2 may be mediated by a differential ratio between repressor (YY1) and activator (PXR, NF1). There are inherent factors which could limit availability of NF1, and thus its capacity to transactivate a gene. In fact, NF1 *trans*-activation represents the summation of the effects of all of the forms of NF1 present in cells. Splice variants may antagonize with each other and reduce availability of NF1 for the *trans*-activation of *CYP3A4* promoter. Two truncated isoforms from NF1 genes have been reported. The NF1-A-short (in rat) and the NFB1-3 (in human) variants derived from alternative splicing of the NF1-A and NF1-B transcript, respectively (Liu, Bernard et al. 1997; Ling, Hauer et al. 2004). Both of which lack a transcriptional activation domain. By themselves they have no effect on regulation. However, they could heterodimerize with other NF1 proteins containing a transcriptional activation domain and reduce their potential of *trans*-activation. Unfortunately, this mechanism is less likely to occur in kidney where these variants account for a minority of the total NF1-A and NF1-B transcripts (Liu, Bernard et al. 1997; Ling, Hauer et al. 2004).

Secondly, it is possible that NF1 binding to its cognate site in renal cells is impaired by CpG methylation within the consensus NF1 binding site. For example, a differential CpG methylation within the NF1 consensus sequence in liver but not in olfactory mucosa was incriminated to be partly involved in repression of *CYP2A3* gene in liver but not in the olfactory mucosa of rat (Ling, Hauer et al. 2004). However, this mechanism could be ruled out since an overexpression of NF1-A1.1 *trans*-activated *CYP3A4* promoter in either LS174T or MDCK.2 cells (Fig. 30B). This

suggests that the *CYP3A4* derived NF1-binding site is not modified by a CpG methylation in cell specific manner.

The renal repression activity attributed to YY1 on the *CYP3A4* promoter may, however, result from its ability to inhibit the NF1 activator bound at its binding site. This is evidenced by several observations. The binding of NF1 and YY1 was shown to be two independent events. Distinct YY1 and NF1 complexes were obtained with a probe encompassing NF1 and YY1 binding sites. Additionally, YY1-DNA and NF1-DNA complexes disappeared selectively with fragment containing either YY1 binding site or NF1 binding site (Saito, Takahashi et al. 2001). We also showed that no protein-protein interaction might be required for the repression activity by YY1. Indeed, YY1 exerts its effect even in the absence of the GA region required for all protein-protein interactions reported thus far (Fig. 27B). We postulate that YY1 may block the activity of NF1 in MDCK.2 cells (Fig. 31). In the most plausible scenario, the repression by YY1 could be more active via the DNA bending mechanism (Natesan and Gilman 1993). The effects of NF1 are affected by modifications of the DNA architecture. For example, affinity of NF1 for nucleosomal DNA is 100-300-fold lower than its affinity for free DNA (Blomquist, Li et al. 1996).

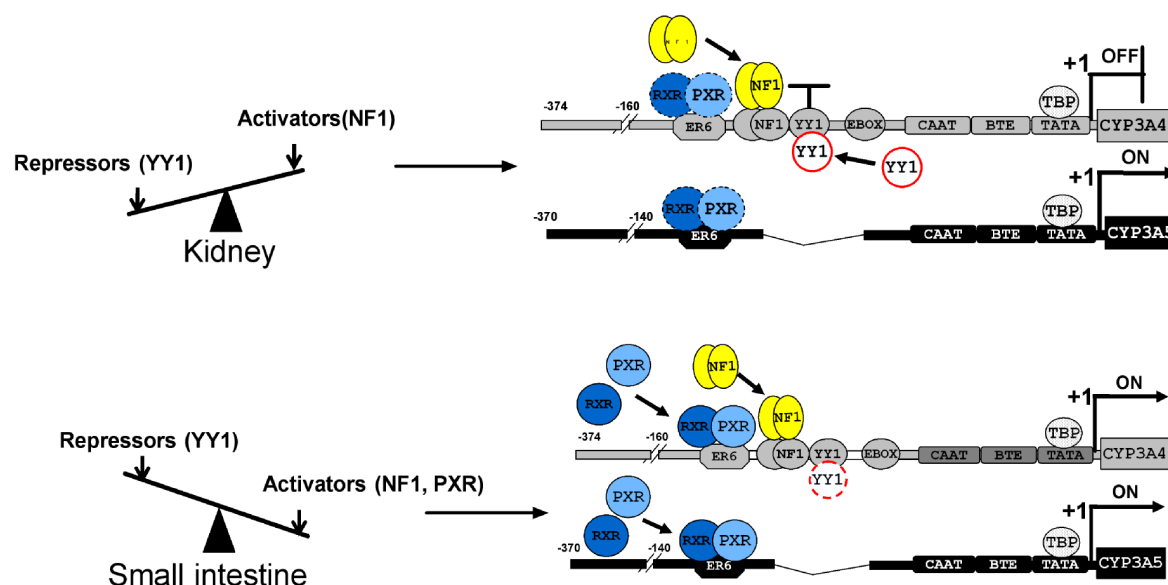


**Fig. 31. Models for the differential transcriptional regulation of *CYP3A4* and *CYP3A5*.** *CYP3A5* promoter lost a 57 bp region containing a functional YY1 repression system. *CYP3A5* is expressed (ON) in renal cells where PXR is not expressed. On the contrary, the YY1 repression system may inhibit (OFF) *CYP3A4* in renal cells by blocking activity of NF1. In intestinal cells, both *CYP3A5* and *CYP3A4* are expressed (ON). The combined activity of PXR and NF1 may override repression by the YY1 repression system. Full circles indicate activity, whereas the broken circles indicate no or weak

activity of the corresponding factor. TBP: transcription binding proteins. Stop bar indicates repression. Transcription start site is indicated as +1.

In this mechanism, whether the bending by YY1 results in activation or repression depend on the orientation of the YY1 binding site (Kim and Shapiro 1996). We identified the binding YY1 site on the anti-parallel strand of the *CYP3A4* promoter. Therefore, it is possible that the binding of YY1 changes the curvature of the DNA. As a result, NF1 binding site may be pushed in the opposite direction relative to the basic transcription binding sites. In intestinal cells, the combined co-activation by PXR and NF1 may override the repressing effect of YY1. Finally, *CYP3A5* promoter, which is not under the control of this system involving PXR, NF1 and YY1, is expressed in both renal and intestinal cells.

## 6. Conclusion

In this study, we showed that the 6.2 kb of the upstream of the human *CYP3A5* promoter mediated a broad tissue basal activity of *CYP3A5 in vivo*. Using *CYP3A5-luc* transgenic mice, we also confirm that *CYP3A5* is induced *in vivo* in the small intestine. We provided also evidence indicating that during evolution, *CYP3A5* got lost a suppressing Yin Yang 1 (YY1)-binding site from the *CYP3A5* promoter, allowing the PXR-independent *CYP3A5* expression outside the liver and small intestine. *CYP3A5* enzyme may have evolved in primates to be employed in endobiotic homeostasis protected against potentially deleterious effects of xenobiotic-driven induction. Finally, the differential expression of *CYP3A4* and *CYP3A5* in the small intestine and kidney represents a combined effect of the loss of the YY1-binding site from the *CYP3A5* promoter, a point mutation attenuating the suppressing effect of YY1 binding site which further facilitated *CYP3A4* expression together with *CYP3A4* promoter activation by NF1 and the renal non-expression of PXR, acting in concert via an unknown exact molecular mechanism. To our knowledge, this is a first evolutionary description of the mechanism uncoupling the inducible and constitutive expression in a major detoxifying enzyme. Similar mechanisms may have evolved for other detoxifying proteins, many of which metabolize endobiotics.

## 7. Perspectives

This study has left unanswered or generated new questions. Hence, for future work it would be interesting to:

- (1) determine factors necessary for the hepatic expression of *CYP3A5* in mouse liver. This could be accomplished *in vitro* by transient transfections of *CYP3A5* constructs in mouse liver models. Additionally, knowing that *CYP3A5* activity does not strictly depend on PXR it would be also of interest to analyse induction of *CYP3A5* *in vivo* in other organs such as lung and skin, using glucocorticoid agonists (e.g. Dexametasone);
- (2) determine whether the CLEM module is the reason for the hepatic constitutive expression of *CYP3A5* or for the common constitutive regulation of *CYP3A4* and *CYP3A5*. Our data indicate that the proximal *CYP3A5* is sufficient for a constitutive and induction activity of *CYP3A5* promoter. Besides the lack of *CYP3A5* transgene activity in liver its activity is surprisingly low in the kidney. This may be due to the lack of a strong enhancer module. CLEM module contains a functional HNF4 $\alpha$  site critical for the constitutive hepatic expression of *CYP3A4* gene (Matsumura, Saito et al. 2004). The HNF4 $\alpha$  is a tissue-specific transcription factor known to regulate a large number of genes in hepatocytes. HNF4 $\alpha$  is also highly expressed in renal tubules (Lucas, Grigo et al. 2005) where *CYP3A5* is expressed. Investigation of the constitutive hepatic and renal expression of a chimeric CLEM-*CYP3A5* could be performed first *in vitro* and later on *in vivo*;
- (3) determine whether the repression of *CYP3A4* by YY1 described herein for the kidney constitutes a general mechanism also applicable to other extrahepato-intestinal organs such as prostate, adrenal gland and lung;
- (4) analyse the regulation effect of an increased level of YY1 in cancer cells on *CYP3A4* expression. Therefore, YY1 level could be quantified as a marker along side the *CYP3A5* and other transcription factors such as PXR, CAR, NF1 and HNF4 $\alpha$ ;
- (5) address the exact mechanism of YY1 repression on *CYP3A4* promoter. To this end *in vivo* analysis of the co-occupancy of YY1, PXR and NF1 would be determined in both human renal and intestinal cells using immunoprecipitation method. The analysis *in vitro* would be carried-out with construct made with the YY1-binding site inserted in the opposite orientation with the expectation that activation of *CYP3A4* promoter would occur;
- (6) analyse the cooperativity of YY1 with other factors, especially considering the unique NF-Y binding site generated on the *CYP3A5* promoter following the deletion of the 57-bp fragment. Our data also indicated that *CYP3A5* activity increased upon an overexpression

by YY1 in renal and intestinal cells (Fig. 27B and data not shown). Therefore, it would be interesting to determine whether the similar cooperative activation of E2F factor by YY1 and NF-Y (van Ginkel, Hsiao et al. 1997) is applicable to the *CYP3A5* proximal promoter. This assay could be done using a mammalian two hybrid system. This study can potentially lead to the development of strategies need for the control of the renal *CYP3A5* activity in patient treated with drugs with narrow therapeutic index.

## 8. Abstract

The human cytochrome P450 3A4 (CYP3A4), the predominant but variably expressed cytochrome P450 in adult liver and small intestine is involved in the metabolism of over 50% of currently used drugs. Its paralog CYP3A5 plays a crucial role in the disposition of several drugs with low therapeutic index, including tacrolimus. Limited information is available for the CYP3A5 transcriptional regulation and its induction by xenobiotics remains controversial. In the first part of this study, we analysed the CYP3A5 transcriptional regulation and its induction by xenobiotics *in vivo* using transgenic mice. To this end, two transgenic strains were established by pronuclear injection of a plasmid, expressing firefly luciferase driven by a 6.2 kb of the human CYP3A5 promoter. A detailed analysis of both strains shows a tissue distribution largely reflecting that of CYP3A5 transcripts in humans. Thus, the highest luciferase activity was detected in the small intestine, followed by oesophagus, testis, lung, adrenal gland, ovary, prostate and kidney. However, no activity was observed in the liver. CYP3A5-luc transgenic mice were similarly induced in both sexes with either PCN or TCPOBOP in small intestine in a dose-dependent manner. Thus, the 6.2 kb upstream promoter of CYP3A5 mediates the broad tissue activity in transgenic mice. CYP3A5 promoter is inducible in the small intestine *in vivo*, which may contribute to the variable expression of CYP3A in this organ.

The hepato-intestinal level of the detoxifying oxidases CYP3A4 and CYP3A5 is adjusted to the xenobiotic exposure mainly via the xenosensor and transcriptional factor PXR. CYP3A5 is additionally expressed in several other organs lacking PXR, including kidney. In the second part of this study, we investigated the mechanism of the differential expression of CYP3A5 and CYP3A4 and its evolutionary origin using renal and intestinal cells, and comparative genomics. For this examination, we established a two-cell line models reflecting the expression relationships of CYP3A4 and CYP3A5 in the kidney and small intestine *in vivo*. Our data demonstrate that the CYP3A5 expression in renal cells was enabled by the loss of a suppressing Yin Yang 1 (YY1)-binding site from the CYP3A5 promoter. This allowed for a renal CYP3A5 expression in a PXR-independent manner. The YY1 element is retained in the CYP3A4 gene, leading to its suppression, perhaps via interference with the NF1 activity in renal cells. In intestinal cells, the inhibition of CYP3A4 expression by YY1 is abrogated by a combined activating effect of PXR and NF1 acting on their respective response elements located adjacent to the YY1-binding site on CYP3A4 proximal promoter. CYP3A4 expression is further facilitated by a point mutation attenuating the suppressing effect of YY1 binding site. The differential expression of CYP3A4 and CYP3A5 in these organs results from the loss of the YY1 binding element from the CYP3A5 promoter, acting



in concert with the differential organ expression of PXR, and with the higher accumulation of PXR response elements in *CYP3A4*.

## 9. Zusammenfassung

Das humane Zytochrom P450 3A4 (CYP3A4) stellt den größten aber sehr variablen Anteil der Zytochrom P450-Enzyme in der Leber und im Dünndarm Erwachsener dar und ist am Stoffwechsel von über 50% heutig eingesetzter Medikamente beteiligt. Sein Paralog CYP3A5 spielt eine entscheidende Rolle bei der Disposition einiger Arzneimittel mit niedrigem therapeutischem Index, darunter Tacrolimus. Über die transkriptionelle Regulation von CYP3A5 ist nur wenig bekannt und seine Induzierbarkeit durch Xenobiotika bleibt umstritten. Zu Beginn dieser Arbeit wurde die transkriptionelle Regulation von CYP3A5 und seine Induzierbarkeit durch Xenobiotika *in vivo* an transgenen Mäusen untersucht. Mittels der Mikroinjektionsmethode wurden zwei transgene Mausstämme etabliert, welche das Luziferasegen des Glühwürmchens unter der Kontrolle von 6,2 kbp des humanen *CYP3A5*-Promotors exprimieren. Eine detaillierte Analyse beider Mausstämme zeigte ein weitgehend mit dem humanen CYP3A5 übereinstimmendes Expressionsmuster. Demnach wurde die höchste Luziferaseaktivität im Dünndarm nachgewiesen, gefolgt von der Speiseröhre, den Hoden, der Lunge, den Nebennieren, den Eierstöcken, der Prostata und den Nieren. Es wurde jedoch keine Aktivität in der Leber detektiert. In CYP3A5-luc transgenen Mäusen beider Geschlechter konnte dosisabhängig eine ähnlich starke Steigerung der Luziferaseaktivität durch PCN oder TCPOBOP im Dünndarm gemessen werden. Zusammengefasst vermitteln die 6,2 kbp des *CYP3A5*-Promotors die Aktivität in vielen Geweben der transgenen Mäuse. Die Induzierbarkeit von CYP3A5 im Dünndarm könnte ein Grund für die hohe Expressionsvariabilität der CYP3A-Enzyme in diesem Organ sein.

Die Menge der detoxifizierenden Oxidasen CYP3A4 und CYP3A5 in der Leber und im Dünndarm wird hauptsächlich über den Xenobiotika-Rezeptor und Transkriptionsfaktor PXR gesteuert. CYP3A5 wird aber auch in einigen Organen ohne PXR, wie der Niere, exprimiert. Im zweiten Teil dieser Arbeit wurde der Mechanismus der differentiellen Expression von CYP3A5 und CYP3A4 sowie deren evolutionärer Ursprung an Nieren- und Dünndarmzellkulturen aber auch mit Hilfe von Genomvergleichen untersucht. Zu diesem Zweck wurden ein Zwei-Zelllinien-Modell etabliert, welches die Expressionsverhältnisse zwischen CYP3A4 und CYP3A5 in der Niere und im Dünndarm *in vivo* widerspiegelt. Die gewonnenen Daten zeigen, dass die CYP3A5-Expression in Nierenzellen durch einen Verlust der supprimierenden Yin Yang 1 (YY1)-Bindestelle im *CYP3A5*-Promotor ermöglicht wurde. Die CYP3A5-Expression in der Niere wurde somit von PXR unabhängig. Im *CYP3A4*-Promotor ist das YY1-Element erhalten und führt so, eventuell durch Wechselwirkung mit dem NF1, zu seiner Supprimierung in Nierenzellen. In Dünndarmzellen wird CYP3A4 exprimiert, da der inhibitorische Effekt von YY1 durch die Aktivierung von PXR in Kombination mit NF1, welche an angrenzende Bindestellen im *CYP3A4*-Promotor binden, aufgehoben wird. Die CYP3A4-Expression im Dünndarm wird desweiteren unterstützt durch eine Punktmutation, welche den supprimierenden Effekt von YY1 abschwächt. Die differentielle Expression von CYP3A4 und CYP3A5 in diesen Organen resultiert aus einem Verlust der YY1-

Bindestelle im *CYP3A5*-Promotor bei gleichzeitig differentieller Organexpression von PXR sowie einer größeren Anzahl von PXR-Bindestellen im *CYP3A4*-Promotor.

## 10. References

- (1999). "A unified nomenclature system for the nuclear receptor superfamily." *Cell* **97**(2): 161-3.
- Aleksa, K., D. Matsell, et al. (2005). "Cytochrome P450 3A and 2B6 in the developing kidney: implications for ifosfamide nephrotoxicity." *Pediatr Nephrol* **20**(7): 872-85.
- Anttila, S., J. Hukkanen, et al. (1997). "Expression and localization of CYP3A4 and CYP3A5 in human lung." *Am J Respir Cell Mol Biol* **16**(3): 242-9.
- Arthur, J. M. (2000). "The MDCK cell line is made up of populations of cells with diverse resistive and transport properties." *Tissue Cell* **32**(5): 446-50.
- Austen, M., C. Cerni, et al. (1998). "YY1 can inhibit c-Myc function through a mechanism requiring DNA binding of YY1 but neither its transactivation domain nor direct interaction with c-Myc." *Oncogene* **17**(4): 511-20.
- Axelrod, J. (1955). "The enzymatic demethylation of ephedrine." *J Pharmacol Exp Ther* **114**(4): 430-8.
- Babinet, C. and M. Cohen-Tannoudji (2001). "Genome engineering via homologous recombination in mouse embryonic stem (ES) cells: an amazingly versatile tool for the study of mammalian biology." *An Acad Bras Cienc* **73**(3): 365-83.
- Ball, S. E., J. Scatina, et al. (1999). "Population distribution and effects on drug metabolism of a genetic variant in the 5' promoter region of CYP3A4." *Clin Pharmacol Ther* **66**(3): 288-94.
- Barwick, J. L., L. C. Quattrochi, et al. (1996). "Trans-species gene transfer for analysis of glucocorticoid-inducible transcriptional activation of transiently expressed human CYP3A4 and rabbit CYP3A6 in primary cultures of adult rat and rabbit hepatocytes." *Mol Pharmacol* **50**(1): 10-6.
- Baskin-Bey, E. S., W. Huang, et al. (2006). "Constitutive androstane receptor (CAR) ligand, TCPOBOP, attenuates Fas-induced murine liver injury by altering Bcl-2 proteins." *Hepatology* **44**(1): 252-62.
- Begon, D. Y., L. Delacroix, et al. (2005). "Yin Yang 1 cooperates with activator protein 2 to stimulate ERBB2 gene expression in mammary cancer cells." *J Biol Chem* **280**(26): 24428-34.
- Berggren, S., C. Gall, et al. (2007). "Gene and protein expression of P-glycoprotein, MRP1, MRP2, and CYP3A4 in the small and large human intestine." *Mol Pharm* **4**(2): 252-7.
- Bertilsson, G., J. Heidrich, et al. (1998). "Identification of a human nuclear receptor defines a new signaling pathway for CYP3A induction." *Proc Natl Acad Sci U S A* **95**(21): 12208-13.
- Biggs, J. S., J. Wan, et al. (2007). "Transcription factor binding to a putative double E-box motif represses CYP3A4 expression in human lung cells." *Mol Pharmacol* **72**(3): 514-25.
- Blomquist, P., Q. Li, et al. (1996). "The affinity of nuclear factor 1 for its DNA site is drastically reduced by nucleosome organization irrespective of its rotational or translational position." *J Biol Chem* **271**(1): 153-9.
- Blumberg, B., W. Sabbagh, Jr., et al. (1998). "SXR, a novel steroid and xenobiotic-sensing nuclear receptor." *Genes Dev* **12**(20): 3195-205.
- Bradford, M. M. (1976). "A rapid and sensitive method for the quantitation of microgram quantities of protein utilizing the principle of protein-dye binding." *Anal Biochem* **72**: 248-54.
- Brudno, M., C. B. Do, et al. (2003). "LAGAN and Multi-LAGAN: efficient tools for large-scale multiple alignment of genomic DNA." *Genome Res* **13**(4): 721-31.

- Burk, O., I. Koch, et al. (2004). "The induction of cytochrome P450 3A5 (CYP3A5) in the human liver and intestine is mediated by the xenobiotic sensors pregnane X receptor (PXR) and constitutively activated receptor (CAR)." *J Biol Chem* **279**(37): 38379-85.
- Burk, O., H. Tegude, et al. (2002). "Molecular mechanisms of polymorphic CYP3A7 expression in adult human liver and intestine." *J Biol Chem* **277**(27): 24280-8.
- Burk, O. and L. Wojnowski (2004). "Cytochrome P450 3A and their regulation." *Naunyn Schmiedebergs Arch Pharmacol* **369**(1): 105-24.
- Bushmeyer, S., K. Park, et al. (1995). "Characterization of functional domains within the multifunctional transcription factor, YY1." *J Biol Chem* **270**(50): 30213-20.
- Busi, F. and T. Cresteil (2005). "CYP3A5 mRNA degradation by nonsense-mediated mRNA decay." *Mol Pharmacol* **68**(3): 808-15.
- Cedrone, E., Y. Reid, et al. (2009). "Tissue-culture adapted Influenza virus strains." *ATCC Connection* **29**(2): 4-5, 15.
- Cervený, L., L. Svecova, et al. (2007). "Valproic acid induces CYP3A4 and MDR1 gene expression by activation of constitutive androstane receptor and pregnane X receptor pathways." *Drug Metab Dispos* **35**(7): 1032-41.
- Chawla, A., J. J. Repa, et al. (2001). "Nuclear receptors and lipid physiology: opening the X-files." *Science* **294**(5548): 1866-70.
- Chekmenov, D. S., C. Haid, et al. (2005). "P-Match: transcription factor binding site search by combining patterns and weight matrices." *Nucleic Acids Res* **33**(Web Server issue): W432-7.
- Chen, X., H. Wang, et al. (2009). "Molecular population genetics of human CYP3A locus: signatures of positive selection and implications for evolutionary environmental medicine." *Environ Health Perspect* **117**(10): 1541-8.
- Cheng, X. and C. D. Klaassen (2006). "Regulation of mRNA expression of xenobiotic transporters by the pregnane x receptor in mouse liver, kidney, and intestine." *Drug Metab Dispos* **34**(11): 1863-7.
- Cheung, C., A. M. Yu, et al. (2006). "Growth hormone determines sexual dimorphism of hepatic cytochrome P450 3A4 expression in transgenic mice." *J Pharmacol Exp Ther* **316**(3): 1328-34.
- Chikhirzhina, G. I., R. I. Al'-Shekadat, et al. (2008). "[Transcription factors of the nuclear factor 1 (NF1) family. Role in chromatin remodeling]." *Mol Biol (Mosk)* **42**(3): 388-404.
- Clore, J., A. Schoolwerth, et al. (1992). "When is cortisol a mineralocorticoid?" *Kidney Int* **42**(6): 1297-308.
- Coto, E. and B. Tavora (2009). "Pharmacogenetics of calcineurin inhibitors in renal transplantation." *Transplantation* **88**(3 Suppl): S62-7.
- Cui, C., M. A. Wani, et al. (1994). "Reporter genes in transgenic mice." *Transgenic Res* **3**(3): 182-94.
- Daly, A. K. (2006). "Significance of the minor cytochrome P450 3A isoforms." *Clin Pharmacokinet* **45**(1): 13-31.
- Dennison, J. B., D. R. Jones, et al. (2007). "Effect of CYP3A5 expression on vincristine metabolism with human liver microsomes." *J Pharmacol Exp Ther* **321**(2): 553-63.
- Des Marais, D. L. and M. D. Rausher (2008). "Escape from adaptive conflict after duplication in an anthocyanin pathway gene." *Nature* **454**(7205): 762-5.
- Ding, X. and L. S. Kaminsky (2003). "Human extrahepatic cytochromes P450: function in xenobiotic metabolism and tissue-selective chemical toxicity in the respiratory and gastrointestinal tracts." *Annu Rev Pharmacol Toxicol* **43**: 149-73.
- Domanski, T. L., C. Finta, et al. (2001). "cDNA cloning and initial characterization of CYP3A43, a novel human cytochrome P450." *Mol Pharmacol* **59**(2): 386-92.

- Drocourt, L., J. C. Ourlin, et al. (2002). "Expression of CYP3A4, CYP2B6, and CYP2C9 is regulated by the vitamin D receptor pathway in primary human hepatocytes." *J Biol Chem* **277**(28): 25125-32.
- Escriva, H., F. Delaunay, et al. (2000). "Ligand binding and nuclear receptor evolution." *Bioessays* **22**(8): 717-27.
- Evans, A. M. (2000). "Influence of dietary components on the gastrointestinal metabolism and transport of drugs." *Ther Drug Monit* **22**(1): 131-6.
- Evans, W. E. and M. V. Relling (1999). "Pharmacogenomics: translating functional genomics into rational therapeutics." *Science* **286**(5439): 487-91.
- Finta, C. and P. G. Zaphiropoulos (2000). "The human cytochrome P450 3A locus. Gene evolution by capture of downstream exons." *Gene* **260**(1-2): 13-23.
- Folger, K. R., E. A. Wong, et al. (1982). "Patterns of integration of DNA microinjected into cultured mammalian cells: evidence for homologous recombination between injected plasmid DNA molecules." *Mol Cell Biol* **2**(11): 1372-87.
- Garfinkel, D. (1958). "Studies on pig liver microsomes. I. Enzymic and pigment composition of different microsomal fractions." *Arch Biochem Biophys* **77**(2): 493-509.
- Geick, A., M. Eichelbaum, et al. (2001). "Nuclear receptor response elements mediate induction of intestinal MDR1 by rifampin." *J Biol Chem* **276**(18): 14581-7.
- Gellner, K., R. Eiselt, et al. (2001). "Genomic organization of the human CYP3A locus: identification of a new, inducible CYP3A gene." *Pharmacogenetics* **11**(2): 111-21.
- Germain, P., B. Staels, et al. (2006). "Overview of nomenclature of nuclear receptors." *Pharmacol Rev* **58**(4): 685-704.
- Giguere, V. (1999). "Orphan nuclear receptors: from gene to function." *Endocr Rev* **20**(5): 689-725.
- Girnita, D. M., S. A. Webber, et al. (2006). "Disparate distribution of 16 candidate single nucleotide polymorphisms among racial and ethnic groups of pediatric heart transplant patients." *Transplantation* **82**(12): 1774-80.
- Givens, R. C., Y. S. Lin, et al. (2003). "CYP3A5 genotype predicts renal CYP3A activity and blood pressure in healthy adults." *J Appl Physiol* **95**(3): 1297-300.
- Gödtel-Armbrust, U., A. Metzger, et al. (2007). "Variability in PXR-mediated induction of CYP3A4 by commercial preparations and dry extracts of St. John's wort." *Naunyn Schmiedebergs Arch Pharmacol* **375**(6): 377-82.
- Goodwin, B., E. Hodgson, et al. (2002). "Transcriptional regulation of the human CYP3A4 gene by the constitutive androstane receptor." *Mol Pharmacol* **62**(2): 359-65.
- Goodwin, B., E. Hodgson, et al. (1999). "The orphan human pregnane X receptor mediates the transcriptional activation of CYP3A4 by rifampicin through a distal enhancer module." *Mol Pharmacol* **56**(6): 1329-39.
- Graham, G. J. (1995). "Tandem genes and clustered genes." *J Theor Biol* **175**(1): 71-87.
- Graham, S. E. and J. A. Peterson (1999). "How similar are P450s and what can their differences teach us?" *Arch Biochem Biophys* **369**(1): 24-9.
- Granvil, C. P., A. M. Yu, et al. (2003). "Expression of the human CYP3A4 gene in the small intestine of transgenic mice: in vitro metabolism and pharmacokinetics of midazolam." *Drug Metab Dispos* **31**(5): 548-58.
- Greiner, B., M. Eichelbaum, et al. (1999). "The role of intestinal P-glycoprotein in the interaction of digoxin and rifampin." *J Clin Invest* **104**(2): 147-53.
- Grieco, A., A. Forgione, et al. (2005). "Fatty liver and drugs." *Eur Rev Med Pharmacol Sci* **9**(5): 261-3.
- Gronemeyer, H. and V. Laudet (1995). "Transcription factors 3: nuclear receptors." *Protein Profile* **2**(11): 1173-308.
- Gronostajski, R. M. (2000). "Roles of the NFI/CTF gene family in transcription and development." *Gene* **249**(1-2): 31-45.

- Gu, X., S. Ke, et al. (2006). "Role of NF-kappaB in regulation of PXR-mediated gene expression: a mechanism for the suppression of cytochrome P-450 3A4 by proinflammatory agents." *J Biol Chem* **281**(26): 17882-9.
- Gu, X., Z. Zhang, et al. (2005). "Rapid evolution of expression and regulatory divergences after yeast gene duplication." *Proc Natl Acad Sci U S A* **102**(3): 707-12.
- Guengerich, F. P. (1999). "Cytochrome P-450 3A4: regulation and role in drug metabolism." *Annu Rev Pharmacol Toxicol* **39**: 1-17.
- Guigo, R., E. T. Dermitzakis, et al. (2003). "Comparison of mouse and human genomes followed by experimental verification yields an estimated 1,019 additional genes." *Proc Natl Acad Sci U S A* **100**(3): 1140-5.
- Haehner, B. D., J. C. Gorski, et al. (1996). "Bimodal distribution of renal cytochrome P450 3A activity in humans." *Mol Pharmacol* **50**(1): 52-9.
- Hall, T. A. (1999). "BioEdit: a user-friendly biological sequence alignment editor and analysis program for Windows 95/98/NT." *Nucl Acids Symp Ser* **41**: 95-98.
- Hariharan, N., D. E. Kelley, et al. (1991). "Delta, a transcription factor that binds to downstream elements in several polymerase II promoters, is a functionally versatile zinc finger protein." *Proc Natl Acad Sci U S A* **88**(21): 9799-803.
- Harlow, G. R. and J. R. Halpert (1998). "Analysis of human cytochrome P450 3A4 cooperativity: construction and characterization of a site-directed mutant that displays hyperbolic steroid hydroxylation kinetics." *Proc Natl Acad Sci U S A* **95**(12): 6636-41.
- Hashimoto, H., K. Toide, et al. (1993). "Gene structure of CYP3A4, an adult-specific form of cytochrome P450 in human livers, and its transcriptional control." *Eur J Biochem* **218**(2): 585-95.
- Henshall, J., A. Galetin, et al. (2008). "Comparative analysis of CYP3A heteroactivation by steroid hormones and flavonoids in different in vitro systems and potential in vivo implications." *Drug Metab Dispos* **36**(7): 1332-40.
- Hinrichs, A. S., D. Karolchik, et al. (2006). "The UCSC Genome Browser Database: update 2006." *Nucleic Acids Res* **34**(Database issue): D590-8.
- Ho, H., A. Pinto, et al. (2005). "Association between the CYP3A5 genotype and blood pressure." *Hypertension* **45**(2): 294-8.
- Honkakoski, P. and M. Negishi (2000). "Regulation of cytochrome P450 (CYP) genes by nuclear receptors." *Biochem J* **347**(Pt 2): 321-37.
- Honkakoski, P., T. Sueyoshi, et al. (2003). "Drug-activated nuclear receptors CAR and PXR." *Ann Med* **35**(3): 172-82.
- Hukkanen, J., T. Vaisanen, et al. (2003). "Regulation of CYP3A5 by glucocorticoids and cigarette smoke in human lung-derived cells." *J Pharmacol Exp Ther* **304**(2): 745-52.
- Hustert, E., M. Haberl, et al. (2001). "The genetic determinants of the CYP3A5 polymorphism." *Pharmacogenetics* **11**(9): 773-9.
- Hustert, E., A. Zibat, et al. (2001). "Natural protein variants of pregnane x receptor with altered transactivation activity toward cyp3a4." *Drug Metab Dispos* **29**(11): 1454-9.
- Hyde-DeRuyscher, R. P., E. Jennings, et al. (1995). "DNA binding sites for the transcriptional activator/repressor YY1." *Nucleic Acids Res* **23**(21): 4457-65.
- Iwano, S., T. Saito, et al. (2001). "Cooperative regulation of CYP3A5 gene transcription by NF-Y and Sp family members." *Biochem Biophys Res Commun* **286**(1): 55-60.
- Johnson, D. R., C. W. Li, et al. (2006). "Regulation and binding of pregnane X receptor by nuclear receptor corepressor silencing mediator of retinoid and thyroid hormone receptors (SMRT)." *Mol Pharmacol* **69**(1): 99-108.
- Johnson, M., I. Zaretskaya, et al. (2008). "NCBI BLAST: a better web interface." *Nucleic Acids Res* **36**(Web Server issue): W5-9.

- Jover, R., R. Bort, et al. (2001). "Cytochrome P450 regulation by hepatocyte nuclear factor 4 in human hepatocytes: a study using adenovirus-mediated antisense targeting." Hepatology **33**(3): 668-75.
- Jover, R., R. Bort, et al. (2002). "Down-regulation of human CYP3A4 by the inflammatory signal interleukin-6: molecular mechanism and transcription factors involved." Faseb J **16**(13): 1799-801.
- Joy, M. S., S. L. Hogan, et al. (2007). "Cytochrome P450 3A5 expression in the kidneys of patients with calcineurin inhibitor nephrotoxicity." Nephrol Dial Transplant **22**(7): 1963-8.
- Kamdem, L. K., F. Streit, et al. (2005). "Contribution of CYP3A5 to the in Vitro Hepatic Clearance of Tacrolimus." Clin Chem **51**(8): 1374-81.
- Kim, J. and D. J. Shapiro (1996). "In simple synthetic promoters YY1-induced DNA bending is important in transcription activation and repression." Nucleic Acids Res **24**(21): 4341-8.
- Kim, J. D., C. Faulk, et al. (2007). "Retroposition and evolution of the DNA-binding motifs of YY1, YY2 and REX1." Nucleic Acids Res **35**(10): 3442-52.
- Kitada, M., T. Kamataki, et al. (1987). "P-450 HFLa, a form of cytochrome P-450 purified from human fetal livers, is the 16 alpha-hydroxylase of dehydroepiandrosterone 3-sulfate." J Biol Chem **262**(28): 13534-7.
- Kliwer, S. A., J. T. Moore, et al. (1998). "An orphan nuclear receptor activated by pregnanes defines a novel steroid signaling pathway." Cell **92**(1): 73-82.
- Klingenberg, M. (1958). "Pigments of rat liver microsomes." Arch Biochem Biophys **75**(2): 376-86.
- Koch, I., R. Weil, et al. (2002). "Interindividual variability and tissue-specificity in the expression of cytochrome P450 3A mRNA." Drug Metab Dispos **30**(10): 1108-14.
- Kolars, J. C., K. S. Lown, et al. (1994). "CYP3A gene expression in human gut epithelium." Pharmacogenetics **4**(5): 247-59.
- Kolars, J. C., P. Schmiedlin-Ren, et al. (1992). "Identification of rifampin-inducible P450III<sub>A4</sub> (CYP3A4) in human small bowel enterocytes." J Clin Invest **90**(5): 1871-8.
- Kreutz, R., M. Zuurman, et al. (2005). "The role of the cytochrome P450 3A5 enzyme for blood pressure regulation in the general Caucasian population." Pharmacogenet Genomics **15**(12): 831-7.
- Kuehl, P., J. Zhang, et al. (2001). "Sequence diversity in CYP3A promoters and characterization of the genetic basis of polymorphic CYP3A5 expression." Nat Genet **27**(4): 383-91.
- Kumar, S., H. Qiu, et al. (2009). "Ligand diversity of human and chimpanzee CYP3A4: activation of human CYP3A4 by lithocholic acid results from positive selection." Drug Metab Dispos **37**(6): 1328-33.
- Lacroix, D., M. Sonnier, et al. (1997). "Expression of CYP3A in the human liver--evidence that the shift between CYP3A7 and CYP3A4 occurs immediately after birth." Eur J Biochem **247**(2): 625-34.
- Lamba, J. K., Y. S. Lin, et al. (2002). "Genetic contribution to variable human CYP3A-mediated metabolism." Adv Drug Deliv Rev **54**(10): 1271-94.
- Lamba, V., K. Yasuda, et al. (2004). "PXR (NR1I2): splice variants in human tissues, including brain, and identification of neurosteroids and nicotine as PXR activators." Toxicol Appl Pharmacol **199**(3): 251-65.
- Laudet, V., C. Hanni, et al. (1992). "Evolution of the nuclear receptor gene superfamily." Embo J **11**(3): 1003-13.
- LeCluyse, E. L. (2001). "Pregnane X receptor: molecular basis for species differences in CYP3A induction by xenobiotics." Chem Biol Interact **134**(3): 283-9.



- Lefebvre, P., P. M. Danze, et al. (1988). "Association of the glucocorticoid receptor binding subunit with the 90K nonsteroid-binding component is stabilized by both steroidal and nonsteroidal antiglucocorticoids in intact cells." *Biochemistry* **27**(26): 9186-94.
- Lehmann, J. M., D. D. McKee, et al. (1998). "The human orphan nuclear receptor PXR is activated by compounds that regulate CYP3A4 gene expression and cause drug interactions." *J Clin Invest* **102**(5): 1016-23.
- Lewis, B. A., G. Tullis, et al. (1995). "Adenovirus E1A proteins interact with the cellular YY1 transcription factor." *J Virol* **69**(3): 1628-36.
- Li, A. P., D. L. Kaminski, et al. (1995). "Substrates of human hepatic cytochrome P450 3A4." *Toxicology* **104**(1-3): 1-8.
- Li, T. and J. Y. Chiang (2006). "Rifampicin induction of CYP3A4 requires pregnane X receptor cross talk with hepatocyte nuclear factor 4alpha and coactivators, and suppression of small heterodimer partner gene expression." *Drug Metab Dispos* **34**(5): 756-64.
- Li, Y., T. Yokoi, et al. (1997). "In vivo activation of aflatoxin B1 in C57BL/6N mice carrying a human fetus-specific CYP3A7 gene." *Cancer Res* **57**(4): 641-5.
- Lieberthal, J. G., M. Kaminsky, et al. (2009). "The role of YY1 in reduced HP1alpha gene expression in invasive human breast cancer cells." *Breast Cancer Res* **11**(3): R42.
- Lin, T. P. (1966). "Microinjection of mouse eggs." *Science* **151**(708): 333-7.
- Lin, Y. S., A. L. Dowling, et al. (2002). "Co-regulation of CYP3A4 and CYP3A5 and contribution to hepatic and intestinal midazolam metabolism." *Mol Pharmacol* **62**(1): 162-72.
- Ling, G., C. R. Hauer, et al. (2004). "Transcriptional regulation of rat CYP2A3 by nuclear factor 1: identification of a novel NFI-A isoform, and evidence for tissue-selective interaction of NFI with the CYP2A3 promoter in vivo." *J Biol Chem* **279**(27): 27888-95.
- Liu, Y., H. U. Bernard, et al. (1997). "NFI-B3, a novel transcriptional repressor of the nuclear factor I family, is generated by alternative RNA processing." *J Biol Chem* **272**(16): 10739-45.
- Lucas, B., K. Grigo, et al. (2005). "HNF4alpha reduces proliferation of kidney cells and affects genes deregulated in renal cell carcinoma." *Oncogene* **24**(42): 6418-31.
- Luke, M. P., G. Sui, et al. (2006). "Yin Yang 1 physically interacts with Hoxa11 and represses Hoxa11-dependent transcription." *J Biol Chem* **281**(44): 33226-32.
- Ma, X., C. Cheung, et al. (2008). "A double transgenic mouse model expressing human pregnane X receptor and cytochrome P450 3A4." *Drug Metab Dispos* **36**(12): 2506-12.
- Mangelsdorf, D. J., C. Thummel, et al. (1995). "The nuclear receptor superfamily: the second decade." *Cell* **83**(6): 835-9.
- Marill, J., T. Cresteil, et al. (2000). "Identification of human cytochrome P450s involved in the formation of all-trans-retinoic acid principal metabolites." *Mol Pharmacol* **58**(6): 1341-8.
- Martinez-Jimenez, C. P., M. J. Gomez-Lechon, et al. (2005). "Transcriptional regulation of the human hepatic CYP3A4: identification of a new distal enhancer region responsive to CCAAT/enhancer-binding protein beta isoforms (liver activating protein and liver inhibitory protein)." *Mol Pharmacol* **67**(6): 2088-101.
- Matsumura, K., T. Saito, et al. (2004). "Identification of a novel polymorphic enhancer of the human CYP3A4 gene." *Mol Pharmacol* **65**(2): 326-34.
- Matsuzaki, K., T. Arai, et al. (1995). "Formation of 6 beta-OH-deoxycorticosterone from deoxycorticosterone by A6 cells." *Steroids* **60**(7): 457-62.
- McArthur, A. G., T. Hegelund, et al. (2003). "Phylogenetic analysis of the cytochrome P450 3 (CYP3) gene family." *J Mol Evol* **57**(2): 200-11.

- McCune, J. S., L. J. Risler, et al. (2005). "Contribution of CYP3A5 to hepatic and renal ifosfamide N-dechloroethylation." *Drug Metab Dispos* **33**(7): 1074-81.
- McKinnon, R. A., W. M. Burgess, et al. (1995). "Characterisation of CYP3A gene subfamily expression in human gastrointestinal tissues." *Gut* **36**(2): 259-67.
- Meisterernst, M., I. Gander, et al. (1988). "A quantitative analysis of nuclear factor I/DNA interactions." *Nucleic Acids Res* **16**(10): 4419-35.
- Merrihew, R. V., W. C. Clay, et al. (2001). "Chromosomal integration of transduced recombinant baculovirus DNA in mammalian cells." *J Virol* **75**(2): 903-9.
- Miller, K. K., J. Cai, et al. (2004). "Stereo- and regioselectivity account for the diversity of dehydroepiandrosterone (DHEA) metabolites produced by liver microsomal cytochromes P450." *Drug Metab Dispos* **32**(3): 305-13.
- Moilanen, A. M., J. Hakkola, et al. (2007). "Characterization of androgen-regulated expression of CYP3A5 in human prostate." *Carcinogenesis* **28**(5): 916-21.
- Moore, J. T. and S. A. Kliewer (2000). "Use of the nuclear receptor PXR to predict drug interactions." *Toxicology* **153**(1-3): 1-10.
- Moore, J. T., L. B. Moore, et al. (2003). "Functional and structural comparison of PXR and CAR." *Biochim Biophys Acta* **1619**(3): 235-8.
- Moore, L. B., B. Goodwin, et al. (2000). "St. John's wort induces hepatic drug metabolism through activation of the pregnane X receptor." *Proc Natl Acad Sci U S A* **97**(13): 7500-2.
- Morris, D. J., S. A. Latif, et al. (1998). "A second enzyme protecting mineralocorticoid receptors from glucocorticoid occupancy." *Am J Physiol* **274**(5 Pt 1): C1245-52.
- Murray, G. I., M. C. McFadyen, et al. (1999). "Cytochrome P450 CYP3A in human renal cell cancer." *Br J Cancer* **79**(11-12): 1836-42.
- Natesan, S. and M. Z. Gilman (1993). "DNA bending and orientation-dependent function of YY1 in the c-fos promoter." *Genes Dev* **7**(12B): 2497-509.
- Nelson, D. R. (2009). "The cytochrome p450 homepage." *Hum Genomics* **4**(1): 59-65.
- Nelson, D. R., L. Koymans, et al. (1996). "P450 superfamily: update on new sequences, gene mapping, accession numbers and nomenclature." *Pharmacogenetics* **6**(1): 1-42.
- Nelson, D. R., D. C. Zeldin, et al. (2004). "Comparison of cytochrome P450 (CYP) genes from the mouse and human genomes, including nomenclature recommendations for genes, pseudogenes and alternative-splice variants." *Pharmacogenetics* **14**(1): 1-18.
- Nikaido, H. (2001). "Preventing drug access to targets: cell surface permeability barriers and active efflux in bacteria." *Semin Cell Dev Biol* **12**(3): 215-23.
- Nishimura, M., S. Naito, et al. (2004). "Tissue-specific mRNA expression profiles of human nuclear receptor subfamilies." *Drug Metab Pharmacokinet* **19**(2): 135-49.
- Novotna, A., A. Dorickova, et al. (2010). "Investigation of Orlistat effects on PXR activation and CYP3A4 expression in primary human hepatocytes and human intestinal LS174T cells." *Eur J Pharm Sci* **41**(2): 276-80.
- Oesch, F., E. Fabian, et al. (2007). "Drug-metabolizing enzymes in the skin of man, rat, and pig." *Drug Metab Rev* **39**(4): 659-98.
- Oinonen, T. and K. O. Lindros (1998). "Zonation of hepatic cytochrome P-450 expression and regulation." *Biochem J* **329** ( Pt 1): 17-35.
- Omura, T. and R. Sato (1964). "The Carbon Monoxide-Binding Pigment of Liver Microsomes. I. Evidence for Its Hemoprotein Nature." *J Biol Chem* **239**: 2370-8.
- Omura, T. and R. Sato (1964). "The Carbon Monoxide-Binding Pigment of Liver Microsomes. II. Solubilization, Purification, and Properties." *J Biol Chem* **239**: 2379-85.
- Ozdemir, V., W. Kalow, et al. (2000). "Evaluation of the genetic component of variability in CYP3A4 activity: a repeated drug administration method." *Pharmacogenetics* **10**(5): 373-88.

- Paine, M. F., H. L. Hart, et al. (2006). "The human intestinal cytochrome P450 "pie"." Drug Metab Dispos **34**(5): 880-6.
- Pariante, C. M., B. D. Pearce, et al. (2001). "The steroid receptor antagonists RU40555 and RU486 activate glucocorticoid receptor translocation and are not excreted by the steroid hormones transporter in L929 cells." J Endocrinol **169**(2): 309-20.
- Paris, P. L., P. A. Kupelian, et al. (1999). "Association between a CYP3A4 genetic variant and clinical presentation in African-American prostate cancer patients." Cancer Epidemiol Biomarkers Prev **8**(10): 901-5.
- Pascussi, J. M., L. Drocourt, et al. (2000). "Dexamethasone induces pregnane X receptor and retinoid X receptor-alpha expression in human hepatocytes: synergistic increase of CYP3A4 induction by pregnane X receptor activators." Mol Pharmacol **58**(2): 361-72.
- Pascussi, J. M., L. Drocourt, et al. (2001). "Dual effect of dexamethasone on CYP3A4 gene expression in human hepatocytes. Sequential role of glucocorticoid receptor and pregnane X receptor." Eur J Biochem **268**(24): 6346-58.
- Pavek, P. and Z. Dvorak (2008). "Xenobiotic-induced transcriptional regulation of xenobiotic metabolizing enzymes of the cytochrome P450 superfamily in human extrahepatic tissues." Curr Drug Metab **9**(2): 129-43.
- Pavek, P., K. Pospechova, et al. (2010). "Intestinal cell-specific vitamin D receptor (VDR)-mediated transcriptional regulation of CYP3A4 gene." Biochem Pharmacol **79**(2): 277-87.
- Pelkonen, O., P. Myllynen, et al. (2001). "Carbamazepine: a 'blind' assessment of CYP-associated metabolism and interactions in human liver-derived in vitro systems." Xenobiotica **31**(6): 321-43.
- Perera, M. A. (2010). "The missing linkage: what pharmacogenetic associations are left to find in CYP3A?" Expert Opin Drug Metab Toxicol **6**(1): 17-28.
- Qiu, H. (2008). "Comparative genomics and phylogenetics of the vertebrate CYP3 family." Dissertation am Fachbereich Biologie der Johannes Gutenberg-Universität Mainz.
- Qiu, H., M. Mathas, et al. (2010). "The unique complexity of the CYP3A4 upstream region suggests a nongenetic explanation of its expression variability." Pharmacogenet Genomics **20**(3): 167-78.
- Qiu, H., S. Taudien, et al. (2008). "CYP3 phylogenomics: evidence for positive selection of CYP3A4 and CYP3A7." Pharmacogenet Genomics **18**(1): 53-66.
- Raucy, J. L. (2003). "Regulation of CYP3A4 expression in human hepatocytes by pharmaceuticals and natural products." Drug Metab Dispos **31**(5): 533-9.
- Raunio, H., J. Hakkola, et al. (2005). "Regulation of CYP3A genes in the human respiratory tract." Chem Biol Interact **151**(2): 53-62.
- Rebeck, T. R., J. M. Jaffe, et al. (1998). "Modification of clinical presentation of prostate tumors by a novel genetic variant in CYP3A4." J Natl Cancer Inst **90**(16): 1225-9.
- Rebeck, T. R., H. Rennert, et al. (2008). "Joint effects of inflammation and androgen metabolism on prostate cancer severity." Int J Cancer **123**(6): 1385-9.
- Reschly, E. J. and M. D. Krasowski (2006). "Evolution and function of the NR1I nuclear hormone receptor subfamily (VDR, PXR, and CAR) with respect to metabolism of xenobiotics and endogenous compounds." Curr Drug Metab **7**(4): 349-65.
- Riffel, A. K., E. Schuenemann, et al. (2009). "Regulation of the CYP3A4 and CYP3A7 promoters by members of the nuclear factor I transcription factor family." Mol Pharmacol **76**(5): 1104-14.
- Robertson, G. R., J. Field, et al. (2003). "Transgenic mouse models of human CYP3A4 gene regulation." Mol Pharmacol **64**(1): 42-50.
- Saito, T., Y. Takahashi, et al. (2001). "Novel transcriptional regulation of the human CYP3A7 gene by Sp1 and Sp3 through nuclear factor kappa B-like element." J Biol Chem **276**(41): 38010-22.

- Salero, E., C. Gimenez, et al. (2003). "Identification of a non-canonical E-box motif as a regulatory element in the proximal promoter region of the apolipoprotein E gene." Biochem J **370**(Pt 3): 979-86.
- Schuetz, J. D., D. L. Beach, et al. (1994). "Selective expression of cytochrome P450 CYP3A mRNAs in embryonic and adult human liver." Pharmacogenetics **4**(1): 11-20.
- Schuetz, J. D., S. Kauma, et al. (1993). "Identification of the fetal liver cytochrome CYP3A7 in human endometrium and placenta." J Clin Invest **92**(2): 1018-24.
- Shi, Y., J. S. Lee, et al. (1997). "Everything you have ever wanted to know about Yin Yang 1." Biochim Biophys Acta **1332**(2): F49-66.
- Shimada, T., H. Yamazaki, et al. (1994). "Interindividual variations in human liver cytochrome P-450 enzymes involved in the oxidation of drugs, carcinogens and toxic chemicals: studies with liver microsomes of 30 Japanese and 30 Caucasians." J Pharmacol Exp Ther **270**(1): 414-23.
- Sim, S. C., R. J. Edwards, et al. (2005). "CYP3A7 protein expression is high in a fraction of adult human livers and partially associated with the CYP3A7\*1C allele." Pharmacogenet Genomics **15**(9): 625-31.
- Singer, G. A., A. T. Lloyd, et al. (2005). "Clusters of co-expressed genes in mammalian genomes are conserved by natural selection." Mol Biol Evol **22**(3): 767-75.
- Smith, G., S. H. Ibbotson, et al. (2006). "Regulation of cutaneous drug-metabolizing enzymes and cytoprotective gene expression by topical drugs in human skin in vivo." Br J Dermatol **155**(2): 275-81.
- Sonoda, J., L. Pei, et al. (2008). "Nuclear receptors: decoding metabolic disease." FEBS Lett **582**(1): 2-9.
- Su, A. I., T. Wiltshire, et al. (2004). "A gene atlas of the mouse and human protein-encoding transcriptomes." Proc Natl Acad Sci U S A **101**(16): 6062-7.
- Tateishi, T., H. Nakura, et al. (1997). "A comparison of hepatic cytochrome P450 protein expression between infancy and postinfancy." Life Sci **61**(26): 2567-74.
- Tegude, H., A. Schnabel, et al. (2007). "Molecular mechanism of basal CYP3A4 regulation by hepatocyte nuclear factor 4alpha: evidence for direct regulation in the intestine." Drug Metab Dispos **35**(6): 946-54.
- Thompson, E. E., H. Kuttub-Boulos, et al. (2004). "CYP3A variation and the evolution of salt-sensitivity variants." Am J Hum Genet **75**(6): 1059-69.
- Thorey, I. S., J. J. Meneses, et al. (1993). "Embryonic expression of human keratin 18 and K18-beta-galactosidase fusion genes in transgenic mice." Dev Biol **160**(2): 519-34.
- Thorn, M., N. Finnstrom, et al. (2005). "Cytochromes P450 and MDR1 mRNA expression along the human gastrointestinal tract." Br J Clin Pharmacol **60**(1): 54-60.
- Thummel, K. E. and G. R. Wilkinson (1998). "In vitro and in vivo drug interactions involving human CYP3A." Annu Rev Pharmacol Toxicol **38**: 389-430.
- Tirona, R. G. and R. B. Kim (2005). "Nuclear receptors and drug disposition gene regulation." J Pharm Sci **94**(6): 1169-86.
- Tom, B. H., L. P. Rutzky, et al. (1976). "Human colonic adenocarcinoma cells. I. Establishment and description of a new line." In Vitro **12**(3): 180-91.
- Tompkins, L. M. and A. D. Wallace (2007). "Mechanisms of cytochrome P450 induction." J Biochem Mol Toxicol **21**(4): 176-81.
- van Ginkel, P. R., K. M. Hsiao, et al. (1997). "E2F-mediated growth regulation requires transcription factor cooperation." J Biol Chem **272**(29): 18367-74.
- van Herwaarden, A. E., E. Wagenaar, et al. (2007). "Knockout of cytochrome P450 3A yields new mouse models for understanding xenobiotic metabolism." J Clin Invest **117**(11): 3583-92.
- Verkoelen, C. F., B. G. van der Boom, et al. (1999). "Cell type-specific acquired protection from crystal adherence by renal tubule cells in culture." Kidney Int **55**(4): 1426-33.

- Wadman, I. A., H. Osada, et al. (1997). "The LIM-only protein Lmo2 is a bridging molecule assembling an erythroid, DNA-binding complex which includes the TAL1, E47, GATA-1 and Ldb1/NLI proteins." *Embo J* **16**(11): 3145-57.
- Weill, L., E. Shestakova, et al. (2003). "Transcription factor YY1 binds to the murine beta interferon promoter and regulates its transcriptional capacity with a dual activator/repressor role." *J Virol* **77**(5): 2903-14.
- Werck-Reichhart, D. and R. Feyereisen (2000). "Cytochromes P450: a success story." *Genome Biol* **1**(6): REVIEWS3003.
- Westlind-Johnsson, A., S. Malmebo, et al. (2003). "Comparative analysis of CYP3A expression in human liver suggests only a minor role for CYP3A5 in drug metabolism." *Drug Metab Dispos* **31**(6): 755-61.
- Westlind, A., L. Lofberg, et al. (1999). "Interindividual differences in hepatic expression of CYP3A4: relationship to genetic polymorphism in the 5'-upstream regulatory region." *Biochem Biophys Res Commun* **259**(1): 201-5.
- Williams, E. T., K. R. Schouest, et al. (2007). "The chimpanzee cytochrome P450 3A subfamily: Is our closest related species really that similar?" *Comp Biochem Physiol Part D Genomics Proteomics* **2**(2): 91-100.
- Williams, J. A., B. J. Ring, et al. (2002). "Comparative metabolic capabilities of CYP3A4, CYP3A5, and CYP3A7." *Drug Metab Dispos* **30**(8): 883-91.
- Wojnowski, L. and L. K. Kamdem (2006). "Clinical implications of CYP3A polymorphisms." *Expert Opin Drug Metab Toxicol* **2**(2): 171-82.
- Wurtele, H., K. C. Little, et al. (2003). "Illegitimate DNA integration in mammalian cells." *Gene Ther* **10**(21): 1791-9.
- Xie, W., J. L. Barwick, et al. (2000). "Humanized xenobiotic response in mice expressing nuclear receptor SXR." *Nature* **406**(6794): 435-9.
- Xu, C., C. Y. Li, et al. (2005). "Induction of phase I, II and III drug metabolism/transport by xenobiotics." *Arch Pharm Res* **28**(3): 249-68.
- Xu, H., J. K. Uno, et al. (2005). "NF1 transcriptional factor(s) is required for basal promoter activation of the human intestinal NaPi-IIb cotransporter gene." *Am J Physiol Gastrointest Liver Physiol* **288**(2): G175-81.
- Yamakoshi, Y., T. Kishimoto, et al. (1999). "Human prostate CYP3A5: identification of a unique 5'-untranslated sequence and characterization of purified recombinant protein." *Biochem Biophys Res Commun* **260**(3): 676-81.
- Yan, B., D. Li, et al. (2010). "Homologous illegitimate random integration of foreign DNA into the X chromosome of a transgenic mouse line." *BMC Mol Biol* **11**: 58.
- Yan, J. and Z. Cai (2010). "Molecular evolution and functional divergence of the cytochrome P450 3 (CYP3) Family in Actinopterygii (ray-finned fish)." *PLoS One* **5**(12): e14276.
- Yang, W. M., C. Inouye, et al. (1996). "Transcriptional repression by YY1 is mediated by interaction with a mammalian homolog of the yeast global regulator RPD3." *Proc Natl Acad Sci U S A* **93**(23): 12845-50.
- Yang, X. P., L. A. Freeman, et al. (2002). "The E-box motif in the proximal ABCA1 promoter mediates transcriptional repression of the ABCA1 gene." *J Lipid Res* **43**(2): 297-306.
- Yao, Y. L., B. R. Dupont, et al. (1998). "Cloning, chromosomal localization and promoter analysis of the human transcription factor YY1." *Nucleic Acids Res* **26**(16): 3776-83.
- Yengi, L. G., Q. Xiang, et al. (2003). "Quantitation of cytochrome P450 mRNA levels in human skin." *Anal Biochem* **316**(1): 103-10.
- Zhai, Y., H. V. Pai, et al. (2007). "Activation of pregnane X receptor disrupts glucocorticoid and mineralocorticoid homeostasis." *Mol Endocrinol* **21**(1): 138-47.
- Zhang, W., A. F. Purchio, et al. (2003). "A transgenic mouse model with a luciferase reporter for studying in vivo transcriptional regulation of the human CYP3A4 gene." *Drug Metab Dispos* **31**(8): 1054-64.

## 11 Appendix

### 11.1 Bradford assay

Bradford reagent stock: Bio-rad protein assay 500-0006.

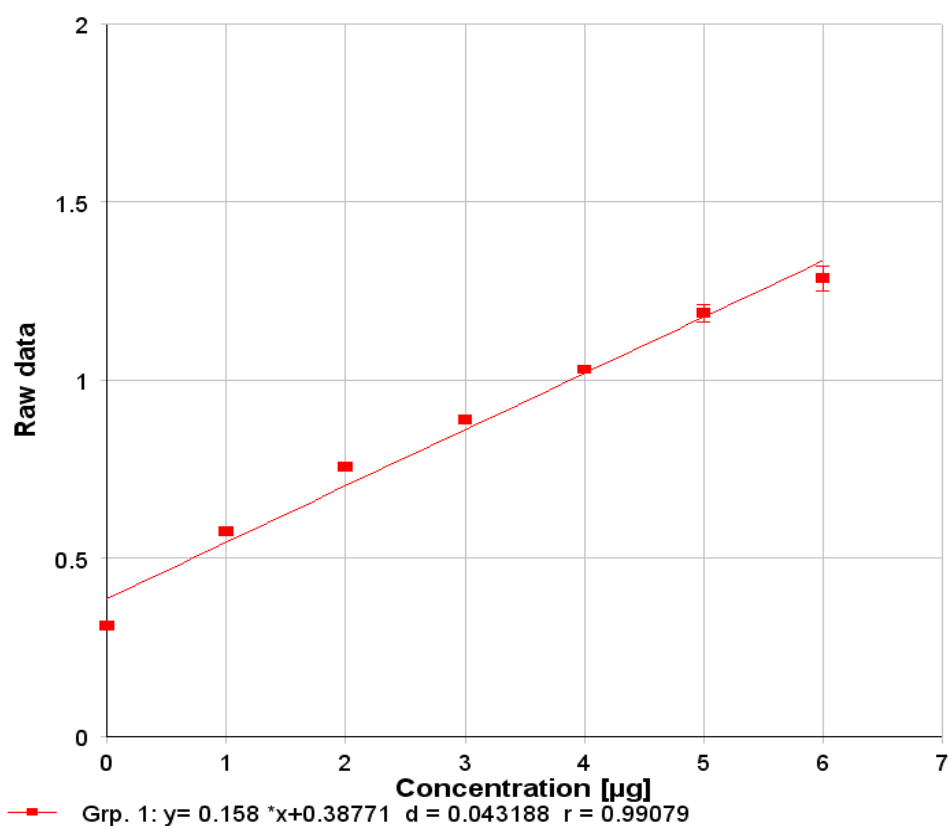
Bradford Assay solution: Prepare a 40% solution by diluted 40 ml of the stock with 60 ml ddH<sub>2</sub>O, filter and store at 4°C until used.

#### Standard curve

BSA (Applichem A1391, Albumin Fraction V): Stock 1mg/ml aliquots stored at -20°C.

BSA Assay solution: Prepare a 1:10 solution by diluted 100 µl of the stock with 900 ml ddH<sub>2</sub>O.

Concentration (µg/well)	0 µg	1 µg	2 µg	3 µg	4 µg	5 µg	6 µg
BSA (1:10) (µl)	0 µl	10 µl	20 µl	30 µl	40 µl	50 µl	60 µl
H <sub>2</sub> O (µl)	100 µl	90 µl	80 µl	70 µl	60 µl	50 µl	40 µl



### Assay on a 96 well plate

The reaction is performed in duplicate for the standard (e.g., S1) and the assay (e.g., X1). For the assay 100  $\mu$ l of the protein solution is mixed with 100  $\mu$ l of 40% Bradford solution. The protein content is determined on a 96 plate reader (Tecan).

	1	2	3	4	5	6	7	8	9	10	11	12
A	S1	S2	S3	S4	S5	S6	S7					
B	S1	S2	S3	S4	S5	S6	S7					
C	X1	X2	X3									
D	X1	X2	X3									

### 11.2 Buffer and solution preparation

#### Medium for *Escherichia coli* culture

NZY+ Broth (per liter): 10 g NZ-Amine (Casein hydrolysate), 5 g yeast extract, 5 g NaCl. Adjust the pH to 7.5 with NaOH. After autoclaving, Add 12.5 ml MgCl<sub>2</sub> (1M), 12.5 ml MgSO<sub>4</sub> (1M) and 10 ml Glukose (2M) steril. Aliquots stored at -20°C.

LB- ("Luria-Bertani") medium (per liter): 2% Bacto-Tryptone; 1% NaCl; 0.5% yeast extract autoclave.

LB agar plates (per liter): LB-medium with 1.5% Bacto-Agar; autoclave, and divide by the plates.

In both cases, Ampicillin is added to 100  $\mu$ g/ml after autoclaving (50°C).

#### 10×TBE

900 mM Tris-Boric acid pH 8,3; 20 mM EDTA pH 8,0

#### Firefly-luciferase Assay buffer

2x Firefly-Luciferase Assay Buffer, pH7.8

60 mM Tricine pH 7.8                      1.075 g/100 ml H<sub>2</sub>O

30 mM MgSO<sub>4</sub>·7H<sub>2</sub>O                      739 mg/100 ml H<sub>2</sub>O

20 mM DTT                                      308 mg/100 ml H<sub>2</sub>O

0.2 mM EDTA                                40  $\mu$ l 0.5 M EDTA pH 8.0/100 ml H<sub>2</sub>O

#### Firefly-luciferase substrate solution

5 ml 2x Firefly-luciferase Assay Buffer

188  $\mu$ l 25 mM D-Luciferin

100  $\mu$ l 27 mM Coenzyme A

53  $\mu$ l 100 mM ATP

4.659 ml ddH<sub>2</sub>O

#### Renilla-luciferase Assay buffer

0.1 M NaCl                                      2.922 g/500 ml

25 mM Tris pH7.5                            1.514 g/500 ml

1 mM CaCl<sub>2</sub> · 2H<sub>2</sub>O                      73.51 mg/500 ml

Coelenterazine, 100  $\mu$ M                      Stock 1 mM (407.5  $\mu$ g/ml) 1 mg-2.454 ml Ethanol

dilution 1 + 9 (100  $\mu$ M) 100  $\mu$ l, Aliquots stored at -20°C.

### Renilla-luciferase substrate solution

100  $\mu$ l Coelenterazine (100  $\mu$ M) in 10 ml Renilla-Luciferase Assay Buffer.

### Nuclear extraction

**Hypotonic buffer A:** 10 mM HEPES pH 7.9, 10 mM KCl, 0.1 mM EGTA, 0.1 mM EDTA, 0.1% benzoase and 2% EDTA-free protease inhibitor cocktail.

**hypertonic buffer B:** 20 mM HEPES pH 7.9, 0.4 M NaCl, 1 mM EDTA, 1 mM EGTA, 1 mM DTT, 0.1% benzoase, 2% EDTA-free protease inhibitor cocktail.

4% gel DNA polyacrylamide gel electrophoresis sufficient for one hoefer minigel (EMSA).

30% Acrylamide-/bis-Methylenbisacrylamide	H <sub>2</sub> O	5xTBE	10% APS	TEMED
0.8 ml	4 ml	1.2 ml	150 $\mu$ l	10 $\mu$ l

### DNA extraction from mouse tail biopsy: Stock solutions

#### A. Lysis buffer

1.0 M Tris, pH 8.5

5.0 M NaCl

0.5 M EDTA

10% SDS

ddH<sub>2</sub>O to 1000 ml

#### B. Proteinase K (from Roth, 10 mg/ml)

Proteinase K 100 mg, ddH<sub>2</sub>O to 10 ml

#### D. Tris- EDTA (TE; 10:1)

1.0 M Tris, pH 8.0

0.5 M EDTA

ddH<sub>2</sub>O to 1000 ml

100% and 70% cold Ethanol.

### Cell culture medium

Cell Culture medium for **LS174T cells:** 86% (v/v) DMEM; 10% (v/v) FBS; 2 mM L-Glutamin; 1 mM Natriumpyruvat; 1 $\times$  Non-essential amino acids; 100 U/ml Penicillin; 100  $\mu$ g/ml Streptomycin.

Cell Culture medium for **MDCK.2 cells:** 86% (v/v) DMEM; 10% (v/v) FBS; 2 mM L-Glutamin; 1 mM Natriumpyruvat; 100 U/ml Penicillin; 100  $\mu$ g/ml Streptomycin.

Cell Culture medium for **HepG2 cells:** 88% (v/v) MEM; 10% (v/v) FBS; 2 mM L-Glutamin; 100 U/ml Penicillin; 100  $\mu$ g/ml Streptomycin.



## **Scientific publications**

Dieudonné Nem, Dorothea Baranyai, Huan Qiu, Ute Gödtel-Armbrust, Sebastian Nestler and Leszek Wojnowski. Pregnane X Receptor and Yin Yang 1 contribute to the Differential Tissue Expression and Induction of CYP3A5 and CYP3A4 (Plosone, in press).

Marianne Mathäs, Oliver Burk, Huan Qiu, Christian Nußhag, Ute Gödtel-Armbrust, Dorothea Baranyai, Shiwei Deng, Kristin Römer, Dieudonné Nem, Björn Windshügel, Leszek Wojnowski. Evolutionary History and Functional Characterization of the Amphibian Xenosensor CAR (Molecular Endocrinology, in press).

Qiu, H., Mathas, M., Nestler, S., Bengel, C., Nem, D., Godtel-Armbrust, U., Lang, T., Taudien, S., Burk, O. and Wojnowski, L. (2010). The unique complexity of the CYP3A4 upstream region suggests a nongenetic explanation of its expression variability. *Pharmacogenet Genomics* 20, 167-78.

## **Congress contribution:**

Nem, D., Gödtel-Armbrust, U., Nestler, S. and Wojnowski L. *In vivo* and *in vitro* analysis of the human CYP3A5 promoter activity (talk, “51. Jahrestagung der Deutschen Gesellschaft für Pharmakologie und Toxikologie”, Mar. 2010, Mainz, Germany).

## Curriculum vitae

### **Personal information**

First, last name: Dieudonné Nem

Date of Birth: 25. 10. 1976

Place of Birth: Bayangam, Cameroon

Marital Status: Married

Nationality: Cameroonian

Gender: Male

Private address: Max-Hufschmidt Str.17, 55130 Mainz, Germany.

Tel: 0049 176 68457323

E-Mail: nem\_dieudonne@yahoo.fr

Work address: Department of Pharmacology, University Medical Center, Johannes Gutenberg University Mainz. Obere Zahlbacher Str.67, 55101 Mainz, Germany.

Tel: 0049 6131 179219

### **Education and professional experience**

Apr. 2008-present

Department of Pharmacology

University Medical Center

Johannes Gutenberg University, Mainz, Germany

Major: Biology

Degree: PhD

### **Fellowship:**

Oct. 2007-present

DAAD (German Academic Exchange Office) Fellowship.

### **2005-2007**

Teacher in Life and Ground Sciences at Nkondjock's high school, Cameroon.

2003-2005

Higher teacher's training school, University Yaounde I, Yaounde Cameroon

Major: Biology and geology

Degree: Secondary Diploma of Education rank II in Life and Ground Sciences.

2001-2005

Department of Biochemistry, University Yaounde I, Yaounde Cameroon

Major: Biochemistry

Degree: Master of Biochemistry.

1997-2001

Department of Biochemistry, University Yaounde I, Yaounde Cameroon

Major: Biochemistry

Degree: Bachelor of Biochemistry.

1989-1997

Junior and high schools in Foumban (Cameroon).

Degree: Baccalaureate in Mathematics and Life Sciences.

1981-1989: Nursery and primary schools in Foumban (Cameroon).